REVIEWS OF GEOPHYSICS AND SPACE PHYSICS, VOL. 18, NO. 1, PAGES 269–311, FEBRUARY 1980

The Heat Flow Through Oceanic and Continental Crust and the Heat Loss of the Earth

J. G. SCLATER, C. JAUPART, AND D. GALSON

Department of Earth and Planetary Sciences, Massachusetts Institute of Technology, Cambridge, Massachusetts 02139

Simple thermal models based on the creation and cooling of the lithosphere can account for the observed subsidence of the ocean floor and the measured decreased in heat flow with age. In well-sedimented areas, where there is little loss of heat due to hydrothermal circulation, the surface heat flow decays uniformly from values in excess of 6 μcal/cm^2 s (250 mW/m^2), for crust younger than 4 Ma (4 m.y. B.P.), to close to 1.1 μcal/cm^2 s (46 mW/m^2) through crust between 120 and 140 Ma. After 200 Ma the heat flow is predicted to reach an equilibrium value of 0.9 μcal/cm^2 s (38 mW/m^2). The surface heat flow on continents is controlled by many phenomena. On the time scale of geological periods the most important of these are the last orogenic event, the distribution of heat-producing elements, and erosion. To better understand the effects of age, each continent is separated into four provinces on the basis of radiometric dates. Reflecting the preponderance of Precambrian crust, two of these provinces cover the Archean to the middle Proterozoic, and the third covers the late Proterozoic to the Mesozoic. The mean heat flow decreases from a value of 1.84 μcal/cm^2 s (77 mW/m^2) for the youngest province to a constant value of 1.1 μcal/cm^2 s (46 mW/m^2) after 800 Ma. The nonradiogenic component of the surface heat flow decays to a constant value of between 0.65 and 0.5 μcal/cm^2 s (25 and 21 mW/m^2) within 200–400 Ma. Using theoretical models, we compute the heat loss through the oceans to be 727 $\times$ 10^{10} cal/s (30.4 $\times$ 10^{12} W). The comparison between the theoretical and measured values allows an estimate of 241 $\times$ 10^{10} cal/s (10.1 $\times$ 10^{12} W) for the heat lost owing to hydrothermal circulation. We show that the heat flow through the marginal basins follows the same relation as that for crust created at a midocean spreading center. These basins have a corresponding heat loss of 71 $\times$ 10^{10} cal/s (3.0 $\times$ 10^{12} W). The heat loss through the continents is calculated from the observations and is 208 $\times$ 10^{10} cal/s (8.8 $\times$ 10^{12} W). Our estimate of the value for the shelves is 67 $\times$ 10^{10} cal/s (2.8 $\times$ 10^{12} W). The total heat loss of the earth is 1002 $\times$ 10^{10} cal/s (42.0 $\times$ 10^{12} W), of which 70% is through the deep oceans and marginal basins and 30% through the continents and continental shelves. The creation of lithosphere accounts for just under 90% of the heat lost through the oceans and hence about 60% of the worldwide heat loss. Convective processes, which include plate creation and orogeny on continents, dissipate two thirds of the heat lost by the earth. Conduction through the lithosphere is responsible for 20%, and the rest is lost by the radioactive decay of the continental and oceanic crust.

We place bounds of between 0.6 and 0.9 μcal/cm^2 s (25 and 38 mW/m^2) for the mantle heat flow beneath an ocean at equilibrium and between 0.40 and 0.75 μcal/cm^2 s (17 and 31 mW/m^2) for the heat flow beneath an old stable continent. The computed range of geotherms for an equilibrium ocean overlaps the range of stable continental geotherms below a depth of 100 km. The mantle heat flow beneath a continent decays with a thermal time constant similar to that of the oceanic lithosphere. The continental basins subside with the same time constant. These observations are evidence that there is no detectable difference between the thermal structure of an equilibrium ocean and that of an old continent. Thus the concept of the lithosphere as a combination of a mechanical and a thermal boundary layer can be applied to both oceans and continents. We evaluate the constraints placed on models based on this concept by seismological observations. In the absence of compelling evidence to the contrary we favor these models because they provide a single explanation for the thermal structure of the lithosphere beneath an equilibrium ocean and a stable continent.

CONTENTS

Introduction 269
Heat flow through the ocean floor 270
  Introduction 270
  Data analysis 270
  Thermal models of the lithosphere 270
  Hydrothermal circulation 271
  Reinterpretation of oceanic heat flow measurements 272
  Marginal basin heat flow 277
  Mantle convection and thermal structure 279
Continental heat flow 281
  Introduction 281
  Geological models for continental formation 281
  Continental heat flow measurements 283
  Heat flow and age 284
  Heat flow and surface heat production 286
  Thermal models 291
Heat loss of the earth 292
  Introduction 292
  Heat loss through the oceans 292
  Heat loss through the continents 293
  Total heat loss of the earth 294
Thermal structure and thickness of the lithosphere 295
  Introduction 295
  Comparison of the 'equilibrium' ocean and old continent geotherm 295
  Comparison with geothermometry and geobarometry data 296
  Relation between reduced heat flow and age 297
  Subsidence of continental basins 297
Convection in the mantle and the thermal structure of the lithosphere 299
Conclusions 300
Appendix A: Relation between area and age for oceanic crust 301
  Magnetic Anomaly Identifications 301
  Deep Sea drilling sites and bathymetric contours 301
  Time scale 301
  Why specific isochrons were chosen 301
  Position of the isochrons 302
  Area versus age for the oceans 303
Appendix B: Relation between area and age for continents 303
Appendix C: The modified plate model 305

Paper number 9R1283.

INTRODUCTION

In the past 15 years our understanding of the earth has changed. Rather than regard the oceans and continents as static and unrelated, we now think of them as mobile and in-

terconnected. The theory of plate tectonics accounts for the major features on the surface of the earth by the motion and interaction of a finite number of rigid plates. These plates are defined tectonically and include both oceans and continents.

The oceanic crust is younger than 180 Ma (180 m.y. B.P.), whereas parts of the continents have existed throughout the whole geological time span: the oldest continental crust is Archean and older than 3800 Ma. The mechanisms of heat transfer beneath continents and oceans may be different, and we consider the oceans and continents separately rather than studying a single plate.

In the past 10 years many new heat flow measurements have been reported in the geophysical literature. They have been assembled under the auspices of the International Heat Flow Commission of the International Association of Seismology and Physics of the Earth's Interior. In 1976, Jessop et al. published an updated and revised version of the previous compilations of *Lee and Uyeda* [1965] and *Simmons and Horai* [1968]. In our analysis we use this compilation and include additional data published since then but before June 1977. Our approach differs from previous work [*Lee and Uyeda*, 1965; *Simmons and Horai*, 1968; *Von Herzen and Lee*, 1969; *Chapman and Pollack*, 1975*a*], principally because we concentrate on examining the oceanic and continental values with local geologic variables in mind. Only when these local variables are understood is it possible to separate deep-seated thermal properties from superficial noise.

Our objective is to increase our understanding of the large-scale mechanism of heat transport within the earth. We separate this review into two parts.

In the first section, which is almost totally empirical, we present a general synthesis of oceanic and continental heat flow data and examine both sets of data within the framework of the theory of plate tectonics. Care is taken in the oceans to account for hydrothermal circulation, and on the continents, consideration is given to the relation between heat flow and surface heat production. We use our understanding of geologic perturbations to establish a relation between heat flow and age for both continents and oceans and account for this relation by models of oceanic and continental heat flow which are compatible with the theory of plate tectonics and uniformitarian in principle. We compare the heat loss through continents and oceans, estimate the amount of heat dissipated by the creation of the oceanic lithosphere, and compute the total heat loss for the earth.

Given the success of the plate theory in accounting for geophysical observations from the oceans, attempts are now being made to apply this quantitative approach to the continents. The success has not been overwhelming, but a productive line of research has been to relate the past geologic record to processes which are active today. In the second section we use this approach and the data and models from the preceding section to examine the thermal structure of the oceanic and continental lithospheres. In particular, we investigate whether or not it is possible to extend the simple thermal models for the oceans to the continents.

The approach that we take is similar to that used in an earlier paper by *Sclater and Francheteau* [1970]. The present analysis places more emphasis on removing the effects of local geology and has the benefit of three advances in the field. These are (1) that the scatter in the oceanic heat flow is now understood, (2) that continental heat flow and radioactive data are more extensive, and (3) that models based on the theory of plate tectonics are having some success in accounting for the subsidence of continental basins.

(For our computations and presentation of the data we use calories. These units permit comparison with previous reviews. Also, we present the data in SI units. They follow those in calories and are enclosed by parentheses.)

HEAT FLOW THROUGH THE OCEAN FLOOR

Introduction

We superimposed all the heat flow values upon an isochron chart of the oceans (Plate 1). A detailed account of the methods used to determine the age of the ocean floor can be found in Appendix A. The data include the compilation of *Jessop et al.* [1976] as well as papers published since this compilation by *Herman et al.* [1977], *Langseth and Hobart* [1976], *Langseth and Zielinski* [1976], *Anderson and Hobart* [1976], *Anderson et al.* [1976*a*, *b*, 1977] and *Sclater et al.* [1976*a*].

For purposes of comparison we separated the data set into six groups; North and South Pacific, North and South Atlantic, the Indian Ocean, and the marginal basins. We define as 'marginal' all basins isolated from active spreading centers by clearly defined tectonic barriers. For example, in the western Pacific all the basins to the west of the major trench system are included. They extend from the Tasman and South Fiji Basin in the south to the Bering Sea and Arctic Basin in the north. Our definition also encompasses the Caribbean, the Mediterranean, the Black and Caspian seas, and the Scotia Sea together with the Andaman and Sunda seas in the Indian Ocean.

Unfortunately the 1:10,000,000 scale that we used was not sufficiently large. Hence in our averaging we may have omitted a few values, especially on younger ocean crust. A careful double check of these areas with the original references showed that the errors introduced were insignificant.

Data Analysis

We computed the mean and standard deviation for all data lying between two isochrons. Throughout the study we use the term age province to define the area between two consecutive isochrons. In particular, the youngest province covers crust created between the present and 4 Ma, and the oldest, crust created prior to 160 Ma.

In all the oceans we observe the same distribution of heat flow (Table 1 and Figure 1). For the young crust the mean is high, ranging from 2 to 6 μcal/cm^2 s (84 to 251 mW/m^2), and is associated with a large scatter of about 2 μcal/cm^2 s (84 mW/m^2). Beyond 60 Ma the mean heat flow has a relatively constant value of around 1.2 μcal/cm^2 s (50 mW/m^2), and the associated scatter is small, less than 0.5 μcal/cm^2 s (21 mW/m^2). The abnormally high scatter in the younger two provinces of the Indian Ocean is a direct consequence of the high but very variable heat flow observed in the Red Sea. The marginal basin heat flow has the same distribution as the oceans.

Thermal Models of the Lithosphere

The oceanic crust is created at a spreading center by intrusion of magma. The magma cools and anneals itself to the recently created crust and moves away from the spreading center as more magma is intruded. The oceanic crust increases in age, loses heat to the seawater, and contracts. This model explains qualitatively the decrease in heat flow with age and the subsidence of midocean ridges. The raw heat flow data are highly scattered. Hence more emphasis has been placed upon

TABLE 1. Oceanic Heat Flow Data

	Age, Ma												
	0–4	4–9	9–20	20–35	35–52	52–65	65–80	80–95	95–110	110–125	125–140	140–160	>160
							North Pacific						
N	268	207	214	126	57	23	36	57	35	33	72	19	12
m	4.04	2.49	1.90	1.59	1.21	1.35	1.48	1.34	1.16	1.11	1.12	1.23	1.29
σ	3.57	1.74	1.26	0.89	0.76	0.52	0.63	0.35	0.46	0.22	0.42	0.37	0.85
							South Pacific						
N	87	64	99	47	51	7	13	6	24	10	19		
m	3.01	2.49	1.82	1.15	1.10	1.12	0.93	1.27	1.30	1.16	0.96		
σ	2.03	2.11	1.30	0.74	0.83	0.53	0.66	0.85	0.41	0.26	0.32		
							Indian Ocean						
N	70	71	67	42	50	122	96	49	35	34	42		
m	2.86	5.23	1.22	1.07	1.49	1.61	1.57	1.28	1.32	1.45	1.16		
σ	1.85	9.9	1.04	0.67	0.72	0.86	0.86	0.75	0.46	0.90	0.39		
							North Atlantic						
N	56	78	63	65	62	82	85	65	43	30	45	47	14
m	3.31	2.13	1.80	1.56	1.62	1.43	1.23	1.19	1.28	1.31	1.29	1.13	1.11
σ	2.69	1.68	1.55	1.06	1.04	0.66	0.50	0.31	0.27	0.36	0.30	0.40	0.22
							South Atlantic						
N	25	24	37	24	32	31	47	27	56	55			
m	2.61	1.31	1.23	1.45	1.32	1.35	1.26	1.35	1.32	1.36			
σ	2.25	1.27	0.73	1.02	0.53	0.53	0.53	0.35	0.46	0.36			
							All Oceans						
N	506	444	470	304	252	265	277	204	193	162	178	66	26
m	3.55 (149)	2.80 (117)	1.69 (71)	1.43 (60)	1.36 (57)	1.49 (62)	1.37 (57)	1.28 (54)	1.28 (54)	1.31 (55)	1.16 (49)	1.16 (49)	1.19 (50)
σ	3.01 (126)	4.30 (180)	1.24 (52)	0.92 (38)	0.83 (35)	0.73 (31)	0.68 (28)	0.48 (20)	0.40 (17)	0.51 (21)	0.38 (16)	0.39 (16)	0.59 (25)
							Marginal Basins						
N		122	46	402	48	32	118			141			
m		2.14	1.92	1.92	1.54	1.28	1.43			101			
σ		1.46	1.16	0.72	0.66	0.74	0.43			0.71			

N is the number of heat flow stations, m is the mean heat flow in μcal/cm^2 s (mW/m^2), and σ is the standard deviation in μcal/cm^2 s (mW/m^2).

the study of ocean floor topography in developing quantitative models for the creation of the oceanic lithosphere.

Sclater et al. [1971] have shown that most midocean ridges are created at a depth of 2500 m and subside to depths greater than 6000 m (Figure 2*a*). For crust younger than 80 Ma the depth increases linearly with the square root of age [*Davis and Lister,* 1974]. For older ocean floor this relation breaks down, and the depth increases exponentially to a constant value of 6400 m (Figure 2*b*) [*Parsons and Sclater,* 1977]. This two-stage relation between depth and age can be explained by the formation of a thermal boundary layer. The magma cools and solidifies as it moves away from the spreading center, and the thickness of the rigid layer thus created increases (Figure 3*a*). *Parker and Oldenburg* [1973] predicted from a one-dimensional cooling model that the layer thickness should increase as the square root of time. This upper layer behaves as a rigid body and is known as the lithosphere. After it reaches a certain thickness at about 80 Ma, it does not thicken any further. This represents the basic justification for modeling the thermal boundary layer as a plate of constant thickness [*McKenzie,* 1967] (Figure 3*b*). *Parsons and Sclater* [1977] demonstrated that for crust younger than 80 Ma both the plate and the boundary layer models are essentially identical, and they used the two different approaches to compute first-order relations which match the topographic data (Table 2).

From these models it is possible to compute the heat flow through the ocean floor. *Lister* [1977] predicted a simple relation between heat flow and $1/t^{1/2}$. *Parsons and Sclater* [1977] showed that this relation should break down at about 120 Ma and that the heat flow should then follow an exponential decay to a value of around 0.9 μcal/cm^2 s (38 mW/m^2) (Table 2).

In order to compare the observations with these models we averaged the heat flow values for all the oceans. As is the case for the individual oceans, the mean and scatter decrease with age (Figure 4*a*). In the older provinces the mean values fall close to those predicted by the plate model, although the scatter prevents the interpretation of the results unambiguously in terms of exponential flattening. For crust younger than 50 Ma the mean values fall well below the theoretical (Figure 4*b*). In order to explain both the topography and the heat flow it is necessary to account for the high scatter and the low mean values for young ocean crust.

Hydrothermal Circulation

Anderson and Hobart [1976], in their analysis of the Galapagos spreading center, have presented an excellent example of the characteristic distribution of heat flow near a spreading center (Figure 5). The values are highly scattered, and many low values are observed on crust between 3 and 4 Ma. Beyond 5 Ma the values show less scatter and fall close to the theoretical. This change in the heat flow distribution is associated with a sudden increase in sediment thickness. *Davis and Lister* [1977] have presented a remarkably similar distribution over the Juan de Fuca Ridge.

The oceanic crust is created by the intrusion of basaltic flows and dykes. Where the intruded magma comes into contact with seawater, it cools rapidly, horizontal and vertical cracks are created on both a large and a small scale, and active convection of seawater occurs. Independently, *Talwani et al.* [1971] and *Lister* [1972] suggested this model to explain the high scatter in heat flow values near a spreading center. The high water temperatures associated with such convection have been observed by conventional techniques in Iceland [*Palmas-*

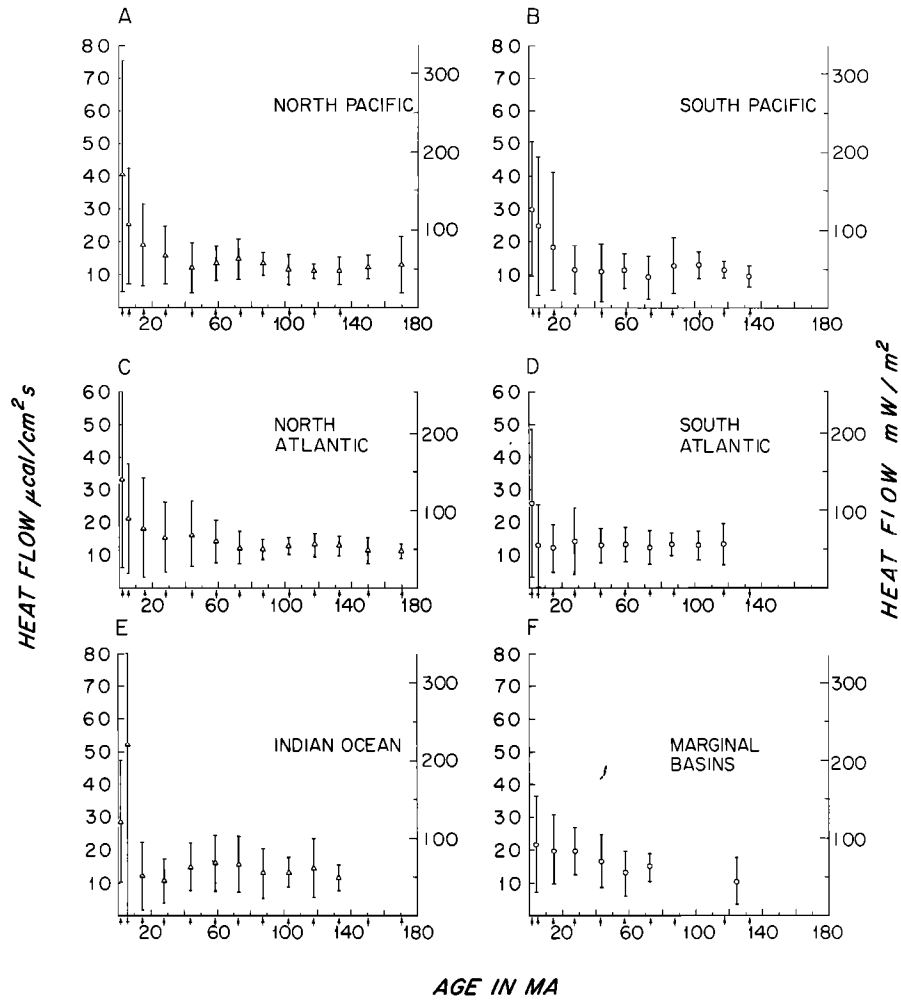

Fig. 1. Mean heat flow and standard deviation as a function of age for five major oceans and the marginal basins.

son, 1967] and over the Galapagos spreading center [*Williams et al.,* 1974]. Extremely hot water at oceanic spreading centers has been observed during dives of the submersible R/V *Alvin* at the Galapagos spreading center and East Pacific Rise [*Corliss et al.,* 1979; J. Edmond, personal communication, 1979]. *Lister* [1977] has proposed a two-stage model for seawater convection through oceanic crust. In the active stage the seawater penetrates into the newly erupted rock, which then cools, contracts, fractures, and hence permits further penetration. The crust cools to a depth where active penetration is halted by the overburden pressure or volume alteration of the intruded mafic rock. These systems are thought to have a lifetime of a few hundred years over a penetration depth of 6–8 km [*Francis et al.,* 1978]. In the passive stage, hydrothermal circulation continues to occur because the permeable water-saturated crust is heated from below as the lithosphere moves away from the spreading center. This passive system exists as long as the permeability and temperature gradients are large enough.

Lister [1972], *Sclater et al.* [1974], and *Davis and Lister* [1977] have shown that the pattern of heat flow over a mid-ocean ridge can be explained by this model (Figure 6). Most deep-sea sediments have a low permeability (J. Crowe and A. Silva, unpublished data, 1979) and in sufficient thickness are impermeable to seawater. Where the permeable crust is not covered, water circulates freely. A highly variable heat flow results, and the mean is lower than is predicted because conventional techniques cannot measure the heat loss by advection. When the crust is covered by a thick blanket of sediment, circulation still occurs, but no heat is lost by advection because the thick sediments are impermeable to seawater. In these areas the measured mean flux is a reasonable estimate of the heat flow at depth.

It is not our purpose in this paper to review the subject of hydrothermal circulation of seawater through the oceanic crust. An exhaustive investigation is presented by *Lister* [1974]. *Anderson* [1979] has reviewed the temperature gradient observations which may indicate seawater flow in thin sediments overlying permeable ocean crust. *Corliss* [1971] and *Bottinga* [1974] have analyzed the effect that this circulation has on the composition of the oceanic crust. Readers should consult these papers to obtain more detailed information concerning this rapidly expanding scientific field.

Reinterpretation of Oceanic Heat Flow Measurements

Recognizing the importance of hydrothermal circulation, *Sclater et al.* [1976*a*] reanalyzed all published data on the Pacific. They characterized the environment according to sediment thickness and topographic roughness. Each station was assigned an environmental quality factor grading from A through D (Figure 7). Only the grade A stations where the

THE AGE OF THE OCEANS

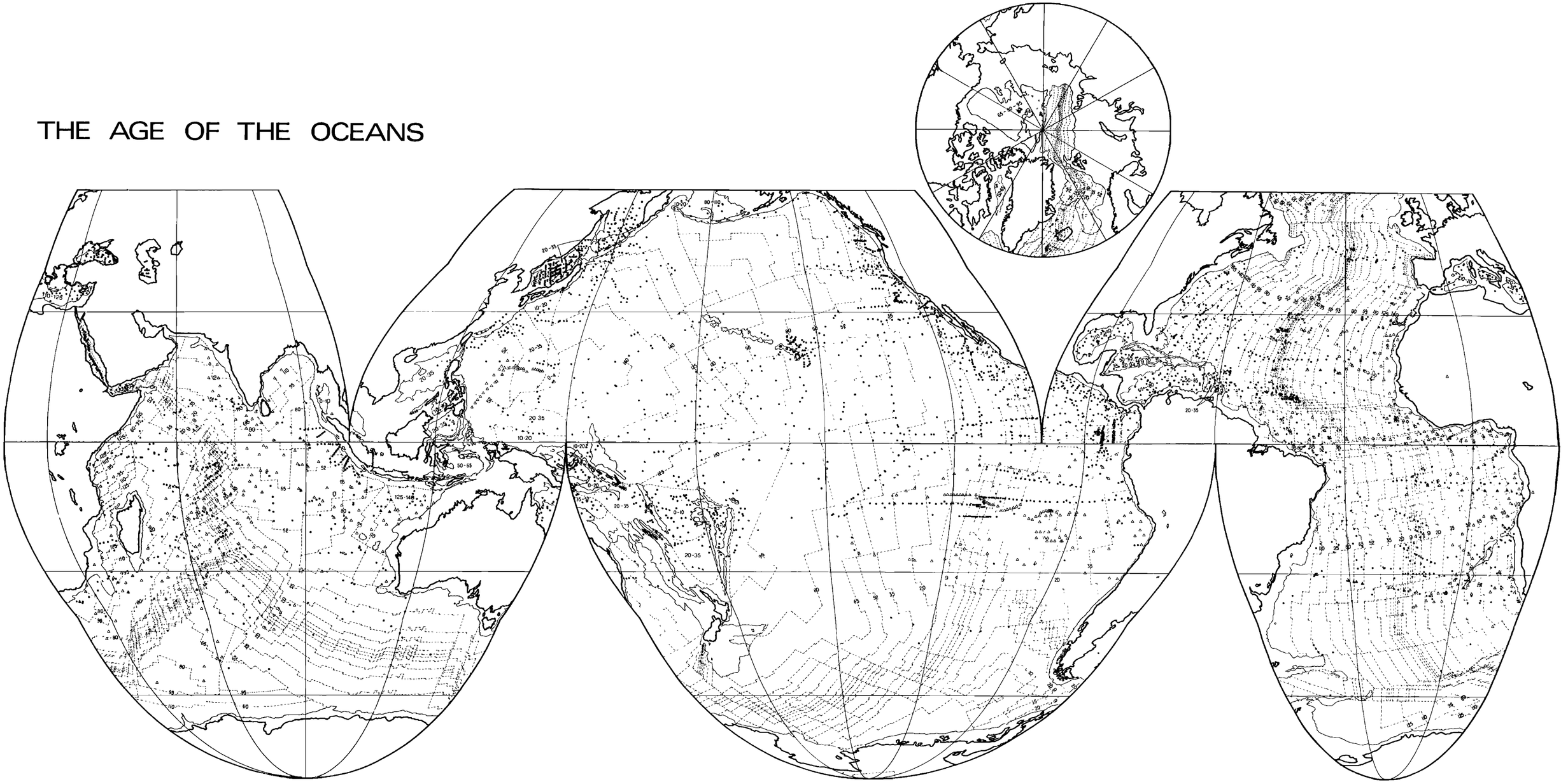

Plate 1. Heat flow stations and ocean floor isochrons (dashed lines) on an equal area map of the oceans [*Goode*, 1923]. Circles are data from *Jessop et al.* [1976]. Triangles represent data published since this compilation.

THE AGE OF THE CONTINENTS

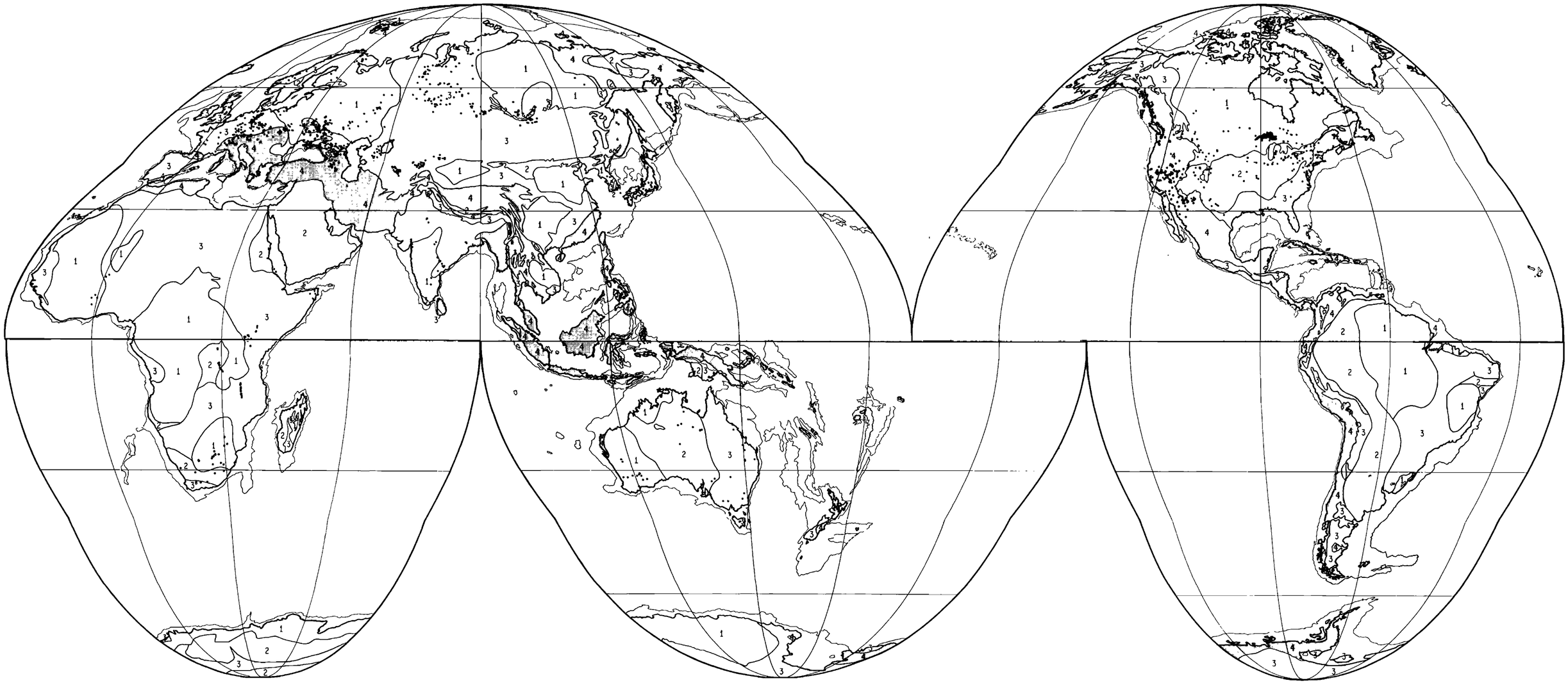

Plate 2. Heat flow stations on a chart of the continents separated into four different age provinces. Province 4 is 0–250 Ma; province 3 is 250–800 Ma; province 2 is 800–1700 Ma, and province 1 is >1700 Ma. Province 4, the Mesozoic and Cenozoic, has been shaded.

IDENTIFIED MAGNETIC LINEATIONS ON THE OCEAN FLOOR

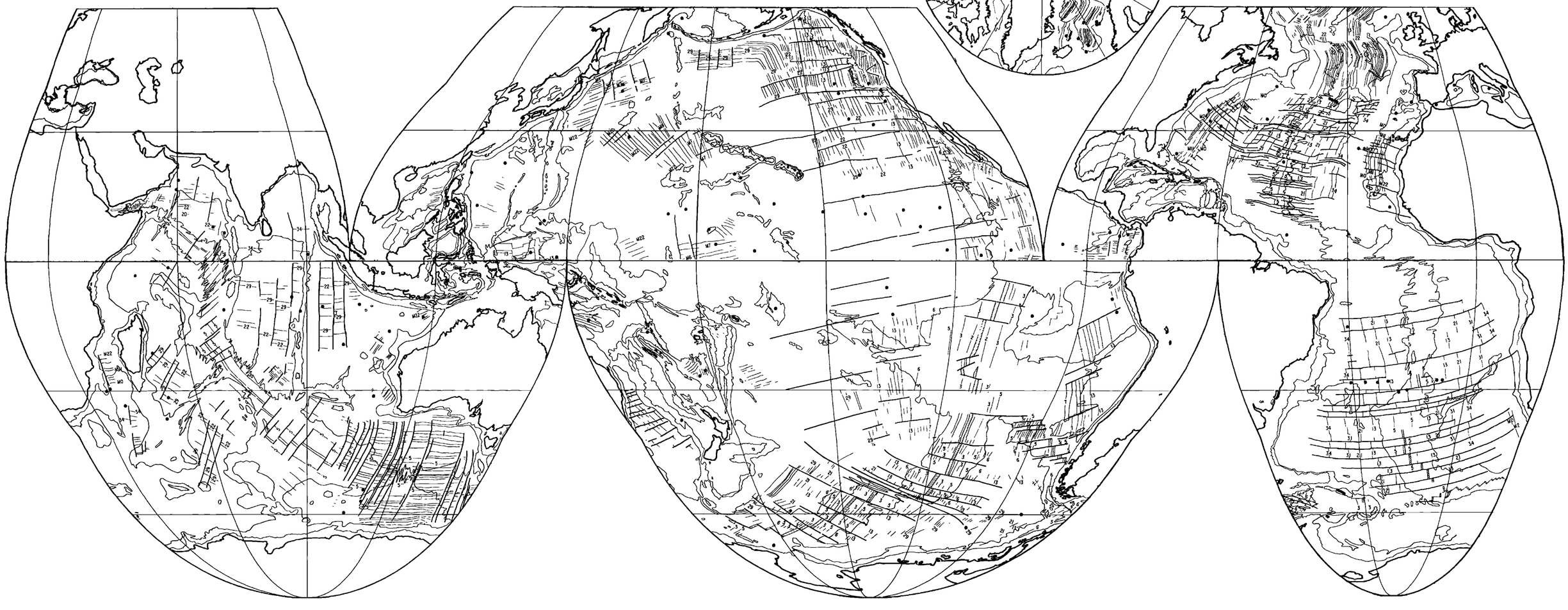

Plate A1. Identified magnetic lineations and the 2000- and 4000-m contours on *Goode's* [1923] equal area map of the oceans. Deep-sea drilling sites where basement was sampled are represented as solid circles.

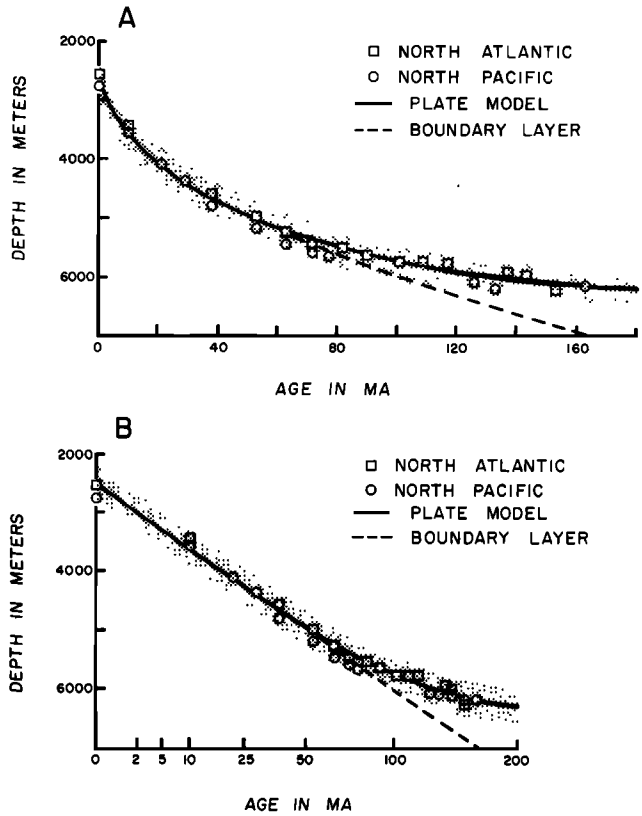

Fig. 2. (*a*) Relation between mean depth and age for the North Atlantic and North Pacific. The shaded area represents an estimate of the scatter in the original points used to determine the mean data. The solid curve is the theoretical elevation from the plate model. The dashed curve is the elevation calculated by assuming that the lithosphere thickens with time. (*b*) Plot of depth versus the square root of age, emphasizing the $t^{1/2}$ dependence of depth for crust younger than 80 Ma. Note that the boundary layer model breaks down at 80 Ma and that a much better fit in older crust is given by the plate model.

basement is completely covered by sediment were assumed to give reliable heat flow values. Using these stations, *Sclater et al.* [1976*a*] found that the scatter was reduced (Figure 8 and Table 3) and that the mean values fall close to the theoretical value (Figure 9). Further surveys on the Juan de Fuca Ridge [*Davis and Lister,* 1977] and in the vicinity of anomaly 13 on the Reykjanes Ridge yielded identical results [*Sclater and Crowe,* 1979] (Figures 8 and 9). Two well-sedimented areas in the Pacific, the equatorial sediment bulge and the Guatemala Basin, fall well below the theoretical heat flow. No detailed survey has been carried out over the Guatemala Basin. But J. Crowe and R. P. Von Herzen (personal communication, 1979) have shown that the low and variable heat flow values on the equatorial sediment bulge are associated with extreme basement relief and unusually permeable sediments.

Partially as a result of the above analyses, authors now show or describe the local environment of all heat flow stations. We examined these new data and found, particularly in the Indian Ocean [*Anderson et al.,* 1977] and the Norwegian Sea [*Langseth and Zielinski,* 1974], a large number of measurements on well-sedimented basement. A few measurements are reported for the Pacific [*Anderson et al.,* 1976*b*] but are too widely distributed to justify our replotting them. We averaged the grade A stations from the Indian Ocean within various age provinces and also, where the age was unknown, by individual basin. The scatter in the data is low (Figure 10 and Table 4), and the mean values lie close to the theoretical (Figure 11). We reexamined data in the Norwegian Sea by plotting them on an isochron chart of the area (Figure 12). As there were not enough data within a given age province to compute a reliable mean, we considered each of the grade A stations individually. The values which are all on young crust fall close to the theoretical expression for the heat flow (Figure 11).

At an active spreading center near the zone of intrusion the relation appears to break down. For example, *Lawver et al.* [1975] have measured the heat flow through the very young but well-sedimented Guyamas Basin in the Gulf of California. They found that in crust less than 2 million years old the mean heat flow falls below the theoretical value. A likely explanation is the discontinuous nature of the intrusion process [*Lister,* 1977], which is not adequately represented in present thermal models. Fortunately, the effect of the initial conditions on these models is small (cf. Appendix C) and only important for ages less than 5 Ma. It does not affect significantly our estimates of heat loss.

From this reexamination of the heat flow data we have established that for crust older than 2 Ma and covered by a thick layer of impermeable sediments there is a simple relation between heat flow and age. This relation is very close to that given by the models which account for the subsidence of the midocean ridges.

Marginal Basin Heat Flow

Watanabe et al. [1977] have recently reviewed the heat flow through the back-arc basins of the western Pacific. They emphasized that though the volcanic zone has a highly variable heat flow, there is still a detectable dependence on age in the back-arc basins. Rather than follow the strictly empirical approach of these authors we examined the data which include these back-arc areas, using our understanding of the heat loss through normal ocean floor. We considered each basin individually and calculated a mean and a standard deviation for the heat flow (Tables 5*a*–5*c*). They vary significantly from one basin to another.

We found it difficult for two reasons to follow the procedure developed in the deep oceans to establish a convincing relation between heat flow and age. First, the age of most marginal basins is unknown, and second, where it is known on the basis of magnetic lineations or deep-sea drilling holes, there are few heat flow measurements. The Scotia Sea is an example of such a basin. It has well-identified lineations but no heat flow values. We found six basins with reliable heat flow measurements (environmental quality grade A) and age estimates. These basins include the Tyrrhenian Sea and Balearic Basin

TABLE 2. Simple Relations Between Depth, Heat Flow, and Age [after *Parsons and Sclater,* 1977]

Age	Relation
	Depth
0–70	$d(t) = 2500 + 350t^{1/2}$
>20	$d(t) = 6400 - 3200e^{(-t/62.8)}$
	Heat Flow
0–120	$q(t) = 11.3/t^{1/2}\,(473/t^{1/2})$
>60	$q(t) = 0.9 + 1.6e^{(-t/62.8)}\,(37.5 + 67e^{(-t/62.8)})$

Here t is in millions of years, $d(t)$ is in meters, and $q(t)$ is in μcal/cm^2 s (mW/m^2). The decay of the radioactive elements contributes 0.1 μcal/cm^2 s (4 mW/m^2) to the heat flow.

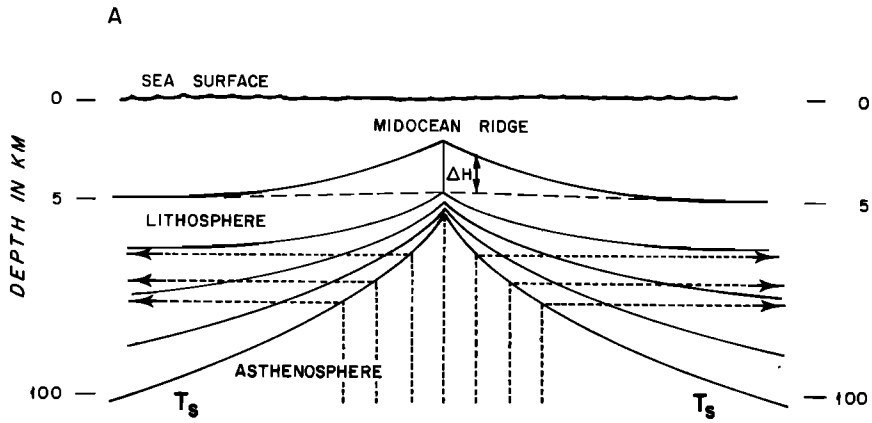

Fig. 3*a*. Schematic model for a thermal boundary layer showing the material flow (dashed lines) and the concept of a thickening lithosphere. The solidus temperature T_s separates solid and partially molten states: the solid lithosphere above is cooler than T_s, and the asthenosphere below is hotter. The solid lines indicate isothermal surfaces within the cooling lithosphere. ΔH is the subsidence of the ridge crest.

in the Mediterranean, the Parece Vela and the West Philippine basins in the Philippine Sea, and finally, the Coral and Bering seas. The sources for the age and heat flow data can be found in Tables 5*a*–5*c*. The two basins in the Mediterranean have been corrected for recent sediment accumulation (Table 6). In each of these basins the mean heat flow is close to the theoretical value predicted by the thermal models for normal ocean crust (Figure 13). This supports the ideas of *Karig* [1970] and others that marginal basins are formed by extensional processes similar to those occurring at active spreading centers.

In order to compare the marginal basins with the deep oceans we wished to separate the data into the same age provinces and plot the mean and standard deviation versus age. As the age of many marginal basins is unknown, this is not as straightforward as it first appears. For those basins where magnetic lineations have been identified or where deep-sea drilling holes have been sited, ages can be assigned in a fairly straightforward manner. For the others this information is not available, and a different approach must be taken. Various authors [*Sclater et al.*, 1976*a*; *Louden*, 1976; *Watanabe et al.*, 1977] have observed that the Parece Vela and West Philippine basins are about 0.5–1 km deeper than ocean crust of the same age. Thus the relation between depth and age for the deep oceans is not a reliable indicator of age for the marginal basins. In contrast, the 'reliable' heat flow values from these basins fit the relation between heat flow and age found in well-sedimented areas of the deep-ocean floor. Where the heat flow has been measured in a well-sedimented basin, we use this relation to determine the age (Tables 5*a*–5*c*). In light of the high sedimentation rate of these basins, such ages should be treated with caution. The ages predicted in this manner for four basins in the western Pacific are of particular interest. The Ryukyu Trough is Miocene or younger, and the Japan, China, and Okhotsk seas are Oligocene. For basins where no magnetic, deep-sea drilling, or heat flow information is available we estimated the age from the surrounding geology.

Having assigned ages to all the marginal basins, we separated the data into age provinces and plotted the mean and standard deviation versus age (Figure 1*f*). In the young regions the mean value is high, and the scatter large. With increasing age both the mean and the scatter decrease. This dis-

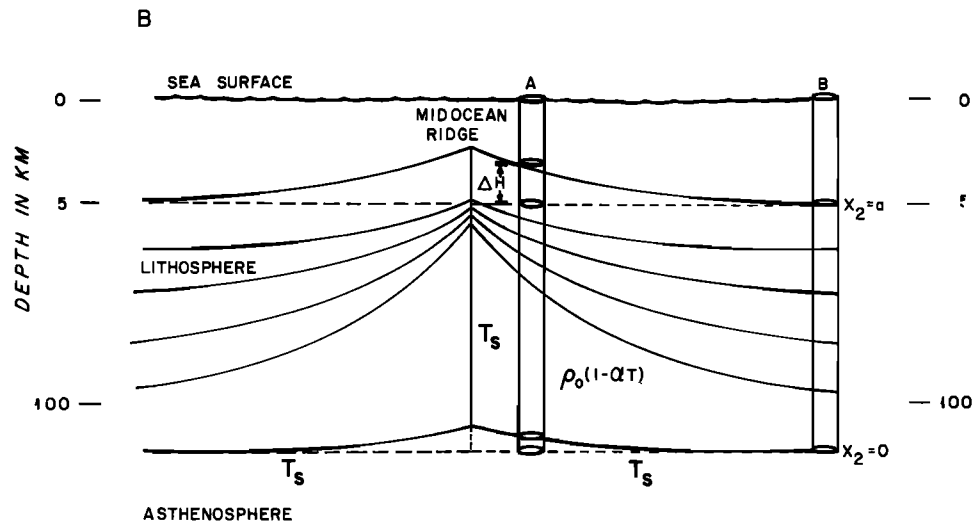

Fig. 3*b*. Plate model. The elevation ΔH is calculated by assuming that columns A and B of unit area must have equal masses above a common level $x_2 = 0$.

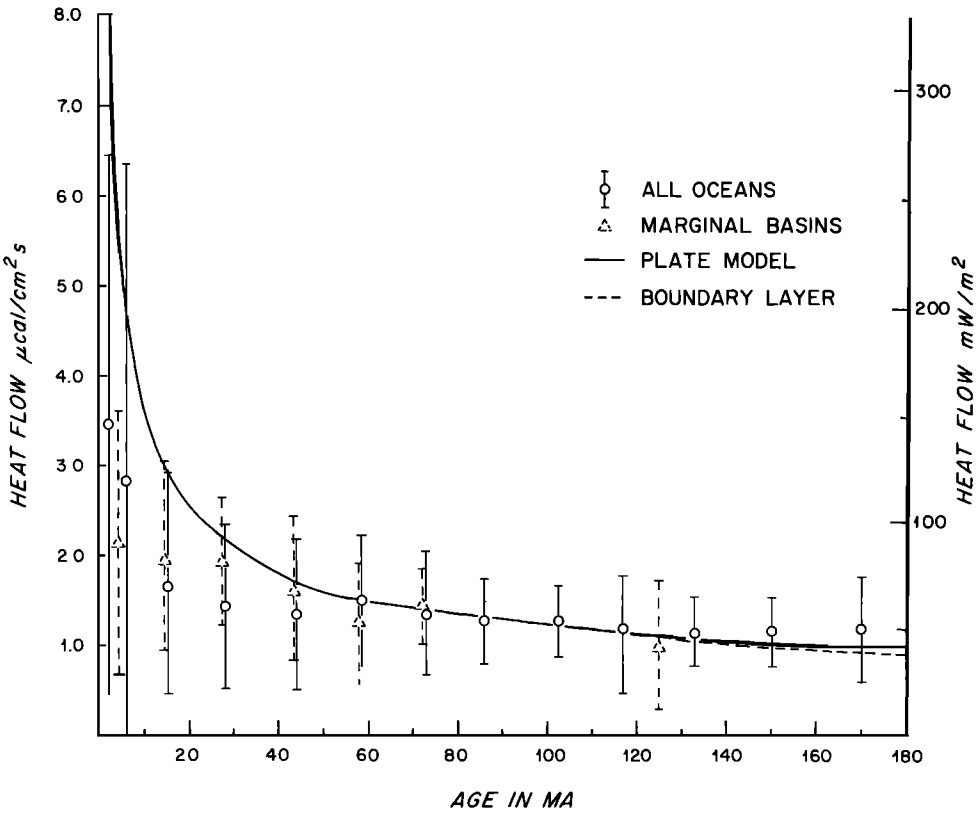

Fig. 4*a*. Mean heat flow and standard deviation for all the oceans and for the marginal basins as a function of age. Also shown are the expected heat flows from the plate and boundary layer models.

tribution of values is remarkably similar to that for normal ocean floor (Figure 4*a*).

Mantle Convection and Thermal Structure

A variety of geophysical observations, including mean heat flow, bathymetry, and velocity of surface waves, depend upon the age of the oceanic crust. *Forsyth* [1977] has reviewed these and shown that all reflect changes in the thermal structure at depth. He concluded that all the data were compatible with the model of a cooling plate 125 km thick in a periodotitic mantle. As an alternative to the plate model, *Parker and Oldenburg* [1973] suggested that the bottom boundary increased in depth with age. *Crough* [1975] and *Oldenburg* [1975] have shown that by including an input of heat from below, this model gives the exponential decrease in depth of the old ocean floor.

The thickening boundary layer model and constant temperature plate model approximate each other [*Parsons and*

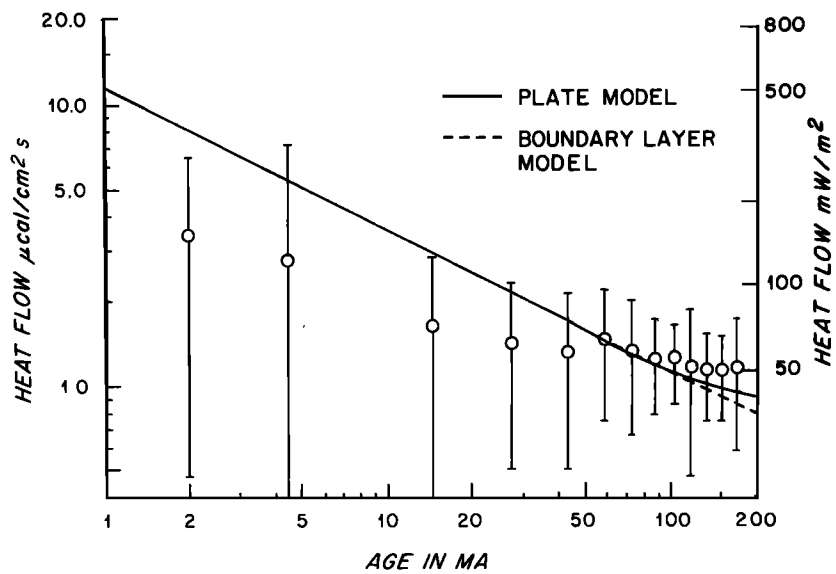

Fig. 4*b*. Log-log plot of the mean heat flow and standard deviation as a function of age for the oceans. Note that for crust younger than 50 Ma the mean values fall below the expected heat flow.

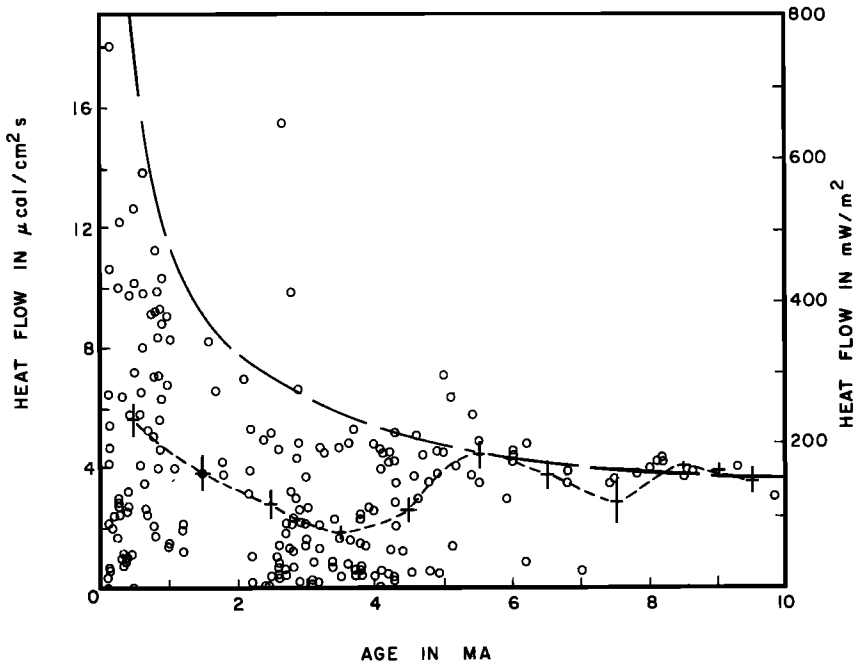

Fig. 5. Heat flow values plotted as a function of age on the Galapagos spreading center. Only those values which are on oceanic crust of well-defined age were used for this plot. Circles represent heat flow values. Pluses are 1-m.y. means. The long-dashed curve is the heat flow expected from the thermal model of *Parsons and Sclater* [1977], and the short-dashed curve connects the mean of the observed data [after *Anderson and Hobart*, 1976].

McKenzie, 1978]. They differ principally in their lower boundary condition. In essence, there are two ways of handling this condition: the first is to specify the heat flux at the base of the plate and allow the plate thickness to vary; the second is to keep the plate thickness constant and to specify the temperature at the base. Two mechanisms have been suggested to maintain the constant heat flux at the lower boundary: shear stress heating associated with plate motion [*Schubert et al.*, 1976] or the heat produced by a uniform distribution of radioactive elements in the upper 300 km of the mantle [*Forsyth*, 1977]. In contrast, various authors [*Richter*, 1973; *Richter and Parsons*, 1975; *McKenzie and Weiss*, 1975] have suggested that small-scale convection in the upper mantle can maintain the necessary vertical heat transport and the temperature near the base of the lithosphere is maintained at a constant value. The lithosphere consists of two parts, a rigid mechanical upper layer and a viscous thermal boundary layer (Figure 14). As it cools, both layers increase in thickness. At about 60 Ma the thermal boundary layer becomes unstable. Small-scale convection develops and creates a thermal structure closely analogous to that modeled by a flat plate [*Parsons and McKenzie*, 1978].

We favor the small-scale convection model for two reasons. First, as it is generally accepted that convection occurs in the mantle, there is no necessity for shear stress heating or large heat production rates. Second, the thermal stabilities of the constant heat flux models have not been investigated, and they are incomplete. The convection model can be approximated by a constant temperature at a fixed depth with all the convective transport of heat confined to the origin. This al-

TABLE 3. Mean and Standard Deviation of Heat Flow Data in Selected Well-Sedimented Areas of Known Age in the Pacific and North Atlantic

	Age Range, Ma	N	m	σ	$\bar{\sigma}$	σ%
1. Northwestern Pacific	120–140	30	1.13 (47)	0.14 (6)	0.03 (1)	12
2. East of Hawaii	90–100	8	1.57 (66)	0.15 (6)	0.05 (2)	9
3. North of Hawaii	80–90	18	1.36 (57)	0.24 (10)	0.06 (2)	17
4. Equatorial Pacific, 114°W	15–20	7	2.40 (100)	0.58 (24)	0.22 (9)	24
5. North of the Galapagos spreading center	5–10	6	4.21 (176)	0.51 (21)	0.21 (9)	13
6. South of the Costa Rica Rift	5–10	4	3.97 (166)	0.41 (17)	0.21 (9)	11
7. Combination of areas 5 and 6	5–10	10	4.12 (173)	0.46 (19)	0.15 (6)	12
8. South of Carnegie Ridge	10–20	9	2.85 (120)	0.52 (22)	0.17 (7)	18
9. Equatorial Pacific, 130°–150°W	35–75	6	0.92 (39)	0.48 (20)	0.20 (8)	52
10. Explorer Ridge, 49°N	3.5–7	24	5.72 (239)	2.30 (96)	0.47 (20)	40
11. Juan de Fuca Ridge, 47°N	3–4	4	6.40 (268)	2.90 (121)	1.40 (58)	45
12. Reykjames Ridge, anomaly 13	32–38	16	1.98 (83)	0.24 (10)	0.06 (2)	3

N is the number of values, m is the mean heat flux in μcal/cm^2 s (mW/m^2), σ is the standard deviation in μcal/cm^2 s (mW/m^2), $\bar{\sigma}$ is the standard error in μcal/cm^2 s (mW/m^2), and σ% the standard deviation as a percentage of the mean.

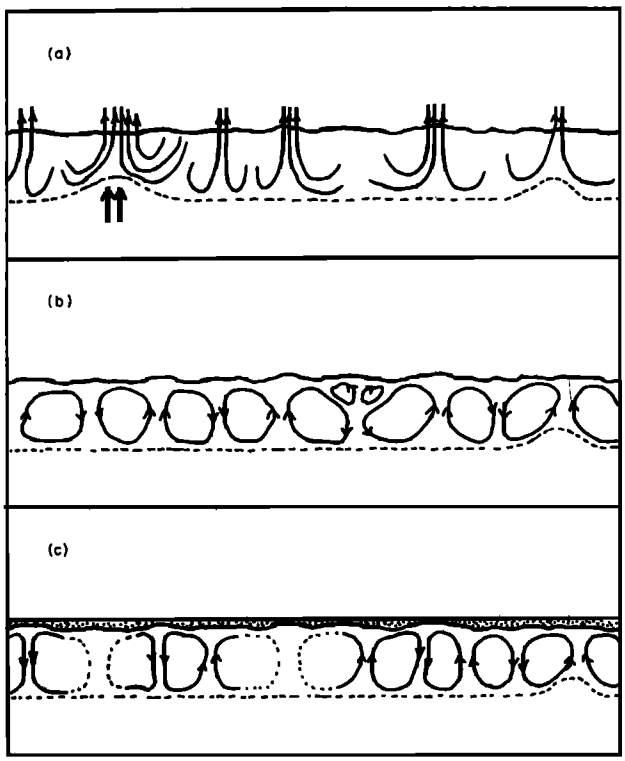

Fig. 6. (*a*) Pattern of convection to be expected near a ridge crest, where the permeable layer is open to the ocean. (*b*) Convective pattern forced by topography in an area of permeable crust bounded by a thin impermeable blanket of sediment. (*c*) The case of permeable crust with a rough boundary, buried by flat-lying sediments. The varying thermal resistance of the sediment blanket overpowers the direct effect of the topography [from *Lister*, 1972].

lows a straightforward comparison of the heat lost by plate creation with that lost by conduction through the plate. With the constant heat flux condition the plate boundary does not remain at a fixed depth, and the heat lost owing to advection from the mantle has to be calculated continuously along the bottom of the plate.

CONTINENTAL HEAT FLOW

Introduction

The interpretation of continental heat flow measurements is difficult for many reasons. The continental crust has an age span greater than 3800 Ma and has been modified continuously by geologic processes. The interpretation involves many variables whose effects, in particular radioactivity, are not properly understood. Any reasonable model must incorporate a number of independent factors, and it is necessary to examine the measurements according to their local context and to integrate them within a geologic framework. We use as a basis the theory of plate tectonics. Continents are modified through time by several processes, the most important being island arc vulcanism, arc-arc amalgamation [*Burke et al.*, 1976], continental collision [*Molnar and Tapponier*, 1976], continental stretching [*Artemjev and Artyushkov*, 1971], and finally erosion.

Most of the continents are Precambrian in age, and we have concentrated on this geologic period to investigate the relation between heat flow and age. A study of Phanerozoic continental crust would require the consideration of the specific tectonic history of each region and is beyond the scope of this paper. We study the relation between heat flow and age and estimate the contribution of the decay of radioactive elements within the crust. From this analysis we develop a coherent geologic model to account for the observations.

Geological Models for Continental Formation

Recent compilations of radiometric ages for exposed geologic formations have revealed that the continents consist primarily of Precambrian crust [*Hurley and Rand*, 1969]. More than two thirds of the crust falls within this age range when areas covered by more recent sedimentation are added [cf. *Goodwin*, 1976, Figure 2] On close inspection it appears that much of the Precambrian crust was created before 2.5 billion years ago in what is called the Archean. Detailed mapping of these terrains reveals that the petrology, geochemistry, and geological associations are remarkably similar to modern examples of island arc and microcontinental collisions [*Tarney et al.*, 1976; *Katz*, 1976]. These observations have led to the general acceptance that the Archean crust was produced by processes which are still active today. However, there are conflicting theories for the origin and evolution of the continental crust. Most of them lie between two extreme models. In the first, most of the present continental mass has differentiated during late permobile times (3000–2500 Ma). The continents do not grow much after the Archean but are modified by relatively continuous arc-arc amalgamation and continent-continent collision resulting from highly active plate motions [*Windley*, 1978]. The alternative concept is that the continents grow through time by irreversible chemical differentiation of the upper mantle and by accretion of newly differentiated material particularly at or near the margins. The accretionary processes are the same as those in the first model, i.e, arc-arc amalgamation and continent-continent collision. In an ex-

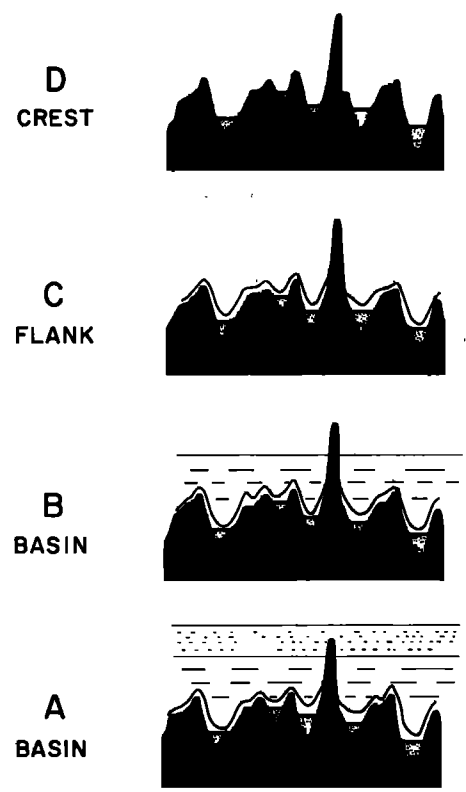

Fig. 7. Schematic diagram of the environmental grades A–D [from *Anderson et al.*, 1977].

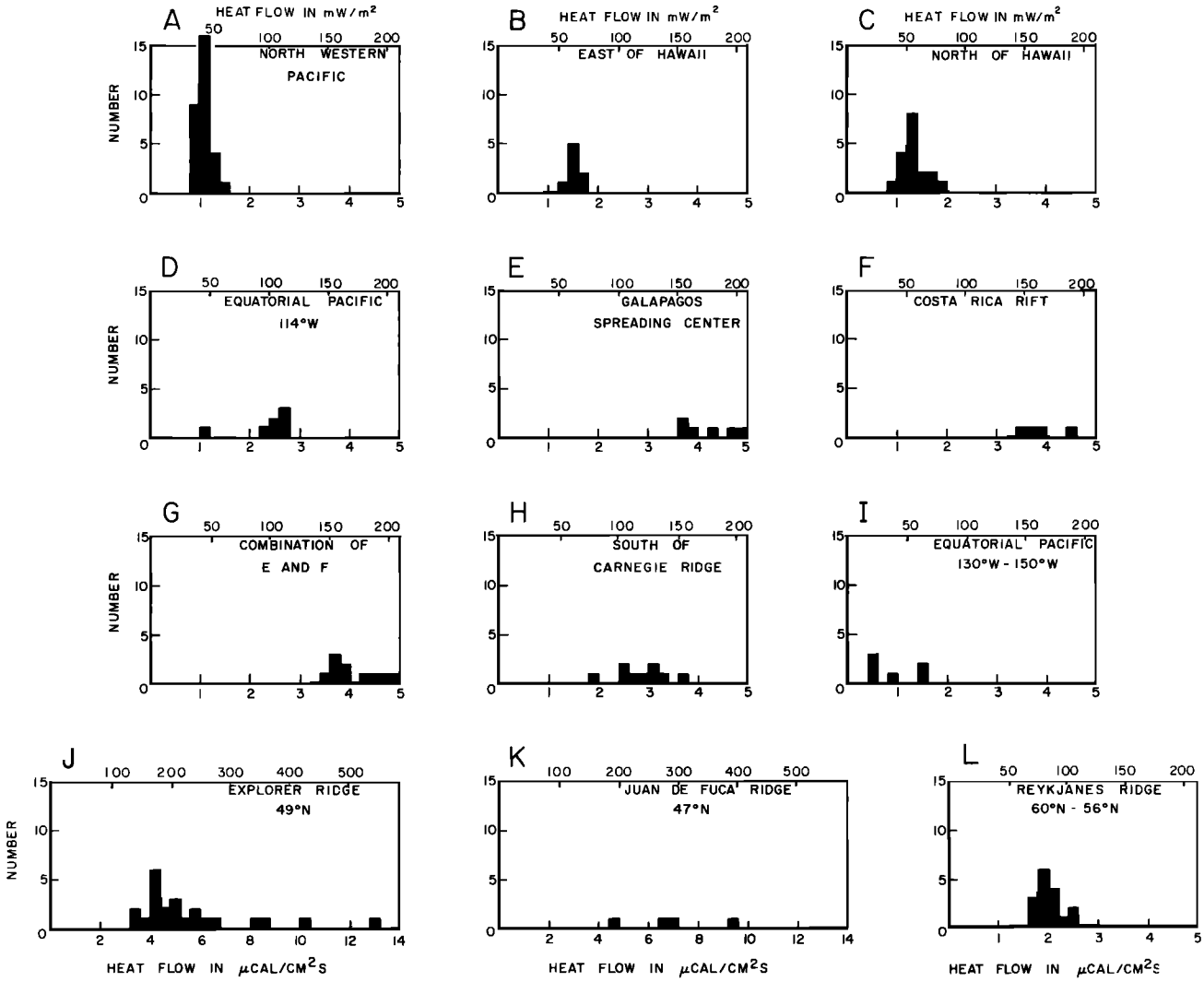

Fig. 8. Histograms of the 'reliable' heat flow values from areas in the North Pacific (Figures 8*a*–8*k*) and from one area in the North Atlantic (Figure 8*l*). The means and standard deviations are given in Table 3.

treme version the continents formed in small globular masses which grow in size through time from a central core [*Moorbath*, 1977]. Obviously, some combination of the two models can explain the observations, and in permobile times they were identical. At this time the loss of heat due to radioactive decay was greater than today [*Lambert*, 1976] and probably resulted in the existence of more plates and a greater area of young oceanic crust [*Bickle*, 1978]. However, irrespective of the model favored, it is to be expected that Precambrian crust will exhibit large differences in age. This is observed, and the radioactive ages extend from 3800 to 600 Ma.

For our purposes it is not important which model is preferred. Both the reworked or newly created continents are assigned the age of the last orogenic event, and both involve a vertical and horizontal gradation of the metamorphosed rocks as is observed today. One important consequence is that the lower continental crust is depleted in chemically combined water and radioactive trace elements such as uranium, thorium, and potassium.

Reworking or accretion of continental crust has probably occurred over short intervals of time (200 m.y.) at specific periods in the past [*Moorbath*, 1977; *Windley*, 1978]. There were two major pulses in the Archean, one at the beginning, 3800–3700 Ma, the other at the end, 2900–2700 Ma. In the Proterozoic pronounced pulses occurred between 1900 and 1700 Ma and around 1500 and 1000 Ma. A series of distinct orogenies have taken place almost continuously throughout the Phanerozoic.

TABLE 4. Mean and Standard Deviation of Grade A Environment Heat Flow Measurements in Various Age Provinces of the Indian Ocean

Age Range, Ma	*N*	*m*	σ
		Indian Ocean	
35–52	6	1.49 (62)	0.15 (6)
52–65	22	1.64 (69)	0.39 (16)
65–80	17	1.55 (65)	0.36 (15)
80–95	19	1.25 (52)	0.22 (9)
95–110	14	1.17 (49)	0.18 (8)
110–125	4	1.20 (50)	0.37 (15)
125–140	14	1.14 (48)	0.21 (9)
		Somali Basin	
	12	1.34 (56)	0.16 (7)

N is the number of values, *m* is the mean in μcal/cm² s (mW/m²), and σ is the standard deviation in μcal/cm² s (mW/m²).

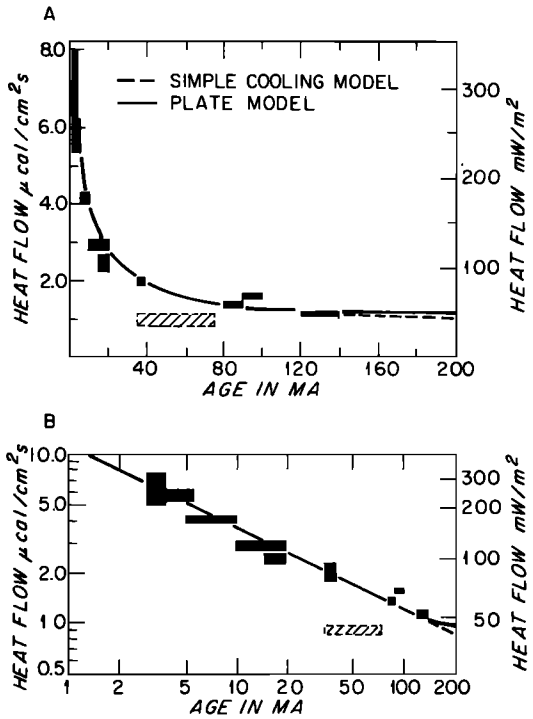

Fig. 9. (*a*) Mean heat flow as a function of age for the well-sedimented areas in the North Pacific and one area in the North Atlantic. Solid rectangles represent the errors in heat flow and age. The solid curve is the theoretical heat flow from the plate model, and the dashed curve that from the boundary layer model. The hatched area represents the value from the equatorial Pacific. (*b*) Log/log plot of heat flow as a function of age for the average values from the well-sedimented areas.

We decided to separate the continents into four age groups. The first comprises all continents with ages greater than 1700 Ma including the Archean, the Aphebian, and the orogenic pulse between 1900 and 1700 Ma. The second group extends from 1700 to 800 Ma and covers the entire Helikian and the first portion of the Hadrinian. The third group is from 800 Ma, the early Hadrinian, to the start of the Mesozoic at 250 Ma. Finally, the fourth group is the Mesozoic and Cenozoic. It encompasses the present episode of plate motion and creation of sea floor. All the relevant information documenting our estimates of the age of crust on individual continents can be found in Appendix B.

A detailed discussion of the philosophy fundamental to our approach in determining the age of the basement can be found in the work of *Hurley and Rand* [1969]. In essence, we have tried to assign the age of the last thermal event rather than the primary age. These two ages are sometimes quite different. As we separate the continents into only four age groups, the error introduced in the heat loss calculations is not large. However, these differences could present a problem to the interpretation of the relationship between heat flow and age, especially in the late Proterozoic and Phanerozoic. We return to this question at the end of our discussion of continental heat flow.

Continental Heat Flow Measurements

The variation of heat flow on continents is a function of a variety of geologic factors and a suite of environmental and measurement problems. The major geologic factors include orogenic history, the amount of radioelements in the crust, and erosion. The principal environmental problems are large-scale water circulation and past climatic changes. In addition, there are difficulties with early thermal conductivity determinations. Many were made on unsaturated samples and are too low [*Simmons and Nur,* 1968], and others consist of a few values supplemented by a relation between conductivity and rock type. Fortunately, in general the errors associated with these measurements are less than 20% and fall well within the range of variations associated with geologic and environmental causes.

In 1968, Polyak and Smirnov suggested that the average heat flow decreased with orogenic age. Later, *Sclater and Francheteau* [1970] and *Chapman and Pollack* [1975*a*] confirmed this rough relation. The heat flow is generally high and very scattered in young regions and decays to a value of around 1.0 μcal/cm^2 s (42 mW/m^2) in the early Proterozoic.

Estimating the contribution of the radioactive decay of U, Th, and K to the surface heat flow was a formidable problem until Birch, Roy, and their co-workers [*Birch et al.*, 1968; *Roy et al.*, 1968] established that the heat flow and the surface ra-

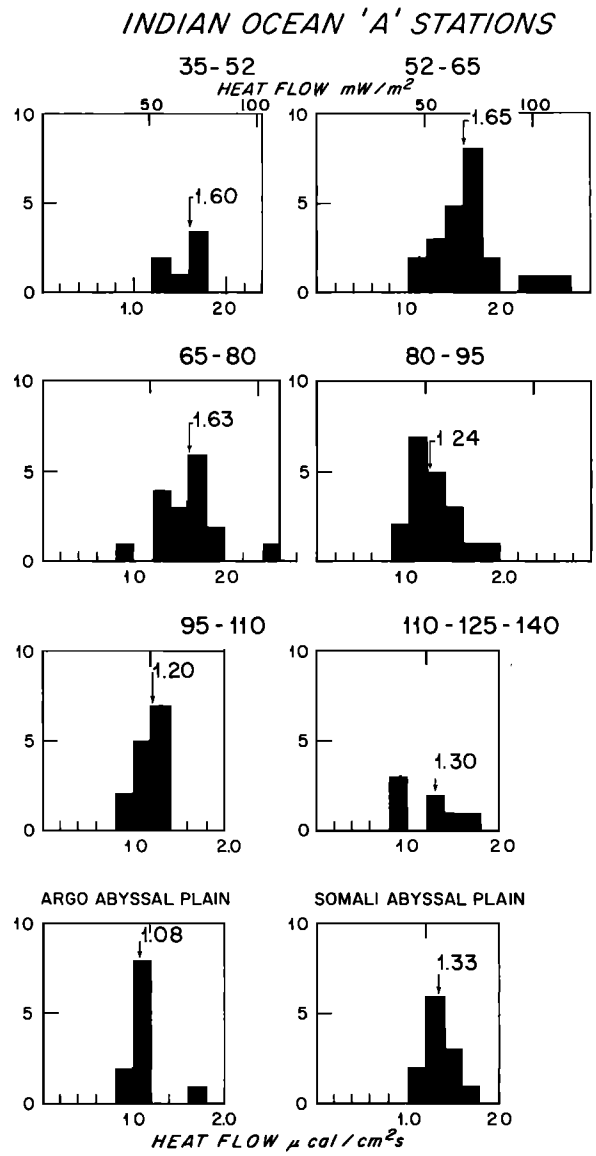

Fig. 10. Histograms of the reliable heat flow values from the Indian Ocean. The means and standard deviations are given in Table 4.

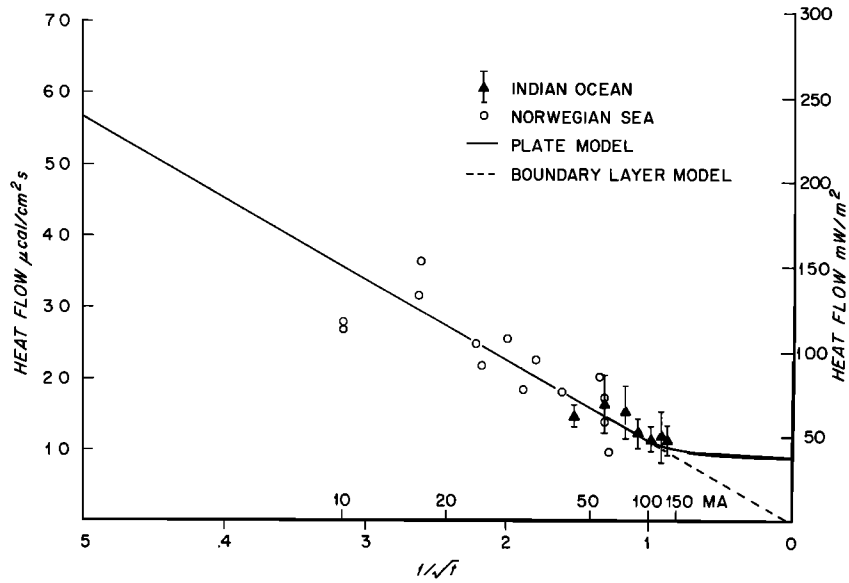

Fig. 11. Mean heat flow and standard deviation from the age provinces in the Indian Ocean plotted against $1/t^{1/2}$. Also presented are grade A environment stations from the Norwegian Sea. The expected heat flows from the plate and boundary layer models are shown.

diogenic heat production were linearly related within tectonically defined regions which they called heat flow provinces. *Lachenbruch* [1970] suggested that the upward migration of the radiogenic elements could account for this relation.

The validity of isolated heat flow measurements has been questioned by *Lewis and Beck* [1977] and *Lachenbruch and Sass* [1977]. These authors have demonstrated that the slow circulation of water affects many measurements in western North America. The climatic history also perturbs the heat flow at depth. *Horai* [1969], *Jessop* [1971], and *Beck* [1977] have suggested that in North America the last glaciation can reduce the near surface temperature gradient by as much as 20%. There is, however, a great deal of controversy about the matter [*Sass et al.*, 1971]. Both factors can lead to underestimates of the heat flow; their combined effects could amount to 30% of the actual value.

Heat Flow and Age

We superimposed the land data from *Jessop et al.* [1976] upon a world map with each continent separated into four provinces (Plate 2). We considered the continents individually and constructed a histogram of the values for each age interval (Figure 15).

We did not apply any selective criteria based on quality and

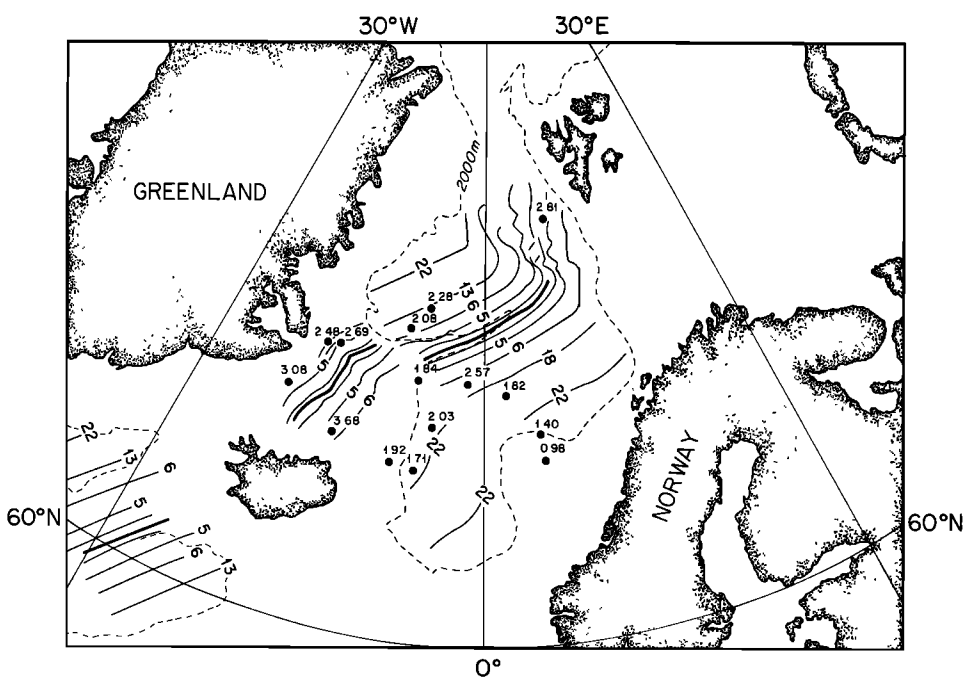

Fig. 12. Grade A environment stations on a polar projection chart of the magnetic lineations in the Norwegian Sea [after *Langseth and Zielinski*, 1976].

TABLE 5a. Age, Observed Heat Flow, and Area for the Arctic Ocean and Northwest Pacific Marginal Basins

Marginal Basin	Age,* Ma	N	m	σ	Area, 10^6 km^2	Basis of Age Estimate
Arctic Ocean	65–80	47	1.58 (66)	0.40 (17)	2.27	heat flow, this paper
Bering Sea	125–140	7	1.16 (49)	0.30 (13)	0.81	*Cooper et al.* [1976]
Kamchatka Basin	9–20				0.10	guess
Sea of Okhotsk	20–35	80	2.01 (84)	0.81 (34)	0.20	heat flow, this paper
Sea of Japan	20–35	191	2.20 (92)	0.56 (23)	0.44	heat flow, this paper
Ryukyu Trough	9–20	10	2.97 (124)	1.59 (67)	0.02	heat flow, this paper
Shikoku Basin	9–20	12	1.20 (50)	1.03 (43)	0.57	*Watts et al.* [1977]
Mariana Trough	0–4	11	1.22 (51)	1.02 (43)	0.36	*Karig* [1971]
Parece Vela Basin	20–35	29	1.42 (59)	1.01 (42)	1.40	*Fischer et al.* [1971]
West Philippine	35–52	28	1.45 (61)	0.77 (32)	1.81	*Louden* [1976]
Basin	52–65	18	1.18 (49)	0.92 (39)	1.00	*Louden* [1976]
South China Sea†	20–35	8	1.74 (73)	0.80 (33)	1.24	heat flow, *Watanabe et al.* [1977]
Carolina Basin	9–20	2	2.04 (85)	0.01	0.24	*Bracey* [1975]
	20–35	6	1.57 (66)	0.09 (4)	0.75	*Bracey* [1975]
	35–52‡	3	2.33 (98)	0.28 (12)	0.80	*Bracey* [1975]
Andaman Sea	0–9	5	2.45 (103)	1.67 (70)	0.15	*Lawver et al.* [1975*b*]
Sulu Sea	9–20	8	1.94 (81)	0.61 (26)	0.04	heat flow, this paper
Celebes Sea	20–35	8	1.64 (69)	0.49 (21)	0.23	heat flow, this paper

N is the number of values, m is the mean in μcal/cm^2 s (mW/m^2), and σ is the standard deviation in μcal/cm^2 s (mW/m^2).
*Assigned age province.
†New values [*Anderson et al.*, 1978] give a higher mean and less scatter and indicate an age closer to 25 Ma.
‡Parts south of the equator.

TABLE 5b. Age, Observed Heat Flow, and Area for the Mediterranean and Caribbean Marginal Basins

	Age,* Ma	N	m	σ	Area, 10^6 km^2	Basis of Age Estimate
			Mediterranean			
Tyrrhenian Sea	6–10	13	2.69 (113)	1.12 (53)	0.72	*Barberi et al.* [1978]
North Balearic Basin	20–35	13	1.75 (73)	0.68 (28)	0.31	*Hsu et al.* [1978]
South Balearic Basin	20–35	19	1.42 (59)	1.19 (50)	0.18	*Bayer et al.* [1973], *Hsu et al.* [1978]
Eastern Mediterranean	110–140	33	0.75 (31)	0.48 (28)	0.40	heat flow, this paper
Black Sea	old	51	1.04 (44)	0.87 (25)	0.41	heat flow, as above
Caspian Sea	old	20	1.95 (85)	1.24 (52)	0.42	heat flow, this paper
			Caribbean			
Cayman Trough	0–4	2	2.19 (92)	0.12 (53)		J. Morgan (personal communication, 1979)
	4–9	3	1.99 (83)	0.34 (14)		
	9–20				0.23	
	20–35	3	1.72 (72)	0.55 (23)		
	35–52	3	1.59 (67)	0.47 (20)		
Yucatan Basin	50–65	11	1.45 (61)	0.18 (8)	0.22	heat flow, this paper
Columbia Basin	65–80	37	1.36 (57)	0.50 (21)	0.64	heat flow, this paper
Venezuela Basin	65–80	27	1.30 (54)	0.20 (8)	0.50	heat flow, this paper
Gulf of Mexico	110–140	50	1.13 (47)	0.63 (26)	0.64	heat flow, this paper
Grenada Trough	20–35	7	1.66 (70)	0.35 (15)	0.13	guess
Tobago Trough	20–35	3	1.10 (46)	0.84 (35)		same as Grenada Trough
Scotia Sea	0–35				1.54	*Barker and Burrell* [1977]
Total					5.69	

N is the number of values, m is the mean in μcal/cm^2 s (mW/m^2), and σ is the standard deviation in μcal/cm^2 s (mW/m^2).
*Assigned age province.

TABLE 5c. Age, Observed Heat Flow, and Area for the Southwest Pacific Marginal Basins

	Age,* Ma	N	m	σ	Area, 10^6 km^2	Basis of Age Estimate
Solomon Sea	9–20	2	1.73 (72)	0.17 (7)	0.06	*Luyendyk et al.* [1975]
Woodlark Basin	0–20	12	1.97 (82)	1.01 (42)	0.46	*Luyendyk et al.* [1974]
West Coral Sea	35–52	14	1.53 (64)	0.35 (15)	0.42	*Burns et al.* [1973]
New Hebrides Basin	20–35	13	1.48 (62)	0.50 (21)	0.87	*Burns et al.* [1973]
Fiji Plateau	0–9	45	2.53 (106)	1.60 (67)	1.42	*Chase* [1971]
Lau-Kermadec Trough	0–4	31	1.70 (71)	1.51 (63)	0.60	*Weissel* [1977]
South Fiji Plateau	20–35	22	1.13 (47)	0.78 (33)	1.26	*Weissel et al.* [1977]
Tasman Sea	53–65	3	1.26 (53)	0.15 (6)	0.83	*Weissel and Hayes* [1977]
	65–80	7	1.21 (51)	0.69 (29)	1.46	*Weissel and Hayes* [1977]
Banda Sea	35–52				0.56	guess
Total for southwest Pacific					7.94	
Total for all west Pacific					20.37	
Total for all marginal basins					26.06	

N is the number of values, m is the mean in μcal/cm^2 s (mW/m^2), and σ is the standard deviation in μcal/cm^2 s (mW/m^2).
*Assigned age province.

TABLE 6. Marginal Basins 'Reliable' Heat Flow Estimates

Marginal Basin	N	m	σ	Reference	Age, Ma	Reference
Tyrrhenian Sea*	8	3.27‡ (137)	0.37‡ (15)	*Erickson et al.* [1977]	6–10	*Barberi et al.* [1978]
Balearic Basin†	6	2.17§ (91)	0.25§ (10)	*Erickson et al.* [1977] *Hsu et al.* [1978]	18–32	*Hsu et al.* [1978] *Bayer et al.* [1973]
Parece Vela Basin	6	2.15 (90)	0.16 (7)	*Sclater et al.* [1976*b*]	18–32	*Fischer et al.* [1971]
West Philippine Basin	6	1.72 (72)	0.16 (7)	*Sclater et al.* [1976*b*]	38–50	*Louden* [1976] *Karig et al.* [1974]
West Coral Sea	11	1.64 (69)	0.32 (13)	this paper	45–55	*Burns et al.* [1973]
Bering Sea	7	1.16 (49)	0.30 (13)	this paper	110–125	*Cooper et al.* [1976]

N is the number of values, m is the mean in μcal/cm^2 s (mW/m^2), and σ is the standard deviation in μcal/cm^2 s (mW/m^2).
*All values thought to be close to basement outcrops have been neglected.
†The two values on the Rhone Fan have been neglected.
‡Heat flow is 3.43 ± 0.37 μcal/cm^2 s (144 ± 15 mW/m^2) when it is increased by 5% to account for recent sedimentation [*Erickson et al.*, 1977].
§Heat flow is 2.66 ± 0.30 μcal/cm^2 s (111 ± 13 mW/m^2) when it is increased by 22% to account for recent sedimentation [*Erikson et al.*, 1977].

treated all the data. The heat flow stations are not randomly distributed on the continents, and many of them are located in closely spaced groups. In order to reduce the bias which this introduces we averaged all values which differed by less than 10% and lay within a radius of 30 km. These figures cover most closely grouped values and were chosen intuitively. For groups with a large deviation all values were considered. For Lake Superior and Europe we examined histograms of individual clusters to check that the data were not biased by this approach.

We computed the mean, standard deviation, median, and mean deviation about the median for each province (Table 7). The use of the median and the mean deviation about the median reduces the bias created by erroneous and anomalous values. There is no reason to believe that the values are normally distributed, and the standard deviation and mean deviation about the median give only estimates of the scatter.

Certain simple conclusions can be drawn from this analysis. The Eurasian and North American values have almost identical distributions. In the youngest province the mean heat flow is high (about 2.0 μcal/cm^2 s, or ~80 mW/m^2) and is associated with a large scatter. For all continents in provinces older than 800 Ma the heat flow tends to a constant value lying in the range 1.0–1.2 μcal/cm^2 s (42–50 mW/m^2). Both the mean and the scatter decrease with age (Figure 16). This behavior is evidence that the heat flow is approaching an equilibrium value in provinces older than 800 Ma. We explain the remaining scatter later in this section.

The equilibrium value is higher than previous estimates (Table 7). This increase probably results from a better treatment of the environmental and instrumental factors in the newer values. For example, *Lewis and Beck* [1977] have shown that the variation of heat flow values in a Precambrian greenstone belt in Ontario can only be explained by slow circulation of water at depth and rejected the lower values measured.

An important feature of the histograms is the distribution of heat flow values below 0.6 μcal/cm^2 s (25 mW/m^2). In the older two provinces outside of Africa there are almost no values below 0.6 μcal/cm^2 s (25 mW/m^2). This cutoff is also observed for the younger provinces but is not so obvious owing to the flatness of the distribution.

Heat Flow and Surface Heat Production

The distribution of the main radioactive heat-producing elements, U, Th and K, has received much attention and several of its features are now well documented. The radiogenic heat production is a scalar quantity which is highly variable on the surface of a continent, on both small and large scales. Continuous belts enriched in uranium and thorium have been

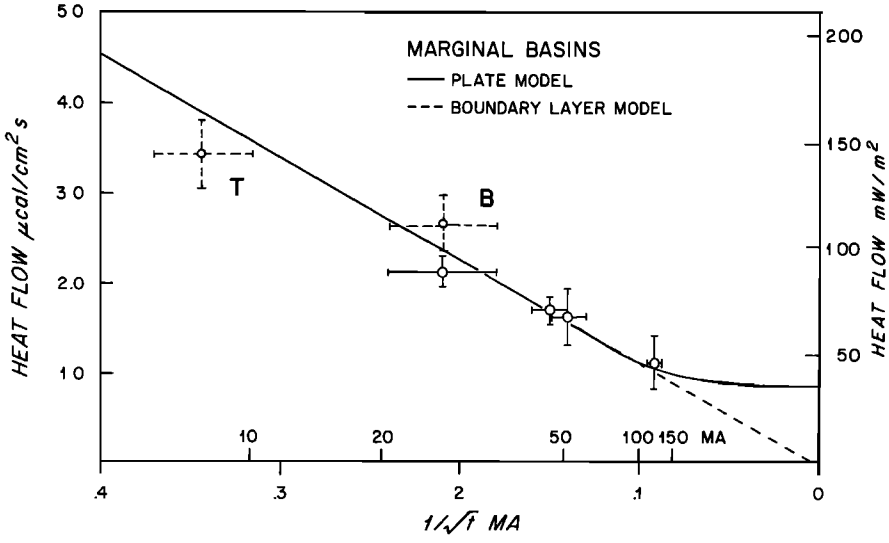

Fig. 13. Mean heat flux and standard deviation from the marginal basins plotted against $1/t^{1/2}$. The expected heat flows from the plate and boundary layer models are also shown. T and B, the dashed bars, represent the values from the Tyrrhenian Sea and Balearic Basin, respectively.

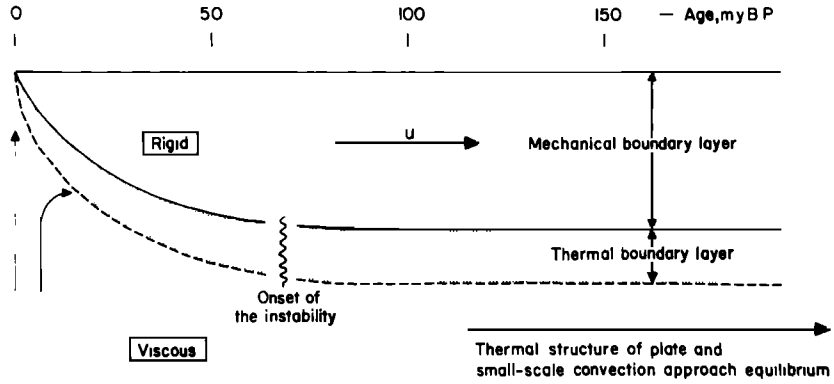

Fig. 14. Schematic diagram showing the division of the plate into rigid and viscous regions and the occurrence of an instability in the bottom viscous part [after *Parsons and McKenzie,* 1978].

reported in Norway [*Killeen and Heier*, 1975], in Australia [*Heier and Rhodes*, 1966], in the United States [*Phair and Gottfried*, 1964], and in the Superior Province in Canada (P. G. Killeen, personal communication, 1978). A general trend of decrease with depth has been shown in a series of plutons in Idaho [*Swanberg*, 1972], in a vertical section of the eastern Alps [*Hawkesworth*, 1974], and in several deep boreholes [*Lachenbruch and Bunker*, 1971; *Lubimova et al.*, 1973].

The radiogenic heat production can be correlated with magmatic differentiation, according to a relationship which is not unique and differs for different magma series [*Tilling et al.*, 1970]. It can also be correlated with a metamorphic index. High-grade metamorphic rocks are significantly lower in Th and U than their counterparts in lower metamorphic grades [*Lambert and Heier*, 1967; *Heier and Adams*, 1965; *Rybach*, 1976]. Typical lower crustal rocks have low heat production rates, ranging from 0.2 to 1.5 × 10^{-13} cal/cm^3 s (0.08 to 0.62 × 10^{-6} W/m^3). In summary, all available data can be accounted for by an upward concentration of the heat-producing elements in the crust combined with lateral concentration differences.

Detailed seismic studies, using reflection and refraction, have revealed that the crust has a complicated structure, heterogeneous to the depth of the Moho. The crustal thickness is highly variable, both on a small scale, for a given tectonic unit, and on a large scale, from one unit to another [*Mueller*, 1978; *Berry*, 1973; *Sollogub et al.*, 1973]. Also, *Padovani and Carter* [1977] have shown from petrological studies that the continental crust varies horizontally. This complexity extends throughout the whole crust, as deep seismic soundings [*Smithson*, 1978] have revealed variations at depth comparable to those observed from geological observations at the surface. As a consequence the picture of a layered crust must be either abandoned or, at best, accepted only as a crude average. This complexity prevents the direct estimation of either the amount or the distribution of the radiogenic elements in the crust.

TABLE 7. Heat Flow Statistics for the Continental Age Provinces

Age Province, Ma	N	m	σ	Median	Mean Deviation About Median
		Africa and Madagascar			
250–800	19	1.15 (48)	0.82 (34)	0.93 (39)	0.64 (27)
800–1700	6	1.36 (57)	0.11 (5)	1.34 (56)	0.10 (4)
>1700	39	1.14 (48)	0.52 (22)	1.10 (46)	0.31 (13)
		South America			
0–250	19	1.31 (55)	0.22 (9)	1.22 (51)	0.19 (8)
		North America			
0–250	164	1.97 (82)	1.07 (45)	1.84 (77)	0.64 (27)
250–800	44	1.53 (64)	0.79 (33)	1.40 (59)	0.59 (25)
800–1700	50	1.26 (53)	0.33 (14)	1.20 (50)	0.24 (12)
>1700	216	1.11 (46)	0.38 (16)	1.05 (44)	0.26 (11)
		Australasia			
0–250	18	1.09 (46)	0.76 (32)	0.91 (38)	0.51 (21)
250–800	17	1.81 (76)	0.78 (33)	1.50 (63)	0.62 (26)
800–1700	10	1.76 (74)	0.27 (11)	1.79 (75)	0.17 (7)
>1700	14	1.14 (48)	0.44 (18)	0.97 (41)	0.29 (12)
		Europe and Asia			
0–250	197	1.81 (76)	1.24 (52)	1.53 (64)	0.70 (29)
250–800	420	1.50 (63)	0.44 (18)	1.48 (62)	0.32 (13)
800–1700	72	1.07 (45)	0.15 (7)	1.10 (46)	0.12 (5)
>1700	106	1.05 (44)	0.31 (13)	1.00 (42)	0.21 (9)
		All Continents			
0–250	398	1.82 (76)	1.26 (53)	1.67 (70)	0.76 (32)
250–800	500	1.50 (63)	0.51 (21)	1.46 (61)	0.34 (14)
800–1700	138	1.20 (50)	0.24 (10)	1.17 (49)	0.22 (9)
>1700	375	1.10 (46)	0.38 (16)	1.05 (44)	0.29 (12)

N is the number of values, m is the mean in μcal/cm^2 s (mW/m^2), and σ is the standard deviation in μcal/cm^2 s (mW/m^2).

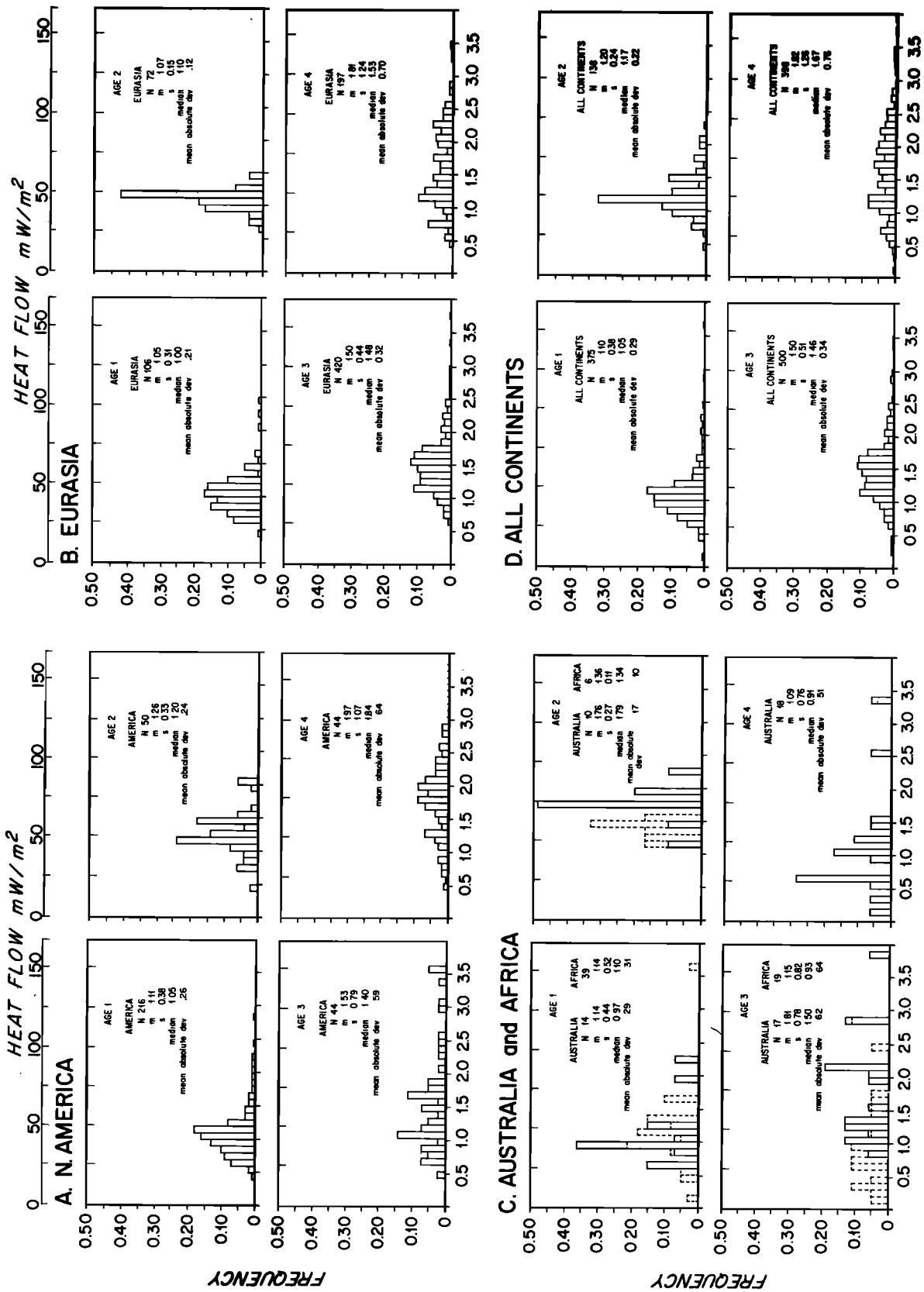

Fig. 15. Histograms of the heat flow values for (*a*) North America, (*b*) Eurasia, (*c*) Africa (dashed lines) and Australia, and (*d*) all continents for the four age provinces.

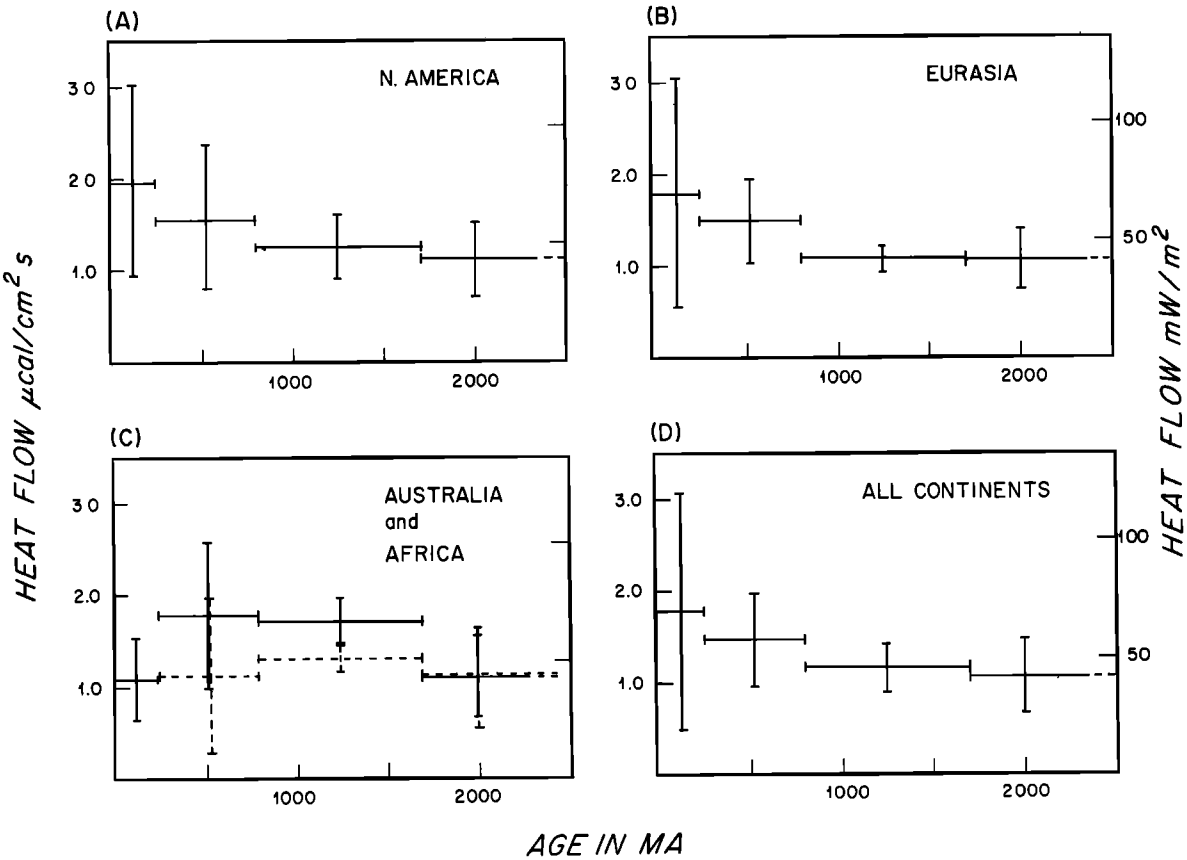

Fig. 16. Heat flow as a function of age for (*a*) North America, (*b*) Eurasia, (*c*) Australia and Africa (dashed lines), and (*d*) all continents.

However, within certain specific areas there is a simple linear relationship between heat flow and surface radioactivity:

$$Q_0 = Q_r + D \cdot A_0 \quad (1)$$

where Q_0 and A_0 are the surface heat flow and radioactive heat production. Q_r, the 'reduced' heat flow, and D are constants [*Birch et al.*, 1968; *Roy et al.*, 1968]. The relationship holds for large areas where the heat production rates and radiometric ages vary considerably. The interpretation of the relation is ambiguous and impossible without a certain number of assumptions. In particular, there is considerable discussion as to the physical meaning of both Q_r and D.

The simplest interpretation is that D represents the thickness of a slab of uniform radioactivity and that Q_r is the heat flux through the base [*Roy et al.*, 1968]. Another interpretation is that D is the inverse of the decrement for an exponentially decreasing rate of radiogenic heat production [*Lachenbruch*, 1970]. In this case,

$$A(z) = A_0 e^{-z/D} \quad (2)$$

where A_0 is the heat production at the surface. Such an interpretation has some justification on geochemical grounds and has limited support from observations. *Lachenbruch* [1970] demonstrated that with this distribution the linear relation is preserved if differential erosion occurs within the heat flow province considered. In this model, D characterizes the degree of upward migration of the radiogenic elements, and Q_r is approximately the heat flow at the base of the crust.

Equation (1) has been used to define heat flow provinces in many parts of the world [*Rao and Jessop*, 1975; *Swanberg et al.*, 1974; *Rao et al.*, 1976; *Chapman and Pollack*, 1975; *Kutas*, 1977] and those that we consider to be reliable are listed in Table 8. The general features of these provinces are for a majority of values to lie on a line defined by Q_r and D and a certain number of values to be offset from the line. These offset values sometimes define a 'heat flow subprovince' where there is a similar relationship, with the same Q_r and a different D [*Blackwell*, 1971]. When the number of data points is small, the uncertainty in the determination of the parameters Q_r and D is great, and it is necessary to select the most reliable ones before attempting any interpretation. We used a criterion based on the number of data points which actually define the linear relationship and the range of heat production rates represented. In particular, we considered a value of Q_r to be meaningful only when low values of crustal heat production were reported.

Recently, *Lachenbruch and Sass* [1977], for the United States, and *Rao and Jessop* [1975], for all stations in the Precambrian, have examined this relationship in more detail. In the United States, for stations west of the Great Plains, i.e., the younger sections of the country, *Lachenbruch and Sass* [1977] find a large scatter in the values and little obvious correlation between heat flow and surface radioactivity (Figure 17). However, within individual orogenic belts and in particular for the Sierra Nevada there is still evidence for a correlation. For older portions of the North American continent the relationship is well established. Elsewhere in the world, *Rao and Jessop* [1975] have found that the relation between heat flow and surface heat production has an overall significance. For example, they have shown that there is a general correla-

TABLE 8. Age and Parameters Defining the Linear Relation Between Heat Flow and Age for Several Continental Heat Flow Provinces

Province	Age, m.y.	N	Q	Q_r	D, km	Reference
Basin and Range (North America)	65–0	86	2.20 (92)	1.41 (59)*	9.4*	*Sass and Lachenbruch* [1978]
Sierra Nevada (North America)	125–0	9	0.93 (39)	0.40 (17)	10.1	*Sass and Lachenbruch* [1978]
Eastern Australia (Australia)	65–0	9	1.72 (72)	1.37 (58)*	(11.1)*	*Sass and Lachenbruch* [1978]
Eastern United States (North America)	400–100	14	1.36 (57)	0.79 (33)	7.5	*Sass and Lachenbruch* [1978]
United Kingdom (Eurasia)	600–300	10	1.40 (59)	0.56 (24)	16.0	*Richardson and Oxburgh* [1978]
Central Shield (Australia)	2000–600	9	1.98 (83)	0.64 (27)*	11.1*	*Sass and Lachenbruch* [1978]
Ukranian Shield (Eurasia)	2500–1900	12	0.87 (37)	0.60 (25)	7.1	*Kutas* [1977]
Western Australia (Australia)	2000	7	0.93 (39)	0.63 (26)	4.5	*Sass and Lachenbruch* [1978]
Canadian Shield (North America)	3000–2000	11	0.93 (39)	0.50 (21) 0.67†	14.4 13.6†	*Jessop and Lewis* [1978]
Baltic Shield (Norway)	3000–2000	5	0.86 (37)	0.53 (22)	8.5*	*Swanberg et al.* [1974]

N is the number of values, Q is the mean heat flow in μcal/cm² s (mW/m²), Q_r is the reduced heat flow in μcal/cm² s (mW/m²), and D is the characteristic depth.

*Unreliable estimate.

†Q_0 and D values allowing for Pleistocene glaciation.

tion between the heat flow and the surface heat production in the Precambrian (Figure 18). The large number of stations where the radioactivity is low constrains the reduced heat flow to lie between 0.5 and 0.7 μcal/cm² s (21 and 29 mW/m²). Work done since 1975 confirms these values (see Table 8). *Rao and Jessop* [1975] have also examined the heat flow through Precambrian greenstone belts and find a range of values from 0.69 to 1.18 μcal/cm² s (29 to 49 mW/m²) with a mean of 0.90 μcal/cm² s (38 mW/m²) (Table 9). These values lie between the intercept heat flow and the mean value for the early Proterozoic and Archean (Table 7). Where the values of radioactivity are consistently low in Precambrian regions, for example, the Superior Province of Canada [*Jessop and Lewis*, 1978], the heat flow has little scatter, and the mean value is close to 1.0 μcal/cm² s (42 mW/m²). Where the values are high, such as the Central Australia Shield, the heat flow is variable, and the mean higher than elsewhere. However, the reduced heat flow is very similar to that through other areas of the Precambrian. Clearly, there is no obvious relation between age and either heat flow or surface radioactivity in the early Proterozoic and Achean. These observations are evidence that steady state conditions are reached and that the scatter in the heat flow is almost solely due to differences in the concentration of heat-producing elements.

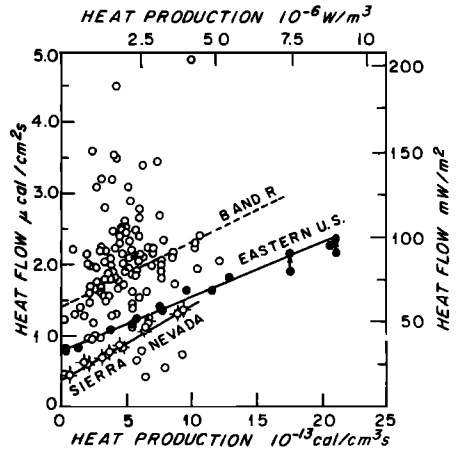

Fig. 17. Observations of heat flow and radioactive heat production from crystalline rocks in the United States; linear regression curves are from *Roy et al.* [1968] for the Basin and Range (dashed curve), eastern United States, and Sierra Nevada provinces. Solid circles represent points east of the Great Plains, and crossed circles represent points interior to the Sierra Nevada physiographic province. Vertical arrows represent corrections for the finite size of plutons [*Roy et al.*, 1968]. Three of the open circles on the eastern United States curve at about 1 μcal/cm² s are from the Klamath Mountains in northern California [from *Lachenbruch and Sass*, 1977].

As we have shown above, the values of the reduced heat flow Q_r obtained in all the old continental provinces are in striking agreement (Table 8). In most of these provinces the heat flow which is actually measured at the surface is close to Q_r for low values of the rate of heat production. Thus Q_r must have a general geophysical significance for old continental crust. On the other hand, the complexity of both the crustal structure and the behavior of U, Th, and K in geologic environments prevents any simple interpretation of the relationship between heat flow and radioactivity. In particular, neither D nor Q_r is known with certainty. D varies significantly from place to place and has little obvious correlation with any physical phenomena. Also, *Richardson and Oxburgh* [1978] and C. Jaupart and G. Simmons (unpublished data, 1978) have shown that metasedimentary and metamorphic terrains surrounding the granitic plutons exhibit the same relation between heat flow and surface radioactivity as the plutons. The reason for this similarity is unknown, but it does imply that the relation cannot be attributed to crustal fractionation alone. At best, the empirical relation is an indication that heat-producing element fractionation in granites and metamorphic and recrystallized clastics are on related scales [*Richardson and Oxburgh*, 1978]. At worst, as it has as yet no sound physical explanation, it could be entirely fortuitous. However, it is still the single quantitative piece of information which gives any indication of the variation of radioactivity with depth. The relationship can only be valid if the radioactive elements are concentrated near the surface. At present, Q_r is the best estimate that we have of the nonradiogenic component of heat flow, and to a first approximation it is the heat flow at the base of the crust.

The distribution of crustal radioactivity distorts the relation between heat flow and tectonic age. For example, the heat flow through the Precambrian rocks in Central Australia and India [*Rao et al.*, 1976] is much higher than is predicted from the gross relation between heat flow and age. However, the reduced heat flow is consistent with that from other shields. In contrast with decrease of surface heat flow versus age (Figure 16) the reduced heat flow drops within 300 Ma to a constant value of 0.6 ± 0.2 μcal/cm² s (25 ± 8 mW/m²) (Figure 19). The sharp decrease occurs over a time span slightly longer than that for the oceans, and the equilibrium value of 0.6 ±

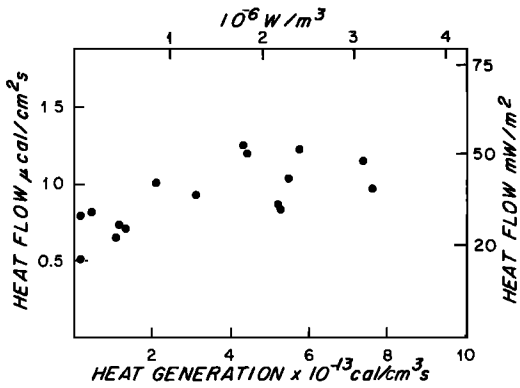

Fig. 18. Heat flow and heat generation for stations in the Precambrian shields [after *Rao and Jessop*, 1975].

0.2 μcal/cm² s (25 ± 8 mW/m²) is close to the predicted equilibrium heat flux of 0.8 ± 0.1 μcal/cm² s (33 ± 4 mW/m²) through the oceans. The two values could be even closer. Most of the continental values are from high northern latitudes and may have to be raised by as much as 0.2 μcal/cm² s (8 mW/m²) to allow for the effect of the last glaciation.

Thermal Models

The above observations can be integrated within the framework of the new ideas on continental formation. Continents are deformed or modified either continuously or discontinuously since permobile times. Greenstone belts are essentially collapsed marginal basins [*Tarney et al.*, 1976], and the granite-gneiss terrain on either side of these belts is deformed calcalkaline tonalitic batholithic rocks [*Tarney and Windley*, 1977; *Windley and Smith*, 1976]. Extra vulcanism is created by continent-continent collision and the formation of major granite plutons. Fractional separation of the radioactive elements takes place, and they are preferentially distributed near the surface.

The high heat flow in the younger regions has four causes: island arc magmatism, plutonism associated with continent-continent collision, erosion [*England and Richardson*, 1977], and crustal thinning [*McKenzie*, 1978; *Lachenbruch*, 1979]. The heat flow in these regions is not uniformly high, and low values can be observed. The classic example (recognized by *Holmes* [1965, Figure 730]) is Japan [*Uyeda*, 1972]. In this area the heat flow changes from less than 1.0 μcal/cm² s (42 mW/m²) along the eastern coast to values as high as 10.8 μcal/cm² s (452 mW/m²) close to the western coast (Figure 20).

TABLE 9. Categorization of Data According to General Rock Type of the Heat Flow Sites [after *Rao and Jessop*, 1975]

Rock Type	*N*	Range	Mean
Ultramafic and anorthosites	5	0.50–0.81	0.74
		(21–34)	(31)
Greenstones	11	0.69–1.18	0.90
		(29–49)	(38)
Mafic igneous (plutonic and volcanic)	11	0.65–1.10	0.90
		(27–46)	(38)
Granites and gneisses	16	0.59–1.44	1.03
		(25–60)	(43)
Sediments	10	1.05–1.20	1.12
		(44–50)	(47)

N is the number of values. The range and mean are in μcal/cm² s (mW/m²).

In general, intrusion and erosional processes are dominant, and the heat flow, though scattered, has a high mean value. With time, tectonic activity terminates, magmatic sources cool, and the rate of erosion decreases. Thus the heat flow tends to equilibrium. In areas where the heat flow is initially low, there is an increased heat input from below, and low values are no longer observed. Sometime between 250 and 800 Ma these perturbations become negligible (Figure 16). To obtain a better estimate of this time scale, it is necessary to concentrate on the Phanerozoic and to take into account variations in surface heat production. From our preliminary plot of reduced heat flow versus age we suggest that the time constant is of the order of 200–300 m.y. (Figure 19). At present it is not possible to give a more precise figure because of the large scatter in the data. Assuming a thermal diffusivity of 0.01 cm²/s, the associated thermal diffusion length scale lies betwen 100 and 200 km.

In the early Proterozoic and Archean crust there is still some scatter in the heat flow. This is probably due to variations in the surface radioactivity. These variations can have two causes. On a large scale (100 km or more) they can be directly associated with horizontal changes in the geologic environment. On a small scale (within an individual pluton) they can be created by weathering [*Lachenbruch*, 1970] and hydrothermal mobilization of the radioactive elements [*Killeen and Heier*, 1975].

One of the areas which does not apparently fit this simple model is the Sierra Nevada. The Sierra Nevada are in western North America. Presumably they were on the continental side of a trench in the Late Cretaceous and early Tertiary. The heat flow distribution in this area (Figure 21) is little different from that observed in Japan (Figure 20). Hence *Roy et al.* [1972] suggested that the low reduced heat flow is the result of a subduction process which terminated in the middle Tertiary.

As most of the continents consist of Precambrian basement, we have concentrated on this portion of the geologic time scale. In order to handle the large quantity of data we have followed a simplistic approach to analyzing the relation between heat flow and radioactive age. It is important to remember the problems associated with this approach. In particular, our age estimates are reliable only for the Archean and some of the early Proterozoic. We run into problems in areas such

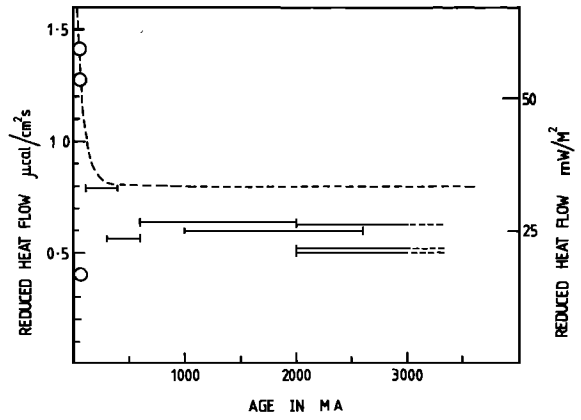

Fig. 19. Reduced heat flow plotted against age. The circles are unreliable estimates from the younger heat flow provinces. The theoretical heat flow (assuming the plate model) through the ocean floor with the crustal contribution subtracted is presented as a dashed curve.

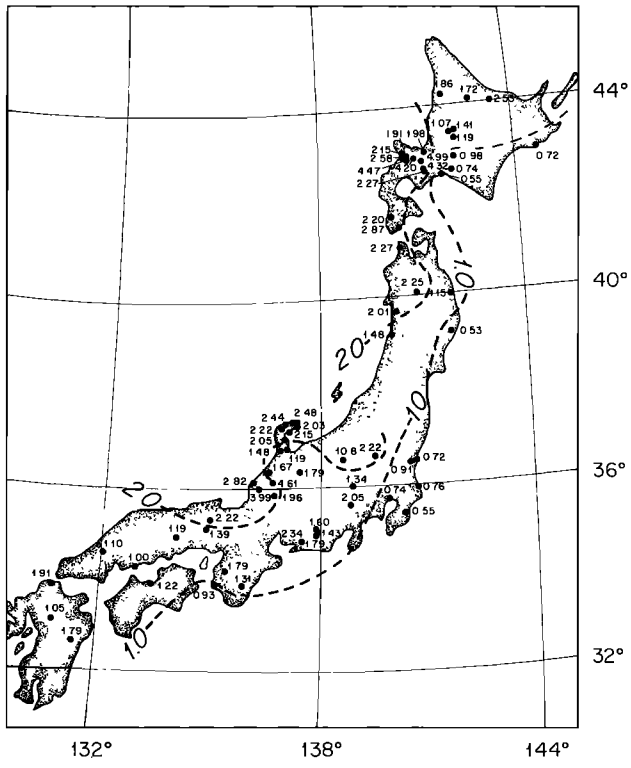

Fig. 20. Heat flow values on the Japanese islands. The dashed lines are the 1.0 and 2.0 μcal/cm² s heat flow contours. Note the band of low heat flow along the east coast of Japan.

as the West Siberian Platform and the sedimentary basins of western Europe where Proterozoic basement is covered by Phanerozoic sediments. These sedimentary basins are almost certainly the result of a Phanerozoic orogenic event which is not reflected in the radioactive dates. The problem becomes extreme in the case of the Sierra Nevada, the belt series of the northern Rocky Mountains, and areas such as the Pannonian Basin, where the heat flow is affected by orogenic events much younger than the radioactive age.

The outflow of heat through the continents is the result of a suite of factors such as orogeny, the vertical distribution of heat-producing elements, and erosion. Because continental creation generally results in a thickening of the crust and change in the vertical distribution of the heat-producing elements, it is not obvious that the decrease in the observed values is directly related to the thermal time constant of the continental lithosphere [*England*, 1978]. We suggest that the reduced heat flow gives the most reliable estimate and find that it is of the order of 300 Ma. To obtain a better value, the relation between surface heat flow, surface heat production, erosion, and orogeny needs to be examined more carefully for the Phanerozoic. Such a study requires an analysis on a local scale and has not been attempted in this paper. However, our analysis yields an upper bound for the time constant of orogenic events. It is interesting to note that orogenies throughout the geologic record occur in pulses of the same duration.

In summary, we observe that continental heat flow is high but variable in young regions and decays to a value of 1.05 ± 0.29 μcal/cm² s (44 ± 12 mW/m²) through the early Proterozoic and Archean crust (Table 7). The high but variable heat flow is related to the processes by which continents are created or modified. Once the effects of these processes have died out, the scatter about the equilibrium flow is caused by variations in surface radioactivity and/or erosion. Our global model is not intended to account for local perturbations, and to get a more detailed picture, it will be necessary to consider processes such as intraplate vulcanism, zones of weaknesses [*Sykes and Sbar*, 1973], and crustal thinning [*Chapman and Pollack*, 1975*b*; *Lachenbruch*, 1979].

HEAT LOSS OF THE EARTH

Introduction

One of the objectives of this review is to compare the heat loss through oceans and continents and to estimate the total heat loss of the earth. For the oceans, as the observed mean values underestimate the heat flow, we have used the theoretical heat flux to compute the loss through a province of a given age. The total heat loss through a single ocean is the sum of the individual values for each province. For the continents, water circulation is less important. We have assumed that the actual observations are reasonable estimates of the heat flow at depth and have used the raw data to compute the loss through each province.

Heat Loss Through the Oceans

In the young crust most of the heat is lost by water circulation. Thus to compute the total heat loss through these regions, it is necessary to use a theoretical value. We cannot use the plate model of *McKenzie* [1967] because on integration it yields an infinite heat flux at the origin. *Davis and Lister* [1974] used an alternative boundary condition for the temperature at the origin. They equated the heat brought up by the ascending magma to the sum of the heat lost horizontally by conduction and that lost vertically by the magma once it is in place. The condition implies a discontinuity between the supply temperature and the temperature at the origin, but it is a reasonable mathematical representation of the discontinuous intrusion process. Though the heat flux at the origin is still infinite, the integrated heat loss is finite. We used this boundary condition to modify the model of *McKenzie* [1967]. Details

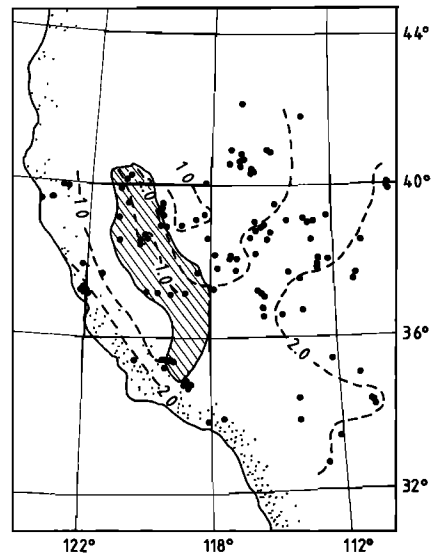

Fig. 21. Contour plot of heat flow for the western United States showing the low associated with the Sierra Nevada batholith (hatched area).

and equations are given in Appendix C. Beyond 1 Ma both this and the original plate model give exactly the same results for both heat flow and topography [*Lister*, 1977].

We compared for each age province (1) the theoretical heat loss through the upper surface, (2) the theoretical flow entering the base of the plate by conduction, and (3) the heat loss given by the observed values (Table 10). The sum of item 1 for all provinces is the theoretical heat loss of the oceans. The sum of item 2 is the heat gained by the oceanic lithosphere, and that of item 3 the measured heat loss of the oceans. Subtracting the heat gained by the lithosphere from the theoretical heat loss gives the heat released by the mantle in plate creation. The radioactive decay of the heat-producing elements was included in the calculation of heat gained. The difference between the theoretical loss and that actually observed represents the heat lost by water flow and by conduction through bare rock.

The total heat loss varies from ocean to ocean. It is largest, about 30%, in the South Pacific, where the spreading rate is fast, and is least, about 10%, in the North Pacific, where the rate is slow. Almost 50% occurs in the Pacific with about 20% in each of the Atlantic and Indian oceans, and 10% in the marginal basins. The total heat loss of the oceans including the marginal basins is 727×10^{10} cal/s (30.4×10^{12} W). It is not uniform with age, as about 50% takes place in the first 20 million years (Table 10). The heat gained by conduction through the base of the plate and by radioactive decay in the crust is small. Over 85% of the heat loss of the oceans occurs by creation and consequent cooling of the lithosphere. The difference between the theoretical heat loss and that observed, 241×10^{10} cal/s (10.1×10^{12} W) represents about one third of the heat lost by oceans. All of this difference takes place in crust younger than 50 Ma, and it is caused principally by the advection of seawater through hot young crust.

Heat Loss Through the Continents

In a previous section we have established a general relation on continents between heat flow and age. Here we use this relation and the separation of the continents into age provinces to estimate their total heat loss. Continental heat flow measurements are considered to be more reliable than those on the ocean floor because they are made at greater depth and involve direct inspection of the local environment. Only large-scale steady state water circulation remains undetected [*Lewis and Beck*, 1977]. In the younger regions the scatter in the heat flow values is high, but the error in the total heat loss is likely to be minimal because the corresponding areas are small. We calculated the total heat loss for each continent separately, first by multiplying the observed mean flow by the area of each age province and then by summing the resultant values (Table 11). For Antarctica, where there are no observations, we used the measured mean value from the rest of the continents. About one fourth of the continents are shelves. To calculate their heat loss, we assumed that about one quarter were created during Cretaceous breakup and have an average age of 120 Ma and a mean heat flow of 1.1 μcal/cm^2 s (46 mW/m^2). For the remaining three quarters the shelves were divided into groups following the ratio of the areas of the age provinces on the corresponding continent. Dividing the total heat loss by the area gives the mean flow through each continent. The values range from 1.19 to 1.52 μcal/cm^2 s (49 to 64 mW/m^2). The Antarctic value is speculative. For the other continents the average heat flow is roughly constant except for Af-

TABLE 10. Heat Loss Through Oceanic Provinces

	Age, Ma												
	0–4	4–9	9–20	20–35	35–52	52–65	65–80	80–95	95–110	110–125	125–140	140–160	>160	Total
North Pacific	20	15	14	12	9	9	7	8	8	4	8	7	3	124 (5.2)
South Pacific	60	32	40	27	17	11	12	9	5	1	2	0	0	216 (9.0)
Indian Ocean	36	18	20	20	17	13	12	9	8	5	2	0	0	160 (6.7)
North Atlantic	11	8	8	7	10	7	8	4	3	2	2	2	1	73 (3.1)
South Atlantic	16	9	10	13	7	4	6	6	6	3	3	0	0	83 (3.5)
Marginal basins	17	9	7	17	7	4	7			2	1	0	0	71 (3.0)
Total heat loss *a*	160	91	99	96	67	48	52	36	30	17	18	9	4	727 (30.4)
Total heat gained *b*	0	0	0	1	4	6	11	11	12	8	10	5	2	70 (2.9)
Total loss observed *c*	51	55	54	59	50	45	52	36	32	20	19	9	4	486 (20.3)
Radiogenic heat loss *d*														31 (1.3)
Estimate of heat loss due to water flow and conduction through bare rock ($a - c$)														241 (10.1)
Estimate of heat loss due to plate creation $[a - (b + d)]$														626 (26.2)

Values are given in 10^{10} cal/s (10^{12} W).

TABLE 11. Heat Losses Through the Continental Age Provinces

	Age, Ma				Continental Shelf	Total Heat Loss	Mean Heat Flow
	0–250	250–800	1700	>1700			
Africa and Madagascar	0.9	18.6	7.3	13.1	4.9	44.8	1.19 (49)
South America	3.4	7.7	5.9	5.7	5.5	28.2	1.26 (53)
North America	11.4	5.7	4.5	11.7	10.9	44.2	1.30 (54)
Australasia	1.0	5.2	5.8	2.1	14.5	28.6	1.52 (64)
Antarctica	2.2	6.9		7.2	6.6	22.9	1.30 (54)
Europe and Asia	31.9	28.3	4.2	13.3	24.7	102.4	1.44 (60)
All continents	50.8	72.4	27.7	53.1	67.1	271.1	1.35 (57)
Addition of heat loss due to volcanic activity						275.1	1.37 (57)
Mean heat flow*	1.78 (75)	1.41 (59)	1.31 (55)	1.10 (46)	1.29 (54)		

Mean heat flow values are given in μcal/cm^2 s (mW/m^2). Heat loss values are given in 10^{10} cal/s (10^{12} W).
*Results from totaling rows or columns may differ slightly from those given owing to rounding. These values do not agree with those from Table 7 because of the different method of averaging.

rica and Madagascar, where the value is lower, and Australia, where the value is higher (Table 11).

We estimate the heat loss through the continents and shelves to be 271 × 10^{10} cal/s (11.3 × 10^{12} W). To this it is necessary to add the amount released by active volcanoes. *Horai and Uyeda* [1969] give a value in the range 4–5 × 10^{10} cal/s (1.7–2.1 × 10^{11} W). Thus we obtain a total value for the continents of 275 × 10^{10} cal/s (11.5 × 10^{12} W) with an error of 50 × 10^{10} cal/s (2.1 × 10^{12} W). The error was estimated by multiplying half the mean absolute deviation by the area of each province and summing these values. Dividing the total heat loss and the error by the area of the continents gives a mean flow of 137 ± 0.25 μcal/cm^2 s (57 ± 11 mW/m^2) (Table 12).

Considering that most of the continental crust is Precambrian, these figures are higher than expected. For example, the mean heat flow is about 0.3 μcal/cm^2 s (13 mW/m^2) higher than the value estimated by *Polyak and Smirnov* [1968] from a similar method. This increase results partially from a more careful consideration of environmental factors and better conductivity measurements in more recent publications. Also, a small amount is a result of concentrating on the orogenic age rather than the age of the last thermal event. We may have included the effects of more recent extensional events in the older province.

TABLE 12. Summary of Area and Heat Loss Information

	Area, 10^6 km^2	Heat Loss, 10^{10} cal/s (10^{12} W)
Continents (including effect of volcanoes)	149.3	208 (8.8)
Continental shelves	52.2	67 (2.8)
Total (continent plus shelves)	201.5	275 (11.5)
Deep oceans	281.7	656 (27.4)
Marginal basins	26.9	71 (3.0)
Total (oceans plus marginal basins)	308.6	727 (30.4)
Worldwide values	510.1	1002 (42.0)
Heat loss by water flow and conduction through bare rock		241 (10.1)
Heat loss by plate creation not including radiogenic heat loss		626 (26.2)
Mean heat flow		
Continents and shelves		1.37* (57)
All oceans (observed)		1.57* (66)
All oceans (theoretical)		2.36* (99)

*Heat flow in 10^{-6} cal/cm^2 s (mW/m^2).

Total Heat Loss of the Earth

We estimate the total heat loss of the earth to be 1002 × 10^{10} cal/s (42.0 × 10^{12} W). More than 70% is lost through the oceans, 7% through the continental shelves, and about 20% through the continents (Table 12). The error, in our estimate of the oceanic heat loss, is between 10 and 20% of the absolute value. If we have not grossly underestimated the effect of water circulation in young continental crust, the error in the continental value is of the same order. In our treatment we have made no attempt to separate the oceanic and continental portions of the shelves. If we assume that one quarter is oceanic, almost 3 times as much heat is lost through the oceans as through the continents. In the case of the oceans, nearly 90% of this heat loss is dissipated by plate creation, and this mechanism is responsible for more than 60% of the heat loss of the earth.

Our estimate of the total heat loss of the earth is almost 40% higher than the value of 6.3 × 10^{12} cal/s (26 × 10^{12} W) given by *Lee and Uyeda* [1965] and is close to the value of 1.0 × 10^{13} cal/s (42 × 10^{12} W) of *Williams and Von Herzen* [1974]. Because their analysis was completed before the development of plate tectonics, *Lee and Uyeda* [1965] were unaware of the importance of water circulation through the oceanic crust. They underestimated the heat lost through the oceans. *Williams and Von Herzen* [1974] made a realistic estimate of the effects of hydrothermal circulation and therefore obtained a reasonable value for the total heat loss.

To a first approximation we can use our analysis (Tables 10–12 and B1) to separate the heat lost at the surface of the earth into (1) that due to convective processes, (2) that resulting from conduction through the lithosphere, and (3) that caused by radioactive decay within the continental crust. If we assume that half the heat flow through the youngest continental crust arises through magmatic activity, then convective processes, which we define here to include plate creation, account for about two thirds of the heat loss of the earth. Assuming a background mantle heat flow of 0.6 μcal/cm^2 s (25 mW/m^2), we calculate the conductive flow through the continents to be 120 × 10^{10} cal/s (5 × 10^{12} W). Adding to this the 70 × 10^{10} cal/s (2.9 × 10^{12} W) gained by the oceanic plate yields a conductive contribution of about 20%. The rest, less than 15%, is contributed by the decay of heat-producing elements in the continental and oceanic crust. These values are based on a number of assumptions and hence are only approximate. But they do emphasize the relative importance of

convection over conduction as the major mechanism by which heat is lost from within the earth.

THERMAL STRUCTURE AND THICKNESS OF THE LITHOSPHERE

Introduction

In the first part of this review we have deliberately concentrated upon the observations and have kept speculation to a minimum. In the second part we investigate the thermal structure beneath oceans and continents and present an integrated review of some of the new but speculative ideas that have recently appeared on the development of the lithosphere. We approach the question of lithospheric thickness from a uniformitarian viewpoint. Can we apply the concept of a thermal boundary layer, which has been so successful in the oceans, to the continents? Further, is this concept of value in examining the creation of continents and their development through time?

Most of the argument concentrates on comparing the relative thickness of the lithospheric plate under an 'equilibrium' ocean with that under the Proterozoic and Archean cratons. Various authors have already estimated these thicknesses. *McKenzie* [1967] and *Sclater and Francheteau* [1970], noting that the heat flows through old oceans and continents were roughly the same and that the surface radioactivity was greater on the continents, suggested that the continental lithosphere was twice as thick. Recently *Jordan* [1975] has suggested that though the rigid portion of the continent is only approximately 100 km thick, another layer lies underneath the old cratons. In his concept, thermal and chemical differences in the continents could extend to 400 km. This layer is attached to and moves with the continental lithosphere. He uses the term 'tectosphere' to describe the region encompassing this layer and the lithosphere. A separate school of thought based on examination of the thermal time constants of the continental lithosphere favors a minimum difference between the plate thicknesses. *Crough and Thompson* [1976] have argued that the reduced heat flow plotted against age fits the same relation as the oceanic heat flow. Also, the exponential subsidence noted by *Sleep* [1971] for Phanerozoic continental basins can only be related to oceanic models if the plate thickness is roughly the same.

Our reanalysis of the heat flow data has shown that rather than being similar the heat flow through an equilibrium ocean is lower than the mean flux through the continents. In this section we compare the mean heat fluxes and use estimates of the distribution of heat-producing elements to compute the temperature as a function of depth underneath the two lithospheres. We compare our range of temperature profiles with geobarometry and geothermometry data beneath continents. Later we consider the relation between reduced heat flow and age and the subsidence of continental basins.

When describing the lithosphere we use the model of a flat plate with a constant temperature at its base. Any process which creates a significant component of additional heat at depth will produce the oceanic observations [*Forsyth*, 1977]. This could be shear stress heating [*Schubert et al.*, 1976], radioactivity in the upper 300 km [*Forsyth*, 1977], or some anomalous heat source [*Crough and Thompson*, 1976]. We prefer the concept of two scales of flow and the idea of a mechanical and thermal boundary layer [*Parsons and McKenzie*, 1978]. The small-scale convection beneath the mechanical boundary layer provides the heat flux which is required to match the observations over old ocean floor. We use this concept as the framework for the rest of this section.

Comparison of the 'Equilibrium Ocean' and Old Continent Geotherm

The oldest ocean crust is found in the western Pacific. It has an age in excess of 180 Ma [*Larson and Hilde*, 1975]. At this age the oceanic lithosphere is not in thermal equilibrium, though both the observations and the theory suggest that it is close [*Parsons and Sclater*, 1977]. The heat flow through the equilibrium ocean is 0.9 ± 0.1 μcal/cm² s (38 ± 4 mW/m²). On the continents, equilibrium conditions are reached by at least the mid-Proterozoic. The heat flux through this region, which is older than 1700 Ma, is 1.10 ± 0.38 μcal/cm² s (46 ± 16 mW/m²) (Table 7) and is 0.2 μcal/cm² s (8 mW/m²) higher than that through the equilibrium ocean. However, because of the large scatter around the continental mean this difference cannot be given too much significance.

To compute the heat flux at the base of the crust and the range in temperatures for the oceanic geotherm, we assume a 10-km crustal layer with a constant heat generation rate of between 1 and 2 × 10^{-13} cal/cm³ s (0.4 and 0.8 × 10^{-6} W/m³) (Figure 22). These values bracket the published estimates for basalt and gabbro. The corresponding contributions to the surface heat flux are therefore 0.1 and 0.2 μcal/cm² s (4 and 8 mW/m²). We obtain two extreme models denoted O_1 and O_2. For O_1 the heat flow is 0.8 μcal/cm² s (34 mW/m²) at the surface and 0.6 μcal/cm² s (25 mW/m²) at the base of the crust, and for O_2 the respective values are 1.0 and 0.9 μcal/cm² s (42

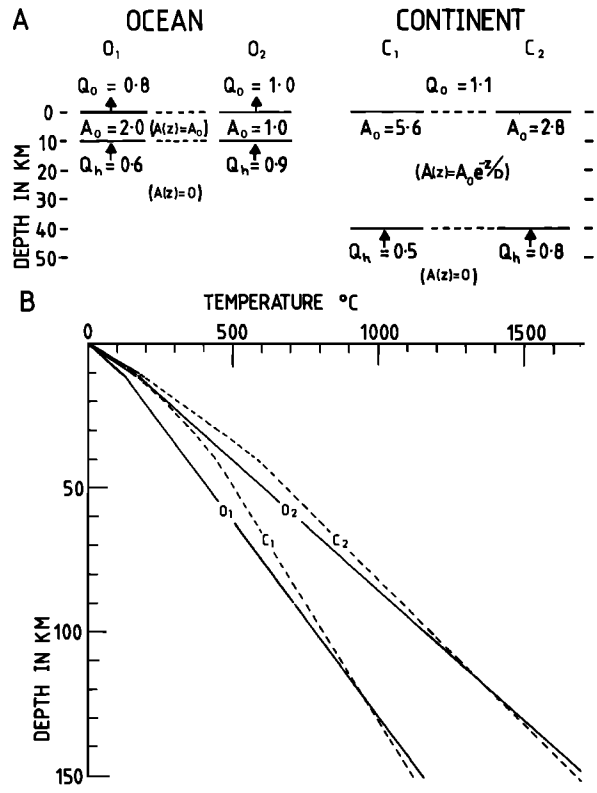

Fig. 22. (*a*) Models used to compute the range of geotherms beneath an 'equilibrium' ocean O_1 and O_2 and an old stable continent (Central Australian Shield (see text for justification)) C_1 and C_2. (*b*) Predicted range in old continental (C_1 and C_2) and 'equilibrium' oceanic (O_1 and O_2) geotherms.

and 38 mW/m^2). We have picked thermal conductivities of 6 and 8 × 10^{-3} cal/cm °C s (2.5 and 3.4 W/m° C) for the crust and mantle. The value for the mantle is the mean thermal conductivity determined from the equations relating heat flow and depth to age for young crust [*Lister*, 1977]. We assume throughout these calculations that the radioactive contribution from the mantle is negligible.

It is difficult to make a realistic estimate of the heat flux through the continental lithosphere and consequently the temperature as a function of depth. The distribution of heat-producing elements with depth is not known with any certainty. As was mentioned before, the scatter in the linear relation of heat flow and radioactivity is large, and it is surprising that Q_r varies so little for provinces older than 250 Ma. The values range from 0.5 μcal/cm^2 s (21 mW/m^2) for the Superior Province to 0.64 μcal/cm^2 s (27 mW/m^2) for the Central Australian Shield. Taking an absolute error of 0.10 μcal/cm^2 s (4 mW/m^2), we arrive at a range of values for Q_r between 0.40 and 0.75 μcal/cm^2 s (18 and 32 mW/m^2). This range represents the best estimate allowed by present data for the heat flux at the base of the crust. All reported values of reduced heat flow are compatible with the upper and lower bounds. This includes the reduced heat flow through the northern latitude provinces (i.e., the Canadian, Baltic, and Ukranian shields and the United Kingdom), which may have to be raised by as much as 0.2 μcal/cm^2 s (8 mW/m^2) to allow for the effects of Pleistocene glaciation. This correction brings their values for Q_r close to the upper bound. Our estimate of the range of heat flow at the base of the continental crust overlaps the estimated range in heat flux of 0.6–0.9 μcal/cm^2 s (24–36 mW/m^2) at the base of the oceanic crust.

For comparison with the oceanic geotherm we computed a range of realistic temperature versus depth profiles for the lithosphere beneath the Central Australian Shield. We chose this shield in order to use real data in an area unaffected by Pleistocene glaciation where D is close to the world average. Two extreme values of Q_r were estimated by plotting the range of straight lines with a constant slope D which can be fit realistically to the heat flow versus surface heat production data (Figure 23). They range between 0.5 and 0.8 μcal/cm^2 s (21 and 34 mW/m^2). We assumed that the heat flux was 1.1 μcal/cm^2 s (46 mW/m^2) at the surface and that the heat-producing elements were concentrated in a crust of depth h. Under these conditions, A_0 depends upon the assumed value for the reduced heat flow Q_r and the model chosen for the distribution of the radiogenic elements in the crust. We chose an exponential decrease with depth. In this model the heat flow from the mantle is approximated by the reduced heat flow [*Lachenbruch*, 1970]. It is important to realize that once the heat flow at the surface and that at the Moho are specified, the temperature at the depth of the Moho is not significantly affected by the form of the radioelement distribution. Under these conditions, A_0 is given by

$$A_0 = (Q_0 - Q_r)/D \tag{3}$$

and the temperature at depth z within the radioactive layer is

$$T = \frac{Q_r Z}{K_1} + \frac{D^2 A_0}{K_1}[1 - e^{-z/D}] \qquad z < h \tag{4}$$

where K_1 is the thermal conductivity of the crustal layer. Below the crustal layer we follow the usual assumptions that steady state conditions prevail and that there is no convection. The temperature at depth z is

$$T = T(h) + \frac{(z-h)}{K_2} Q_r \qquad z > h \tag{5}$$

where K_2 is the conductivity of the upper and lower layers. To compute the probable range in the temperature depth profiles, we used the two extremes for Q_r and assumed values of 0.006 and 0.008 cal/cm °C s (2.5 and 3.4 W/m °C) for K_1 and K_2, respectively.

The range in temperatures allowed by the models that we have chosen is large (Figure 22). Though the continental temperatures are generally higher in the upper portion of the lithosphere, there is a significant overlap below 100 km. The thicker low-conductivity continental crust completely compensates for the slightly higher oceanic mantle heat flow. Given this overlap, the heat flow data are clearly compatible with a model which has a similar temperature structure at depth under both continents and oceans.

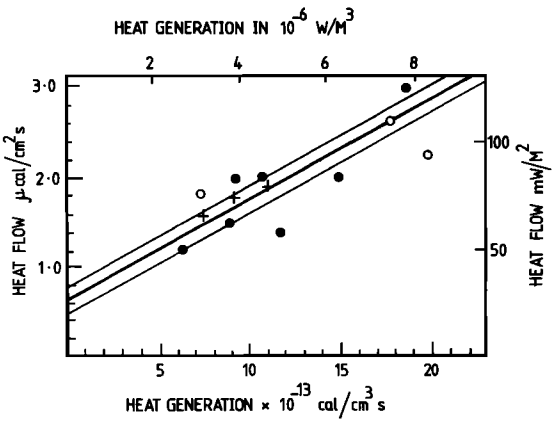

Fig. 23. Heat flow and heat production for the Central Australian Shield Province. The heavy curve represents a least squares fit to the observed data excluding the open circles. Upper and lower curves represent an estimated range of correlations with the same slope compatible with the observed data. Pluses represent gneisses; solid and open circles, granites [after *Sass and Lachenbruch*, 1978].

Comparison With Geothermometry and Geobarometry Data

The pressure-temperature (PT) conditions in the lithosphere can be inferred from the study of mineral assemblages in xenoliths. Before continuing we compare these conditions with our temperature profiles.

The thermodynamical interpretation of analyses of coexisting phases in xenoliths is plagued by two basic problems. First, the assumptions which are involved in the derivation of geothermometers and geobarometers of practical use are not always justified [*Wiltshire and Jackson*, 1975]. They are that the observed minerals are in equilibrium with each other, that the solutions are ideal, and that real systems can be approximated by simple ones. Second, the processes of magma generation and xenolith formation are still not understood and probably involve perturbations of the very temperatures which are to be estimated [*Irving*, 1976; *Hoffman and Hart*, 1978].

Recent improvements have been made to the existing methods, in particular by *Wood and Banno* [1973] for temperature determinations based on the enstatite-diopside equilibrium, by *Akella* [1976] for pressure estimations in the system $CaSiO_3$-$MgSiO_3$-Al_2O_3 applied to the assemblage garnet +

enstatite + diopside, and by *Dixon and Presnall* [1979] for the system $CaO\text{-}MgO\text{-}Al_2O_3\text{-}SiO_2$ applied to the assemblage forsterite + spinel + enstatite + diopside. These new geothermometers and geobarometers are not used consistently throughout the literature and this poses an obvious problem when comparisons are needed. We plot in Figure 24 a number of PT determinations from recent publications or older sources which we corrected ourselves following *Wood and Banno* [1973], *Akella* [1976], and *Dixon and Presnall* [1979]. We stressed in our search the data points for the lowest temperatures. Such studies of xenoliths, while they are not a reliable tool for calculating geotherms, do provide maximum temperature estimates at any depth. They are therefore perfectly acceptable for our purposes.

Not surprisingly, the lowest temperature estimates at any given depth are found beneath old continents (cf. in Figure 24 the data of *Griffin et al.* [1979], *Eggler et al.* [1979], and F. R. Boyd and P. H. Nixon (unpublished data, 1978)). The errors in each PT determination are very large, around ±100°C and ±5 kbar (or ±15 km) [*Mori and Green*, 1975; *Dixon and Presnall*, 1979]. The data provided (Figure 24) are consistent with any of our continental geotherms down to a depth of 100 km. Below this depth the upper conductive profile is ruled out. However, it is not certain that the assumption of conduction is warranted in the mantle. The mechanisms of heat transfer depend critically on the thermal history of the earth and remain largely unknown. If small-scale convection exists in the oceanic lithosphere, it perturbs significantly the conductive temperature profile below a certain depth. This critical depth is defined by a change in the rheology of mantle material from a rigid to a viscous behavior.

Given the errors inherent in geothermometry and geobarometry and the lack of certainty about the dominant heat transport mechanism in the mantle, the present knowledge about the PT conditions in the continental lithosphere precludes any separation between the two temperature profiles that we have computed on the basis of the surface heat flow observations. More data points at shallow depths (above 120 km) are necessary to verify our conclusions.

Relation Between Reduced Heat Flow and Age

One of the major factors affecting continental heat flow values in the Proterozoic and the Archean is the distribution of heat-producing elements. If it is assumed that these elements are concentrated in the crust, then the reduced heat flow is an estimate of the heat contribution from below this radioactive layer. Thus using Q_r, we examined the variation with time of the nonradiogenic component of heat flow. The scatter in the young values is high, and the relation cannot be considered valid for the Cenozoic or late Mesozoic. The reduced heat flow decays within 200–300 Ma to a constant value lying between 0.50 and 0.64 $\mu cal/cm^2$ s (21 and 27 mW/m^2). In this decay, which is more rapid than that shown by the heat flow measurements alone [cf. *Chapman and Pollack*, 1975*a*, Figure 1], the key values are those from New England [*Roy et al.*, 1968] and England and Wales [*Richardson and Oxburgh*, 1978]. It is of interest to note that *Foland and Faul* [1977] have shown that the eastern United States has been subjected to Cenozoic plutonism with the youngest episode terminating around 100 Ma. The spread in tectonic age in the New England province is larger than was previously thought to be the case.

Given the large number of variables which affect the calculation of the reduced heat flow the simplicity of the variation of Q_r with age is surprising. The characteristic time span for the decrease is between 200 and 300 Ma and is close to the thermal time constant for the oceanic lithosphere.

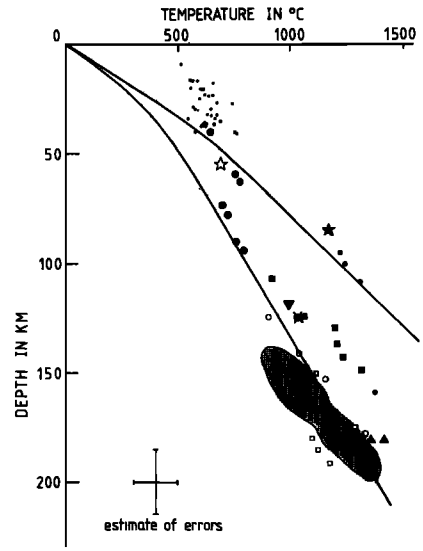

Fig. 24. Comparison of the range of old continental geotherms with geothermometry and geobarometry data. Small and large solid circles represent data of *Griffin et al.* [1979]; open stars, *Smith and Levy* [1976]; open circles, *Bishop et al.* [1979]; solid stars, *Francis* [1976]; medium solid circles, *Aoki and Shiba* [1974]; inverted triangles, *Ernst* [1979]; crossed circles, *Carswell et al.* [1979]; solid squares, *Carter Hearn and Boyd* [1975]; crosses, *Reid et al.* [1975]; open squares, *Eggler et al.* [1979]; triangles, *Gurney et al.* [1975]. The shaded area is taken from F. R. Boyd and P. H. Nixon (unpublished data, 1978).

Subsidence of Continental Basins

The most important observation justifying a simple model of the oceanic lithosphere is the relation between depth and age. *Sleep* [1971] showed that several continental basins have the same exponential subsidence as the oceans. Recently, a series of studies have been made of various Cenozoic and Mesozoic continental shelves and inland basins (Table 13). Their subsidence can be divided into two phases. First, there is a chaotic period during which the basin is formed. In this phase the subsidence history is complex. It can vary from rapid, if a deep graben is created, through slow and linear, if the basin is initiated by a long and continuous event, to no subsidence at all, if the basin starts by uplift. In contrast to the complex initial conditions the subsidence of the second phase is widespread and general. In certain places it is rapid, and the depth increases as the square root of the age. Examples are the Gulf of Lyon [*Watts and Ryan*, 1976] and the Labrador Sea [*Keen*, 1979]. In other places the relation between depth and age is linear, e.g., the Pannonian Basin [*Sclater et al.*, 1979] and the North Sea [*Sclater and Christie*, 1979]. After about 50 million years the depth shows an exponential decrease to a constant value. Examples of this exponential subsidence are the U.S. east coast wells examined by *Sleep* [1971], the Cost B-2 well [*Steckler and Watts*, 1978], and the wells off Nova Scotia [*Keen*, 1979].

Most Phanerozoic continental basins have been subjected to successive pulses of sedimentation. Each major pulse is characterized by complex initial conditions followed by an exponential increase in depth. Examples of such regions are the North Sea and the Sverdrup Basin [*Sweeney*, 1977]. In con-

TABLE 13. A Summary of the Subsidence of Various Phanerozoic Continental Basins and Shelves

Basin or Shelf	Age Range, Ma	Measured Subsidence		Basement Depth, km	Mode of Subsidence	Reference
		Age, Ma	Depth, km			
Pannonian	16–0	16–0	1–4	1–4	linear	*Sclater et al.* [1979]
Gulf of Lyon	25–0	25–0	4	4	$t^{1/2}$	*Watts and Ryan* [1976]
Labrador	75–0	65–0	2–4	2–4	$t^{1/2}$	*Keen* [1979]
North Sea	100–0	100–0	3–5	3–5	linear	*Sclater and Christie* [1979]
Nova Scotia	175–0	140–0	3–5	6–11	$t^{1/2} \rightarrow$ exp	*Keen* [1979]
Cost B-2	175–0	125–0	5	15	exp (−60)	*Steckler and Watts* [1978]
U.S. east coast	175–0	110–0	1–3	?	exp (−50)	*Sleep* [1971]
U.S. Gulf Coast	175–0	110–0	2–4	?	exp (−50)	*Sleep* [1971]
Kansas	330–230	330–230	1–2	1–2	exp (−50)	*Sleep* [1971]
Elk Point	370–230	370–230	3–4	3–4	exp (−50)	*Sleep* [1971]
Appalachian	450–360	450–360	1–3	1–3	exp (−50)	*Sleep* [1971]
Michigan	450–330	450–330	1–3	1–3	exp (−50)	*Sleep* [1971]

The age range for the subsidence data is not always the age range of the basin, as the wells do not always reach the base of the sedimentary layer. We consider only the post–Mid-Cretaceous subsidence of the North Sea.

trast the four Phanerozoic basins, Kansas, Elk Point, Appalachian, and Michigan, have a simpler history [*Sleep,* 1971] (Table 13).

The Phanerozoic, Mesozoic, and Cenozoic basins have two general features. First, the maximum sedimentation is between 10 and 15 km for the continental shelves and between 3 and 8 km for the inland basins. Second, the observable subsidence occurs over a time span of about 200 million years and follows an exponential law with a time constant of 50–60 million years [*Sleep,* 1971; *Steckler and Watts,* 1978]. This time constant is close to the figure of 62.8, which best fits the subsidence history of old ocean floor [*Parsons and Sclater,* 1977].

Three models have been proposed which underline the importance of the lithosphere in the formation of these basins. The first involves thermal doming, followed by erosion and then thermal relaxation with sediment being deposited in the hole left by the eroded material [*Sleep,* 1971]. If the continental plate thickness is of the order of 100–150 km, the subsidence will be exponential with a time constant of roughly 60 million years. This model has two problems. First, only as much sediment can be deposited as is eroded; and second, erosion increases toward the center of the basin. Neither feature is observed. Two other models, the first involving extension by dyke intrusion [*Royden et al.,* 1980] and the second extension by stretching of the lithosphere [*McKenzie,* 1978], have been proposed. Both models involve extension and the replacement of light crust by dense asthenosphere. They do not require extensive erosion to produce the basin.

In passive regions where the dominant regime is extensional the stretching model with lithospheric attenuation is favored. In complex compressional regions, such as the Alps and the Carpathians, the initial subsidence is less uniform, and it is probable that some other mechanism such as localized dyke intrusion or subcrustal extension also occurs. In the following discussion we do not separate between the models and for simplification analyze the data within the framework of the stretching model [*McKenzie,* 1978].

During the extensional phase the upper crust cracks by brittle failure and extends along low-angle listric faults, the lower crust flows ductilely, and the lithosphere attenuates. There is much faulting, and horst and grabens are formed. Though most of the area subsides, some is elevated. Following this phase, general subsidence commences. After 50 million years, processes at the bottom of the lithosphere become dominant, and the basin subsides exponentially to a constant depth.

The similarity between Mesozoic and Cenozoic basins and shelves and the ocean floor can be extended back to the early Proterozoic (Table 14). For example, the Proterozoic basins of southern Africa can be separated into a suite of clearly defined basins with well-dated basement and overlying volcanics [*Anhaeusser,* 1973; *Hoffman,* 1973]. The floors of these basins are continental and the sediments have been deposited uniformly in shallow water. Two other Proterozoic basins, the Hamersley from Western Australia [*Button,* 1976] and the Coronation geosyncline [*Hoffman,* 1973] in northwestern Canada, show similar features. Various authors [e.g., *Hoffman,* 1973; *Windley,* 1978] have pointed out the structural similarity between these basins and Phanerozoic basins and continental shelves. They show almost exactly the same range of maximum subsidence and cover approximately the same time span as the Phanerozoic basins. These observations indicate that the basins were created by similar processes and that the continental lithosphere has had a thickness of 100–150 km throughout geologic history. Inaccuracies in dating and prob-

TABLE 14. A Summary of the Subsidence of Various Archean and Proterozoic Sedimentary Basins

Basin	Age, Ma	Time Span, m.y.	Maximum Subsidence, km	Mean Rate, km/m.y.	Reference
Pongola	3060(2940)–2810	190–70	10.7	0.10	*Anhaeusser* [1973], *Hunter* [1974]
Witwatersrand	2720–2340*	280*	11.9	0.05	*Anhaeusser* [1973], *Hunter* [1974]
Transvaal	2350–2125	225	9	0.04	*Button* [1976]
Hamersley	2350–2000	350	10	0.03	*Button* [1976]
Coronation geosyncline	2100–1800	300	10.7	0.03	*Hoffman* [1973]
Waterburg	1950–1790	160	6.5	0.04	*Anhaeusser* [1973], *Hunter* [1974]

*The age is now thought to be older, and the range >200 m.y. (H. L. Allsopp, personal communication to *van Niekerk and Burger* [1978]).

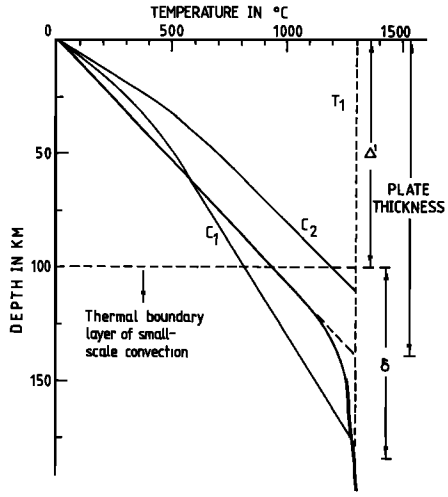

Fig. 25. Comparison of two continental geotherms (C_1 and C_2 from Figure 22) with the equilibrium geotherm in the oceanic plate (heavy curve) showing the role played by small-scale convection in the boundary layer. Δ' is the thickness of the mechanical boundary layer, and δ is the thermal length scale governing the actual temperature structure in the boundary layer. Also shown is the plate thickness obtained by the fit to the depth and heat flow observations [after *Parsons and McKenzie*, 1978].

lems with mapping may have led to overestimates of both the time span and the depth of subsidence of the Proterozoic basins. If indeed the time span and depth have been overestimated, the lithosphere was thinner at that time but certainly not thicker.

In summary, we have shown that an equilibrium ocean and an Archean continent probably have similar temperature structures at depth. This suggests that the continental and oceanic lithospheres have the same thickness. The behavior of the reduced heat flow and the subsidence history of continental basins support this conclusion.

Convection in the Mantle and the Thermal Structure of the Lithosphere

The heat flow through old oceans is close to that through old continents. In the past it was proposed that the radioactive elements were more abundant in the thicker continental crust. Thus the heat flow at the base of the crust was lower under continents than under oceans. However, in our analysis we have found that the heat flow through the old continents is in general higher than that through an equilibrium ocean and that the contribution from radioactivity is lower than was previously assumed. Thus we have proposed a model in which the temperatures at depths greater than 100 km are the same under both an old stable continent and an ocean were it at equilibrium.

Conduction is not the only mechanism of heat transfer in the upper mantle. *Parsons and McKenzie* [1978] proposed a model in which the lithosphere is considered as a thermal boundary layer whose thickness increases with age until it becomes unstable. Below a given temperature it is assumed that the lithospheric material behaves as a solid and forms an upper mechanical boundary layer. At greater temperatures the equivalent viscosity is low, and the material behaves as a fluid over geologic times. The temperature structure is conductive in the solid portion and governed by small-scale convection below. Assuming a mantle heat flow of 0.75 μcal/cm^2 s (31 mW/m^2) and a conductivity of 8×10^{-3} cal/cm °C s (3.4 W/m °C), following *Parsons and McKenzie* [1978], we computed the geotherm beneath an ocean were it at equilibrium (Figure 25). Fundamentally, the model of a flat plate is a way of reconciling the mechanical and thermal behavior of the lithosphere. The two behaviors are not always consistent, and they are also not directly related to the seismic structure in the upper mantle. Note that the total thickness of the thermal boundary layer is greater than the plate thickness as previously determined. The rigid portion in which the dominant heat transfer mechanism is conduction is less than the plate thickness.

We compared our range of continental geotherms with this model (Figure 25). The oceanic geotherm lies between our two continental geotherms and, as was explained before, is compatible with the results derived from geothermometry and geobarometry. There is no evidence for a major difference between the temperature structure under an equilibrium ocean and an old continent.

The original arguments which are presented to justify the difference in lithosphere thickness came from the conductive interpretation of heat flow measurements and surface wave dispersion studies [*Brune and Dorman*, 1963]. We now reevaluate the constraints placed upon thermal models of the upper mantle by seismological observations. Such seismic studies fall into two categories: (1) surface wave dispersion and (2) *S/ScS* time delays. In 1963, *Brune and Dorman* [1963] showed that there were significant differences in the shear wave velocity structure beneath the Canadian Shield and the ocean floor. *Dziewonski* [1971], using 'pure-path' dispersion data, found that these differences were confined to the upper 200 km of the mantle. More recently, *Jordan* [1975] and *Sipkin and Jordan* [1975] on the basis of *ScS* travel times and the discrepancies between models inverted from body and surface wave data have suggested that lateral heterogeneities between oceans and continents extended to depths of 400 km. The analysis of $S/ScS/ScS^2$ travel time delays is difficult, and *Okal and Anderson* [1975] have questioned both their results and their conclusions. In the light of the strong dependence of these delays on the age of the ocean floor [*Sipkin and Jordan*, 1975], the position of the earthquakes chosen for the surface reflection points, and the errors in the delays the difference between the old oceans and the shields is not large. Furthermore, from long-period Rayleigh wave velocities and taking account of lateral heterogeneities within oceanic plates *Okal* [1977] showed that all observational seismic data related to shields were not significantly different from oceanic models below 250 km. He points out that the velocities derived from the models of *Jordan* [1975] are inconsistent with the set of data that he used. *Cara* [1979], using higher Rayleigh wave modes which are more sensitive to the structure at depth, showed that the differences between oceans and continents are confined to depths of less than 250 km. At shallower depths he finds as much variation between the western and eastern United States as between a path across the Pacific and the eastern United States. He also shows that the slight low-velocity zone which is not required when inverting the fundamental mode data for the eastern United States is required by the inversion of the higher modes.

Surface wave data are strongly dependent upon the age of the ocean floor [*Forsyth*, 1977] and show large variations for periods less than 140 s, indicating variation in the shear wave structure above 200 km. Below this depth all the data are compatible with the same model [*Okal*, 1977]. If small-scale

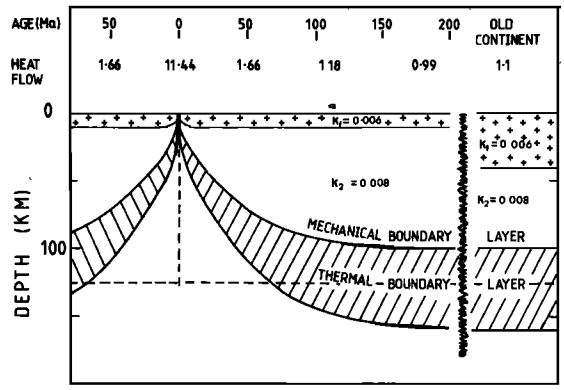

Fig. 26. Schematic diagram modified from *Parsons and McKenzie* [1978] showing the division of the lithosphere into two regions of different rheologies beneath both oceans and continents. All the depth estimates are speculative. The dashed line indicates the plate of constant thickness approximation. The temperature structures beneath the equilibrium ocean and the old continent can be found in Figure 22. The heat flow is in units of 1 μcal/cm^2 s (41.8 mW/m^2).

convection does exist in the upper mantle under both oceans and continents, significant temperature differences are expected as deep as the bottom of the thermal boundary layer (Figure 25). This depth is not known at present, but it is probably deeper than 150 km. The oldest ocean considered by *Forsyth* [1977] is 100–130 Ma and is significantly above thermal equilibrium. It is plausible that temperature variations associated with convection are responsible for lateral differences in seismic structure down to depths of 250 km. Further, the equilibrium oceanic geotherm at depths below 70 km is close to the solidus. *Forsyth* [1977] has suggested that beyond 200 Ma the geotherms may not intercept the wet solidus at any point [*Forsyth,* 1977, Figure 12]. Such a difference would have a large effect on seismic waves but little effect on the temperature structure. This is an alternative and equally plausible explanation as to why a small difference in temperature could correspond to a relatively striking difference in seismic structure beneath oceans and continents.

With presently available information we see no reason to believe that there is difference between the thermal structure under an equilibrium ocean and that under an old stable continent. We suggest that the continents are merely the equilibrium portion of the lithosphere which has not been destroyed in the subduction process (Figure 26). We favor this uniformitarian model because it is simple and compatible with all observations pertaining to the thermal structure of oceans and continents.

Conclusions

The observed subsidence of the ocean floor and the measured decrease of heat flow with age are accounted for by the creation of lithospheric plate. Further, we have shown that the marginal basins exhibit the same relation between heat flow and age as the deep ocean floor. On the continents the heat flow is generally high in the younger regions, decreasing to a constant value after 800 Ma. However, the nonradiogenic component reaches an equilibrium value after only 200–300 Ma.

We have stressed the importance of local geologic variables. For example, hydrothermal circulation and unmeasured loss of heat by advection are responsible for the scatter and low mean values on younger ocean crust. Obviously, no further measurements at sea should be contemplated without due care being given to selecting a suitable environment. On the continents, slow circulation of water has long been known to perturb the surface gradients. Fortunately, such water circulation can usually be detected, and it is possible to avoid such areas. Because of the greater depth of measurement, environmental problems are considered to be less important on continents than on the ocean floor.

We calculate the total heat loss of the oceans to be of the order of 7×10^{12} cal/s (29×10^{12} W), of which 90% is due to plate creation. We estimate that about 30% is not observed because of the unmeasured heat loss by advection near active spreading centers. Our estimate of the heat loss through the continents is 3×10^{12} cal/s (13×10^{12} W). The total heat loss of the earth is of the order of 1×10^{13} cal/s (42×10^{12} W). Over two thirds of the surface heat is lost by plate creation and continental orogeny, 20% by conduction, and the rest by the radioactive decay of heat-producing elements in the crust. Convection is the dominant mechanism by which the internal heat of the earth is released.

We conclude from a careful analysis of the thermal structure of the lithosphere that there is no observable difference between the geotherm for old continents and that for an ocean at equilibrium. However, there is some evidence from seismology that there may be significant shear wave velocity differences at depth even if the temperature differences are not large.

As well as answering some questions this study has revealed a few problems in the interpretation of oceanic heat flow data. One of them is the relation between age and heat flow in marginal basins. Is the simplistic approach taken in this review justified, and why do the depths in this region not show the same relation with age as normal ocean floor? Another problem arises in the well-sedimented areas where the heat flow is lower than expected. Is the difference from the expected heat flow environmentally controlled (i.e., circulation in the basement or sediment), or does it require some modification of our ideas about the tectonic processes active in the crust?

A variety of questions have been raised by our analysis of the continental data. What is the actual distribution of the radiogenic elements in the lower crust? What is the meaning of Q_r and D in the light of the discovery that the linear relation between heat flow and surface heat production holds for metasediments and other metamorphic rocks as well as for granitic plutons?

In our analysis we have concentrated on the radioactive rather than the orogenic age. To examine the actual decay of heat flow with age, the Phanerozoic values need a more careful analysis in which the effects of continental extension, basin formation, mountain building, and erosion are all examined in an integrated approach. Such an analysis is particularly important in view of the rapid decay of the reduced heat flow with age and the 50-m.y. time constant indicated by the subsidence of continental basins through the Proterozoic and Phanerozoic. The study of continental basins through geologic time promises to be a subject worthy of more attention. If our speculations are correct, the lithosphere was sufficiently rigid to support a significant sedimentary load in the Archean. Preliminary data suggest that the plate thickness at that time was the same as it is today. The development of such a thick boundary layer early in the history of the earth must have had a major effect on the loss of heat and thermal convection in the mantle beneath the lithosphere.

We have deliberately taken a uniformitarian approach. This is permitted by our present knowledge. Some problems remain, and the most important is the interpretation of the seismic information. However, it is possible to interpret this information in a variety of different ways, some of which are compatible with our approach to the thermal data. In light of the lack of constraints placed by the seismic information we prefer a simple interpretation of the heat flow data. Hence we favor a model which has a similar thermal structure at depth beneath an equilibrium ocean and an old stable continent.

APPENDIX A: RELATION BETWEEN AREA AND AGE FOR OCEANIC CRUST

We calculated the position of isochrons on the deep-sea floor using three techniques: (1) magnetic anomaly identifications, (2) deep-sea drilling samples, and (3) rotating the present ridge axis through appropriate rotation parameters. For the marginal basins we determined the age of the sea floor using the first two techniques and a relation between age and mean heat flow established earlier in this paper.

Magnetic Anomaly Identifications

We superimposed identified magnetic lineations upon an interrupted equal area chart of the world [*Goode*, 1923]. We started with the compilation of *Pitman et al.* [1974] and updated or changed the lineations in areas where more data have been collected (Plate A1). For the sake of brevity we have cited compilations of data rather than the original publications. The original data can be found by reference to these compilations.

For the Arctic Ocean, Norwegian Sea, and Atlantic Ocean north of 53°N we used the compilation of J. D. Phillips et al. (unpublished data, 1979). For the Labrador Sea the lineations were taken from *Kristoffersen and Talwani* [1977] and for the central North Atlantic from *Pitman and Talwani* [1972]. Off the east coast of North America and the west coast of Africa we employed the compilations of *Schouten and Klitgord* [1977] and H. Schouten and K. Klitgord (unpublished data, 1979). For the central South Atlantic we followed the compilation of *Ladd* [1974] and for the west coast of Africa the lineations of *Rabinowitz and LaBrecque* [1979]. The Scotia Sea lineations, the ridge axis around the Bouvet triple junction, and the Southwest Indian Ridge from Bouvet Island to 40°E are from *Barker and Burrell* [1977], *Sclater et al.* [1976c], and *Sclater et al.* [1978], respectively.

For the North Pacific we used the compilation of *Pitman et al.* [1974], updated in the western Pacific with the data of *Hilde et al.* [1976]. For the marginal basins of the same ocean we followed *Louden* [1976] for the Philippine Sea, *Watts and Weissel* [1975] for the Shikoku Basin, and *Bracey* [1975] for the North Carolina Basin. For the Panama Basin the lineations are from *Lonsdale and Klitgord* [1978].

In the central South Pacific we have followed the lineations of *Handschumacher* [1976] near the ridge axis and for anomalies older than anomaly 13, *Pitman et al.* [1974]. For the Chile Rise and the Bellingshausen Basin we used data of *Weissel et al.* [1977] and for the rest of the South Pacific, *Molnar et al.* [1975]. In the marginal basins of the South Pacific the Tasman Sea lineations are from *Weissel and Hayes* [1977], those in the South Fiji Basin from *Watts et al.* [1977], and those in the Lau Basin from *Lawver et al.* [1975] and *Weissel* [1977]. The lineations presented for the west Coral Sea are from J. K. Weissel (personal communication, 1978).

For the central Indian Ocean and Wharton Basin the magnetic anomaly lineations were taken from *Pitman et al.* [1974]. These have been supplemented by data from *Simpson et al.* [1979] in the North Mozambique Basin and *Bergh and Norton* [1976] in the South Mozambique Basin. The lineations shown off northwestern Australia in the Gascoyne abyssal plain are from *Larson* [1975].

Deep-Sea Drilling Sites and Bathymetric Contours

As a few of the lineations are difficult to identify and much of the sea floor is not covered by lineations, we supplemented our anomaly identifications with deep-sea drilling holes which reached basement (Plate A1). The data for these sites can be found in the *Initial Reports of the Deep Sea Drilling Project*, volumes 1–44, issued by the U.S. Government Printing Office. Also presented are the 2000- and 4000-m contours from the world bathymetric chart of *Chase* [1975]. The 2000-m contour outlines most of the continents and continental shelves surrounding the continents. The 4000-m contour gives a good indication of the position of the midocean ridges within the major oceanic basins.

Time Scale

It is necessary to have a consistent time scale which relates anomaly number and biostratigraphic epoch to time in order to determine absolute age from magnetic anomaly identifications and sediments recovered at the base of deep-sea drilling holes. For magnetic anomaly numbers 0–34 (0–80 Ma), present through the Late Cretaceous, we used *LaBrecque et al.* [1977]. We followed *van Hinte* [1976*a*, *b*] for the Mesozoic lineations and the rest of the Cretaceous and the Jurassic.

Why Specific Isochrons Were Chosen

Except for the first 20 million years we separated the oceans into nine almost equal intervals of time. We chose four intervals between 0 and 20 Ma and nine between 20 and 160 Ma and added everything on crust older than 160 Ma into one time span. The individual isochrons were selected for different reasons. The 9-, 20-, and 35-Ma isochrons were chosen because these are the ages of the easily identifiable magnetic anomalies 5, 6, and 13. The ocean crust cools rapidly immediately after formation. To better estimate the heat loss in the first 9 Ma, we separated this interval into three subdivisions, 0–1, 1–4, and 4–9 Ma. We chose the 52-Ma isochron (anomaly 22) because this is the time at which significant motion started between Australia and Antarctica. The 65-Ma isochron overlies anomaly 29 and marks the Cretaceous-Tertiary boundary. The 80-Ma isochron overlies anomaly 34, which is the last clearly identified magnetic anomaly of the Tertiary-Cretaceous sequence. The 125-Ma isochron (anomaly M7) was selected because this is the time of creation of the South Atlantic and Indian oceans. We chose the 95- and 115-Ma isochrons because they are equally spaced in time between the 80- and 125-Ma isochrons. The 140-Ma isochron overlies anomaly M22. We selected 160 Ma as the final isochron because it is the time of jump in early spreading in the North Atlantic and to permit a separation of the very old crust in the western Pacific. There is no known ocean crust older than 180 Ma.

We have assumed that the 2000-m contour on the continental shelf marks the break between continent and ocean. This is an oversimplification, but on the scale of our analysis any errors introduced can be neglected.

Position of the Isochrons

We used the magnetic anomaly compilation, the basement ages inferred from sediment recovered in deep-sea drilling holes, the above time scales, and published plate reconstructions to draw the isochrons on the equal area chart of the oceans. We determined the position of the isochrons in the Atlantic by rotating the ridge axis about the poles and by the angles given by *Sclater et al.* [1977]. For the Southwest Indian and America/Antarctic ridges we calculated the position of the isochrons by rotating the ridge axis by the rotational parameters given by *Norton and Sclater* [1979]. Care was taken not to violate the basic concepts of plate tectonics in the development of the Azores, central Atlantic, and Bouvet triple junctions.

In the North and South Pacific, except for the Macquarie Ridge, the East Pacific Rise, and the Chile Rise before 9 Ma, we used the magnetic lineations to determine the position of the isochrons. For the two youngest isochrons we rotated the ridge axis through the appropriate rotation parameters of *Minster et al.* [1974]. In the Indian Ocean the isochrons on the Southwest Indian Ridge from present to 80 Ma, on the Central Indian Ridge from present to 35 Ma, and on the Southeast Indian Ridge from 0 to 53 Ma were determined by rotating the ridge axis through the rotation parameters from *Norton and Sclater* [1979]. For the Red Sea we assumed that it had opened at 20 Ma and since then had spread at a constant rate. The rest of the isochrons in the Indian Ocean were interpolated from the published lineations except for the Somali Basin close to the coasts of India and Antarctica. For this crust we determined the position of the isochrons from the early opening history of *Norton and Sclater* [1979] and then transferred them by hand to the large chart. These isochrons are hypothetical.

In the case of the marginal basins we used published magnetic lineations and sediment recovered from deep-sea drilling holes. However these data are not sufficient to permit ages to be assigned to more than half these basins. In the text we justify a relation between heat flow and age for these basins. Where other data are not available, we applied this relation.

For the western Mediterranean we used the heat flow data of *Erickson et al.* [1977]. We assumed that the northern portion of the Messina Basin was young and, on the basis of the low heat flow values, that the rest of the eastern Mediterranean was old. In the Caribbean we assumed that the Cayman Trough was initiated at 50 Ma and has been spreading at a uniform rate since then. For the rest of this area we based our estimate on the age of the surrounding continents and the surface heat flow. Some support for the age that we have assigned to the Venezuela Basin comes from the recognition of east-west lineated anomalies in the Columbia Basin which have been tentatively identified as 29–33 [*Christofferson*, 1973]. For the Scotia Sea we have used the lineations presented by *Barker and Burrell* [1977].

In the Arctic Ocean we estimated the age from the heat flow. For the Bering Sea we followed *Cooper et al.* [1976]. We assumed that the Kamchatka Basin was young and used the heat flow to estimate the age of the Sea of Okhotsk and the Sea of Japan. In the North Pacific marginal basins we estimated the age of the Ryukyu Trough, Celebes Sea, Scotia Sea, Andaman Sea, and South China Sea from the heat flow. We took the age for the Mariana Trough from *Karig* [1971], and for the rest of the basins we used either magnetic lineations (West Philippine Basin and Shikoku Basin) or the sedi-

TABLE A1. Area (in 10^6 km^2) as a Function of Age for the Oceans

	Age, Ma												
	0–4	4–9	9–20	20–35	35–52	52–65	65–80	80–95	95–110	110–125	125–140	140–160	>160	Total Area
North Pacific	1.8	3.2	4.4	5.2	5.2	5.2	5.0	6.0	6.6	3.8	7.2	6.1	2.8	62.5
South Pacific	5.3	6.9	13.0	12.1	9.4	6.8	8.6	7.3	4.1	1.2	1.8	0.2	0	76.7
Indian Ocean	3.2	3.9	6.4	8.9	9.6	8.1	8.9	7.1	7.3	4.3	1.8	0	0	69.5
North Atlantic	1.0	1.8	2.5	3.3	5.3	4.4	5.5	3.3	2.2	2.0	2.2	2.0	0.6	36.1
South Atlantic	1.4	2.0	3.4	5.6	3.9	2.5	4.3	4.2	4.6	2.6	2.4	0	0	36.9
Marginal basins		3.4*	2.1	7.5	3.6	2.7	5.0	0	0		2.6*	0	0	26.9
Total area	14.2	19.7	31.8	42.6	37.0	29.7	37.3	27.9	24.8	15.2	16.7	8.3	3.4	308.6
Heat flow														
Surface	11.3	4.6	3.1	2.25	1.8	1.6	1.4	1.3	1.2	1.15	1.1	1.05	1.0	
Bottom	0	0	0	0.02	0.1	0.2	0.3	0.4	0.5	0.55	0.6	0.65	0.7	
Observed	3.6	2.8	1.7	1.4	1.35	1.5	1.4	1.3	1.3	1.3	1.15	1.15	1.2	

Surface and bottom heat flows are in units of 10^{-6} cal/cm^2 s or units of 42 mW/m^2 (from Table C3) plus 0.1 μcal/cm^2 s, and observed heat flow in 10^{-6} cal/cm^2 s or units of 42 mW/m^2 (from Table 1).
*Values of 3.4 and 2.6 are for the intervals 0–9 and 110–140 Ma, respectively.

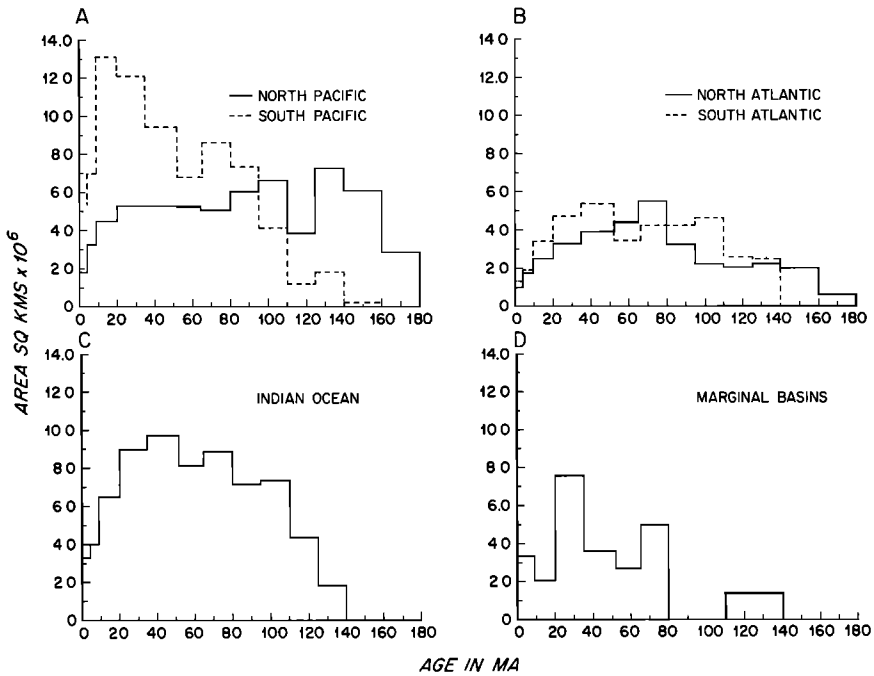

Fig. A1. Step function representation of the area as a function of age for the oceans: (*a*) North and South Pacific, (*b*) North and South Atlantic, (*c*) Indian Ocean, and (*d*) marginal basins.

ment recovered at the base of deep-sea drilling holes (Parece Vela Basin). The age of the Carolina Basin was taken directly from the magnetic lineations [*Bracey*, 1975].

In the southwest Pacific marginal basins we took the age for the Solomon Sea and Woodlark Basin from *Luyendyk et al.* [1973]. We assumed that the east Coral Sea had the same age as the South Fiji Basin, i.e., between 20 and 35 Ma [*Watts et al.*, 1977], and for the west Coral Sea we used data of *Burns et al.* [1973]. For the Fiji Plateau our age estimate is from *Chase* [1971], and we assumed that the Lau and Kermadec basins were between 0 and 4 Ma [*Lawver et al.*, 1975*a*; *Weissel*, 1977]. The lineations in the Tasman Sea were employed to determine the position of the isochrons, and for the Banda Sea in the absence of any concrete information we guessed the age from the depth to be 52–65 Ma.

The age estimates for the marginal basins are not reliable. We have included them for the sake of completeness. As they represent less than 10% of the area of the ocean floor, the errors introduced in the calculated total heat loss are small.

Area Versus Age for the Oceans

Apart from the South Pacific the oceans exhibit the same linear decrease of area with age (Tables 10 and A1 and Figures A1*a*–A2*d*). This similarity is the result of a combination of spreading and crustal consumption. The Atlantic and Indian oceans have roughly the same spreading rate, and the North Pacific, which has twice the spreading rate, has only a western limb. The South Pacific has both limbs to anomaly 22 (53 Ma) and is spreading at 4 times the rate for the Atlantic and Indian oceans. Thus this ridge axis creates most of the youthful sea floor. However, it does not alter the linear decrease of area with age (Figure A2*a*). For our computations of

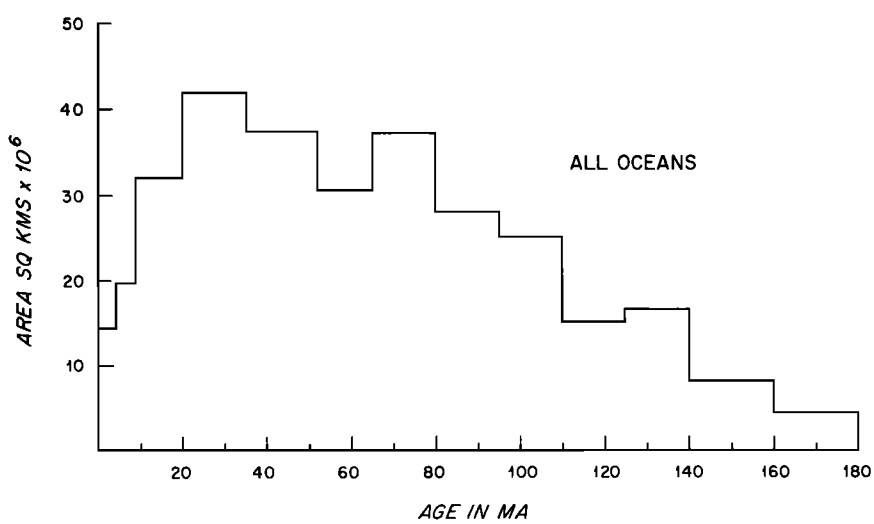

Fig. A2*a*. Step function representation of the area as a function of age for all the oceans, including the marginal basins.

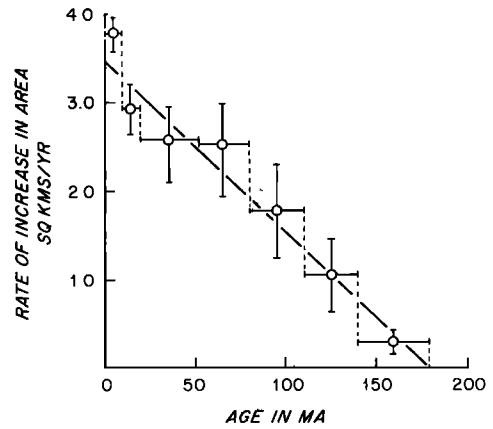

Fig. A2*b*. Rate of increase in area of the oceans as a function of age.

heat loss the age/area distribution has three important features. (1) Almost half the sea floor, not including the marginal basins, is located in the Pacific. (2) The marginal basins, as we define them, represent 8% of the ocean floor. (3) The continental shelves cover about 10% of the surface of the globe. If we assume that the shelves are continental, the ratio of ocean to continent is 3:2. This is different from the 2:1 figure determined from previous studies [*Kossinna,* 1921; *Menard and Smith,* 1966] (Table A1). We compared our values for the oceans with those of *Menard and Smith* [1966]. Once allowance is made for the different definitions of shelf and ocean, the agreement is excellent. From this comparison we estimate that our errors in comparison of areas of continents and oceans are of the order of 2%. The errors in the area of the individual age provinces are difficult to calculate. More than 60% of the ocean is covered by well-identified magnetic lineations, and for a further 20% the position of the isochron can be predicted with some confidence. Thus we estimate our errors in the areas to be less than 20%.

From the histograms of area versus age (Figure A2*a*) we calculated the rate of increase of oceanic crust including marginal basins with age (Figure A2*b*). The amount of crust present decreases linearly with age (Table A1 and Figure A2*b*). Both the values for total area in a given time interval and the rate of decrease of crust are close to those determined by *Berger and Winterer* [1974] in a similar but cruder study. The similarity of the two values is evidence that more careful analysis will not change the conclusion that the oceans have a roughly linear decrease of area with age.

It is tempting to use our analysis to investigate whether or not there was a rapid increase in area of young crust in the Cretaceous [*Hays and Pitman,* 1974]. However, we have not considered the area of material consumed in the trenches, and it is not possible to determine whether or not such an increase occurred. A definitive test awaits global reconstructions of the oceans and continents.

Appendix B: Relation Between Area and Age for Continents

In this study we have chosen four intervals of time. The first interval includes all continent older than 1700 Ma. It spans the Archean and the early Proterozoic and terminates with the orogenic pulse between 1900 and 1700 Ma. The second interval extends through the middle Proterozoic from 1700 to 800 Ma and includes the major continent-forming phase between 1100 and 900 Ma. The third interval runs from 800 Ma to the start of the Mesozoic at 250 Ma. The fourth and final interval is the Mesozoic and Cenozoic, which covers the crust formed or altered during the latest episode of plate motion and creation of sea floor.

For our separation of the continents into the appropriate intervals we have followed *Hurley and Rand* [1969] and *Hurley* [1971]. This material has been supplemented wherever possible by information gathered from geological maps of various continents and by more recent compilation of radiometric age data. We have separated the crust into tectonic provinces and have assumed that all rocks within a province have the age of the last orogeny.

For North America we used the data compilation of *Hurley and Rand* [1969] in conjunction with the tectonic chart of North America by *King* [1969]. For South America we followed *Hurley and Rand*'s [1969] data, extensively modified by new data from *de Almeida et al.* [1974, Figure 1] and *Urien and Zambrano* [1973, Figure 5]. For Africa, to which we added both Arabia and Madagascar, we started with the compilation of *Hurley and Rand* [1969], to which we added data for central Africa from *Choubert and Foure-Muret* [1968]. Our separation of Arabia into different age intervals is speculative (P. M. Hurley, personal communication, 1978). For Eurasia we followed the charts presented by *Hurley* [1971] and supplemented these with data from the *Russian Tectonic Atlas* [*Ministry of Geology,* 1969] and the *Chinese Tectonic Chart of Asia* [*Chinese Geological Society,* 1975]. We assigned the Russian platform between the Urals and the Siberian platform the younger age of the tectonic chart rather than that given by *Hurley* [1971]. In essence, we have given this area the age of the oldest sediments deposited rather than the crustal age of basement. In this particular case we believe such an assignation is justified by the great thickness of sediments which

TABLE B1. Areas of Continental Age Provinces

	Age, Ma				Continental Shelf	Total Area
	0–250	250–800	800–1700	>1700		
Africa and Madagascar	0.5	16.2	5.4	11.5	4.2	37.8
South America	2.6	5.1	4.9	5.2	4.5	22.3
North America	5.8	3.7	3.6	10.5	10.3	33.9
Australasia	0.9	2.9	3.3	1.8	9.9	18.8
Antarctica	1.2	4.6		6.6	5.2	17.6
Europe and Asia	17.6	18.9	3.9	12.7	18.0	71.1
All continents	28.5	51.3	21.2	48.3	52.2	201.5
Area/age (km/yr) $\times 10^{-2}$	11.4	9.3	2.4	2.1		5.0

Values for areas are given in 10^6 km^2. Results from totaling columns may differ slightly from those given owing to rounding.

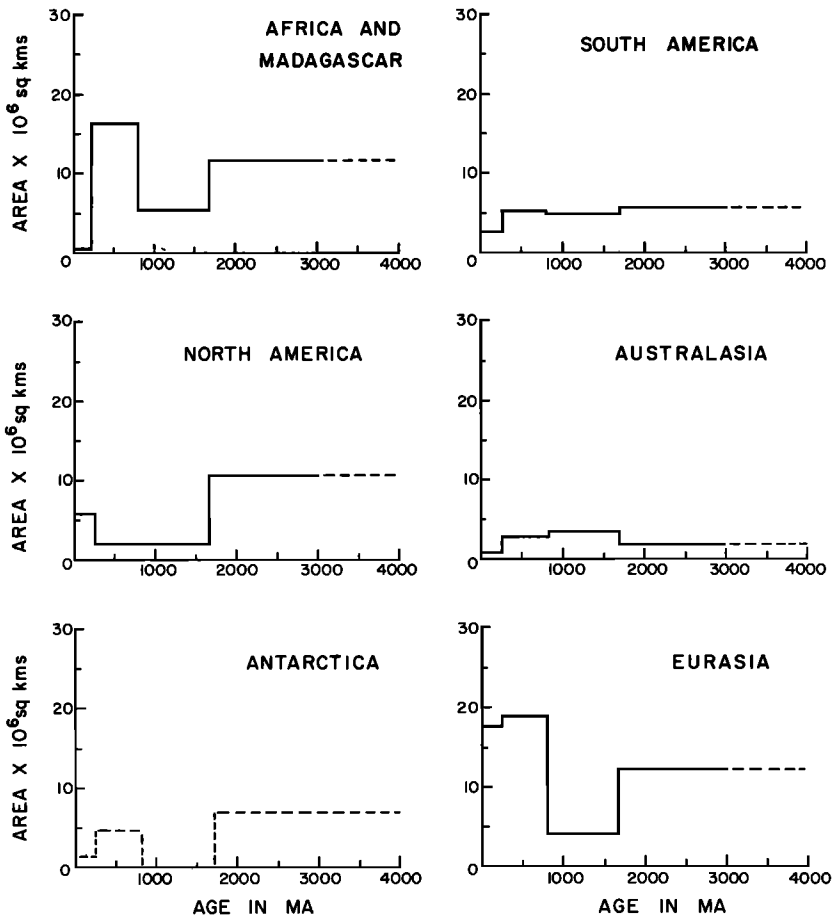

Fig. B1. Step function representation of the area as a function of age for the individual continents.

could only have been created by an orogeny of this age. For India, which we included in Eurasia, we used the chart presented by *Hurley and Rand* [1969] and a more recent compilation of radioactive dates made by *Naqui et al.* [1974, Figure 2]. We took the age ranges for Australia from *Hurley and Rand* [1969, Figure 6], and for Antarctica, for which there are very few data, we employed the same source [*Hurley and Rand,* 1969, Figure 7].

We superimposed the province boundaries which we determined from the papers mentioned above onto *Goode*'s [1923] interrupted equal area map of the world. We also plotted the 2000-m contour, which for the purpose of this paper defines the continental shelf line. Using a planimeter, we computed the area in each of the age intervals and the total amount of shelf around each continent (Table B1, Figure B1).

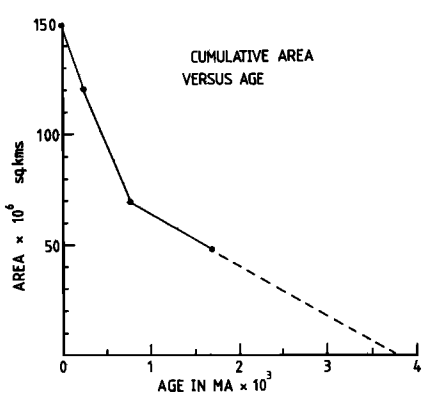

Fig. B2. Cumulative plot of the area of the continents as a function of age.

Almost half the continental area is formed in the two intervals older than 800 Ma (Figure B2). Our distribution of area with age for the continents is similar to that of *Hurley and Rand* [1969] and *Veizer* [1976]. However, we have slightly more continent in the Mesozoic and Cenozoic and a much larger area in the interval prior to 1700 Ma. The increase in the latter interval is expected. As more radiometric age dates on continental basement are published, it is becoming apparent that the area of the oldest portions of the Precambrian has been underestimated in the past. On the other hand the problems of relating radioactive age to orogenic age still exist. Thus we have inadvertently included a few youthful orogenic regions in the older provinces. This is particularly true on the Russian and West Siberian platforms. Until this problem in continental tectonics is resolved, age/area estimates based on basement radioactive ages must be considered at best good estimates rather than quantitative values.

Appendix C: The Modified Plate Model

We follow here the derivation of *McKenzie* [1967], using the boundary conditions of *Davis and Lister* [1974]. In nondimensional variables the differential equation and boundary conditions for the modified plate model are

$$\frac{\partial^2 T}{\partial z^2} - 2R\frac{\partial T}{\partial z} + \frac{\partial^2 T}{\partial x^2} = 0$$

TABLE C1. Surface Heat Flow From Different Models

Age, Ma	Plate Model Spreading Rate, cm/yr			Cooling Half-Space Model, 3 cm/yr	Exponential Approximation, 3 cm/yr	*McKenzie* [1967], 3 cm/yr
	1	3	5			
1	11.60	11.30	11.26	11.30	2.37	11.46
4	5.69	5.62	5.62	5.65	2.30	5.64
9	3.77	3.75	3.74	3.77	2.19	3.75
20	2.51	2.51	2.51	2.53	1.96	2.51
35	1.90	1.90	1.89	1.91	1.72	1.90
52	1.56	1.56	1.55	1.57	1.50	1.56
65		1.39		1.40	1.37	1.39
80		1.26		1.26	1.25	1.26
95		1.16		1.16	1.15	1.16
110		1.08		1.08	1.08	1.08
125		1.02		1.01	1.02	1.02
140		0.97		0.96	0.97	0.97
160		0.92		0.89	0.93	0.92
180		0.89		0.84	0.89	0.89

Heat flow values are in units of μcal/cm^2 s.

$$T(z=1)=0$$
$$T(z=0)=1 \qquad \text{(C1)}$$
$$-\frac{1}{R}\frac{\partial T}{\partial x}+T=1 \quad \text{at} \quad x=0$$

where R is the Peclet number, equal to $ul/2k$; u is the plate velocity, l the plate thickness, and k the thermal diffusivity; x denotes the horizontal coordinate, and z the vertical ($z = 1$ at the upper surface). The third boundary condition equates the heat brought in at the origin with that lost horizontally to the plate [*Davis and Lister*, 1974]. The nondimensional horizontal coordinate x is given by

$$x = ut/l$$

where t is the age of the crust at distance $x = ut$ from the ridge axis.

The solution to (C1) is

$$T = 1 - z + \sum_{N=1}^{\alpha} A_N \exp(-a_n x)\sin(n\pi z) \qquad \text{(C2)}$$

where

$$a_n = -R + (R^2 + n^2\pi^2)^{1/2}$$

and

$$A_N = \frac{2(-1)^{n+1}}{n\pi}\frac{2R}{2R+a_n}$$

The original plate model of *McKenzie* [1967] used the same equations but a different initial condition at $x = 0$. This condition was

$$T = 1 \quad \text{at} \quad x = 0 \qquad \text{(C3)}$$

The solution to these equations is still of the form (C2) with

$$a_n = -R + (R^2 + n^2\pi^2)^{1/2}$$

and

$$A_N = 2(-1)^{N+1}/n\pi$$

For our calculations we use the following parameters which can be found in the work of *Parsons and Sclater* [1977]:

K thermal conductivity, equal to 7.5×10^{-3} cal/°C cm s;
k thermal diffusivity, equal to 8.0×10^{-3} cm^2/s;
l thickness of the plate, equal to 125 km;
T_1 temperature at the base of the plate, equal to 1333°C.

These values yield an asymptotic heat flux of 0.8×10^{-6} cal/cm^2 s as time goes to infinity.

The *McKenzie* [1967] model has the disadvantage of yielding an infinite heat flux at the ridge axis, as the series solution diverges for $x = 0$. The modified plate model is therefore more appropriate for our heat loss calculations. The two plate models only differ significantly in their predictions for times less than 1 Ma, as can be seen in Table C1.

We give in Table C1 the theoretical heat flow at the discrete ages that we used to define the isochrons on the oceanic crust, together with the cooling half-space solution of *Davis and Lister* [1974] and the exponential approximation of *Parsons and Sclater* [1977] which is asymptotic to the plate solution as time goes to infinity. We list in Table C2 the three corresponding expressions. We make the computations for plate velocities of 1, 3, and 5 cm/yr and find little difference in the results, even for the earliest ages. The theoretical values derived from (C2) are in good agreement with the other values.

In Table C3 we give the mean heat flow through the upper and lower surfaces of the plate for the time intervals defined by two consecutive isochrons. The same plate velocities are used, and the results differ slightly before 9 Ma.

All these calculations do not include the contribution of the radioactive decay of U, Th, and K. For equivalence with val-

TABLE C2. Three Expressions Used to Predict the Surface Heat Flow

	Expression	Numerical Approximation
Plate model	$\left(\frac{KT_1}{l}\right)\left\{1+\sum_{N=1}^{\alpha}\frac{4R}{2R+\alpha_N}e^{-a_n x}\right\}$	
Cooling half-space model	$\left(\frac{KT_1}{l}\right)\frac{l}{(\pi k)^{1/2}}\frac{1}{t^{1/2}}$	$11.3/t^{1/2}$
Exponential approximation	$\left(\frac{KT_1}{l}\right)+\left(\frac{2KT_1}{l}\right)\exp\left[-\left(\frac{\pi^2 k}{l^2}\right)t\right]$	$0.8 + 1.6\exp(-t/62.8)$
McKenzie [1967] model	$\frac{KT_1}{l}\left\{1+2\sum_{N=1}^{\alpha}e^{-a_n x}\right\}$	

K is thermal conductivity, and k is thermal diffusivity $K/\rho Cp$.

TABLE C3. Mean Heat Flow Through the Upper and Lower Surfaces of the Lithosphere

	Upper Surface Spreading Rate, cm/yr			Lower Surface Spreading Rate, cm/yr		
Age, Ma	1	3	5	1	3	5
0–1	21.31	22.30	22.40	0.00	0.00	0.00
1–4	7.65	7.51	7.50	0.00	0.00	0.00
4–9	4.53	4.50	4.49	0.00	0.00	0.00
9–20	3.02	3.01	3.01	0.00	0.00	0.00
20–35	2.17	2.16	2.16	0.02	0.02	0.02
35–52	1.71	1.71	1.71	0.10	0.10	0.10
52–65		1.47			0.21	
65–80		1.32			0.31	
80–95		1.20			0.41	
95–110		1.11			0.49	
110–125		1.05			0.56	
125–140		0.99			0.61	
140–160		0.95			0.66	
160–180		0.91			0.69	

Heat flow values are in $\mu cal/cm^2$ s.

ues of *Parsons and Sclater* [1977] a value of 0.1 $\mu cal/cm^2$ s should be added throughout.

Acknowledgments. This paper has a long history. Important initial input came from S. Uyeda, P. D. McKenzie and N. H. Sleep. M. S. Steckler, L. Bales, and L. Dobinov helped with the analysis and plotting of the continental heat flow data. L. Royden wrote the computer programs for Goode's projection, and P. Pollen digitized some of the oceanic contours. P. M. Hurley and C. Burchfiel aided us in the separation of the continents into age provinces. The original manuscript was reviewed by B. F. Windley, P. C. England, and J. H. Sass. We benefited greatly from their comments. E. Nisbet provided information on the early Proterozoic basins, and B. Kennett discussed the implications of the seismological information with us. This study was supported by National Science Foundation grants 76-82076 OCE and DPP76-19053A01. The work was completed when J. G. Sclater was on sabbatical at the Department of Geodesy and Geophysics, University of Cambridge, Cambridge, United Kingdom, and C. Jaupart was enjoying active military duty at the Place Balard air force base in Paris.

REFERENCES

Akella, J., Garnet pyroxene equilibria in the system $CaSiO_3$-$MgSiO_3$-Al_2O_3 and in a natural mineral mixture, *Amer. Mineral., 61,* 589–598, 1976.

Anderson, R. N., Oceanic heat flow, in *The Sea,* vol. 7, Wiley-Interscience, New York, in press, 1979.

Anderson, R. N., and M. A. Hobart, The relation between heat flow, sediment thickness, and age in the eastern Pacific, *J. Geophys. Res., 81,* 2968–2989, 1976.

Anderson, R. N., G. Moore, S. Schilt, R. Cardwell, A. Trehu, and V. Vacquier, Heat flow near a fossil ridge on the north flank of the Galapagos spreading center, *J. Geophys. Res., 81,* 1828–1838, 1976*a*.

Anderson, R. N., M. G. Langseth, V. Vacquier, and J. Francheteau, New heat flow measurements on the Nazca plate, *Earth Planet. Sci. Lett., 29,* 243–254, 1976*b*.

Anderson, R. N., M. G. Langseth, and J. G. Sclater, Mechanisms of heat transfer through the floor of the Indian Ocean, *J. Geophys. Res., 82,* 3391–3409, 1977.

Anderson, R. N., M. G. Langseth, D. E. Hayes, T. Watanabe, and M. Yasui, Heat flow, thermal conductivity, thermal gradient, in *Geophysical Atlas of the East and South East Asian Seas, Map Chart Ser.,* vol. MC-25, edited by D. E. Hayes, Geological Society of America, Boulder, Colo., 1978.

Anhaeusser, C. R., The evolution of the early Precambrian crust of southern Africa, *Phil. Trans. Roy. Soc. London, Ser. A, 273,* 359–388, 1973.

Aoki, K., and I. Shiba, Petrology of websterite inclusions of Itinone-Gata, Japan, *Sci. Rep. Tohoku Univ., Ser. 3, 12,* 395–411, 1974.

Artemjev, M. E., and E. V. Artyushkov, Structure and isostasy of the Baikal Rift and the mechanism of rifting, *J. Geophys. Res., 76,* 1197–1211, 1971.

Barberi, F., et al., Age and nature of basalts from the Tyrrhenian abyssal plain, in *Initial Reports of the Deep Sea Drilling Project,* vol. 42, part 1, edited by K. J. Hsu et al., pp. 509–514, U.S. Government Printing Office, Washington, D. C., 1978.

Barker, P. F., and J. Burrell, The opening of the Drake Passage, *Mar. Geol., 25,* 15–34, 1977.

Bayer, R., J. L. LeMouel, and X. LePichon, Magnetic anomaly pattern in the western Mediterranean, *Earth Planet. Sci. Lett., 19,* 168–176, 1973.

Beck, A. E., Climatically perturbed temperature gradients and their effect on regional and continental heat flow means, *Tectonophysics, 41,* 17–39, 1977.

Berger, W. H., and E. L. Winterer, Plate stratigraphy and the fluctuating carbonate line, *Int. Ass. Sedimentol. Spec. Publ., 1,* 11–48, 1974.

Bergh, H. W., and I. O. Norton, Prince Edward fracture zone and the evolution of the Mozambique Basin, *J. Geophys. Res., 81,* 5221–5239, 1976.

Berry, M. J., Structure of the crust and upper mantle in Canada, *Tectonophysics, 20,* 183–201, 1973.

Bickle, M. J., Heat loss from the earth: A constraint on Archean tectonics from the relation between geothermal gradients and the rate of heat production, *Earth Planet. Sci. Lett., 40,* 301–315, 1978.

Birch, F., R. F. Roy, and E. R. Decker, Heat flow and thermal history in New England and New York, in *Studies of Appalachian Geology,* edited by E. An-Zen, pp. 437–451, Interscience, New York, 1968.

Bishop, F. C., J. V. Smith, and J. B. Dawson, Na, K, P, and Ti in garnet pyroxene and olivine from peridotite and eclogite xenoliths from African kimberlites, *Lithos, 11,* 155–173, 1979.

Blackwell, D. D., The thermal structure of the continental crust, in *The Structure and Physical Properties of the Earth's Crust, Geophys. Monogr.,* vol. 14, edited by J. G. Heacock, AGU, Washington, D. C., 1971.

Bottinga, Y., Thermal aspects of sea-floor spreading and the nature of the suboceanic lithosphere, *Tectonophysics, 21,* 15–38, 1974.

Bracey, D. R., Reconnaissance geophysical survey of the Caroline Basin, *Geol. Soc. Amer. Bull., 86,* 775–784, 1975.

Brune, J., and J. Dorman, Seismic waves and earth structure in the Canadian Shield, *Bull. Seismol. Soc. Amer., 53,* 167–210, 1963.

Burke, K., J. F. Dewey, and W. S. F. Kidd, Dominance of horizontal movements, arc, and microcontinental collisions in the later permobile region, in *The Early History of the Earth,* edited by B. F. Windley, pp. 113–129, John Wiley, New York, 1976.

Burns, R. E., et al., *Initial Reports of the Deep Sea Drilling Project,* vol. 21, 931 pp., U.S. Government Printing Office, Washington, D. C., 1973.

Button, A., Transvaal and Hamersley basins—Review of basin development and mineral deposits, *Minerals Sci. Eng. Repub. S. Afr., 8,* 262–293, 1976.

Cara, M., Lateral variations of *S* velocity in the upper mantle from higher Rayleigh modes, *Geophys. J. Roy. Astron. Soc., 57,* 649–670, 1979.

Carswell, D. A., D. B. Clarke, and R. H. Mitchell, The petrology and geochemistry of ultramafic nodules from pipe 200, in *Proceedings, Second International Kimberlite Conference, Santa Fe, 1977,* AGU, Washington, D. C., 1979.

Carter Hearn, B., Jr., and F. R. Boyd, Garnet peridotite xenoliths in a Montana, USA, kimberlite, *Phys. Chem. Earth, 9,* 247–255, 1975.

Chapman, D. S., and H. N. Pollack, Global heat flow: A new look, *Earth Planet. Sci. Lett., 28,* 23–32, 1975*a*.

Chapman, D. S., and H. N. Pollack, Heat flow and incipient rifting in the Central African Plateau, *Nature, 256,* 28–30, 1975*b*.

Chase, C. G., Tectonic history of the Fiji Plateau, *Geol. Soc. Amer. Bull., 82,* 3687–3710, 1971.

Chase, T. E., Topography of the oceans, *IMR Tech. Rep. Ser. TR57,* Scripps Inst. of Oceanogr., La Jolla, Calif., 1975.

Chinese Geological Society, *Chinese Tectonic Chart of Asia,* Peking, China, 1975.

Choubert, G., and A. Foure-Muret, International tectonic map of Africa, Unesco, Paris, 1968.

Christofferson, E., Linear magnetic anomalies in the Columbia Basin, central Caribbean Sea, *Geol. Soc. Amer. Bull., 64,* 3217–3230, 1973.

Cooper, A. K., D. W. Scholl, and M. S. Marlow, A plate tectonic model for the evolution of the eastern Bering Sea Basin, *Geol. Soc. Amer. Bull., 87,* 1119–1126, 1976.

Corliss, J. B., The origin of metal-bearing submarine hydrothermal solutions, *J. Geophys. Res., 76,* 8128–8138, 1971.

Corliss, J. B., et al., Exploration of submarine thermal springs on the Galapagos Rift, submitted to *Science,* 1979.

Crough, S. T., Thermal model of oceanic lithosphere, *Nature, 256,* 388–390, 1975.

Crough, S. T., and G. A. Thompson, Thermal model of continental lithosphere, *J. Geophys. Res., 81,* 4857–4862, 1976.

Davis, E. E., and C. R. B. Lister, Fundamentals of ridge crest topography, *Earth Planet. Sci. Lett., 21,* 405–413, 1974.

Davis, E. E., and C. R. B. Lister, Heat flow measured over the Juan de Fuca Ridge on a quasi-regular grid, *J. Geophys. Res., 82,* 4845–4853, 1977.

de Almeida, F. F. M., G. Amaral, U. G. Gordani, and K. Kawashita, The Precambrian evolution of the South American cratonic margin south of the Amazon river in the ocean basins and margins, in *The South Atlantic,* vol. 1, edited by A. Naim and F. Stehli, pp. 411–466, John Wiley, New York, 1974.

Dixon, J. R., and D. C. Presnall, Geothermometry and geobarometry of synthetic spinel lherzolite in the system, CaO-MgO-Al_2O_3-SiO_2, in *Proceedings, Second International Kimberlite Conference, Santa Fe, 1977,* AGU, Washington, D. C., 1979.

Dziewonski, A. M., Upper mantle models from 'pure-path' dispersion data, *J. Geophys. Res., 76,* 2587–2601, 1971.

Eggler, D. H., M. E. McCallum, and C. B. Smith, Discrete nodule assemblages in kimberlites from northern Colorado and southern Wyoming: Evidence for a diapiric origin of kimberlite, in *Proceedings, Second International Kimberlite Conference, Santa Fe, 1977,* AGU, Washington, D. C., 1979.

England, P. C., Some thermal considerations of the Alpine metamorphism—Past, present and future, *Tectonophysics, 46,* 21–40, 1978.

England, P. C., and S. W. Richardson, The influence of erosion upon the mineral facies of rocks from different metamorphic environments, *J. Geol. Soc. London, 134,* 201–213, 1977.

Erickson, A. J., G. Simmons, and W. B. F. Ryan, Review of heat flow data from the Mediterranean and Aegean seas, in *International Symposium on the Structural History on the Mediterranean Basins,* edited by B. Bign-Duval and L. Montadert, pp. 2263–2280, Editions Tecknip, Paris, 1977.

Ernst, W. G., Comparative chemical-mineralogist investigation of five western Alpine lherzolite complexes, in *Proceedings Second International Kimberlite Conference, Santa Fe, 1977,* AGU, Washington, D. C., 1979.

Fischer A. G., et al., *Initial Reports of the Deep-Sea Drilling Project,* vol. 6, 1329 pp., U.S. Government Printing Office, Washington, D. C., 1971.

Foland, K. A., and H. Faul, Ages of the White Mountain intrusives, New Hampshire, Vermont and Maine, U.S.A., *Amer. J. Sci., 277,* 888–904, 1977.

Forsyth, D. W., The evolution of the upper mantle beneath mid ocean ridges, *Tectonophysics, 38,* 89–118, 1977.

Francis, D. M., Amphibole pyroxenite xenoliths: Cumulate or replacement phenomena from the upper mantle, Nunivak Island, Alaska, *Contrib. Mineral. Petrol., 58,* 51–61, 1976.

Francis, T. J. G., I. T. Porter, and R. C. Lilwall, Microearthquakes near the eastern end of St. Paul's fracture zone, *Geophys. J. Roy. Astron. Soc., 53,* 201–217, 1978.

Goode, J. P., The homolosine projection, in *An Introduction to the Study of Map Projections,* edited by J. A. Stears, chap. 10, University of London Press, London, 1923.

Goodwin, A. M., Giant impacting and the development of the continental crust, in *The Early History of the Earth,* edited by B. F. Windley, 619 pp., John Wiley, New York, 1976.

Griffin, W. L., D. A. Carswell, and P. H. Nixon, Lower-crustal granulites and eclogites from Lesotho, southern Africa, in *Proceedings, Second International Kimberlite Conference, Santa Fe, 1977,* AGU, Washington, D. C., 1979.

Gurney, J. J., B. Harte, and K. G. Cox, Mantle xenoliths in the Matsku kimberlite pipe, *Phys. Chem. Earth, 9,* 507–523, 1975.

Handschumacher, D. W., Post-Eocene plate tectonics of the eastern Pacific, in *The Geophysics of the Pacific Ocean Basin and Its Margin,* edited by G. H. Sutton et al., pp. 177–202, AGU, Washington, D. C., 1976.

Hawkesworth, C. J., Vertical distribution of heat production in the basement of the eastern Alps, *Nature, 249,* 435–436, 1974.

Hays, J. D., and W. C. Pitman III, Lithospheric plate motion, sea level changes and climatic and ecological consequences, *Nature, 246,* 12–18, 1974.

Heier, K. S., and J. A. S. Adams, Concentration of radioactive elements in deep crustal material, *Geochim. Cosmochim. Acta, 29,* 53–61, 1965.

Heier, K. S., and J. M. Rhodes, Thorium, uranium and potassium concentrations in granites and gneisses of the Rum Jungle Complex, Northern Territory, Australia, *Econ. Geol., 61,* 563–571, 1966.

Herman, B. M., M. G. Langseth, and M. A. Hobart, Heat flow in the oceanic crust bounding western Africa, *Tectonophysics, 41,* 61–77, 1977.

Hilde, T. W. C., N. Isezaki, and J. M. Wageman, Mesozoic sea floor spreading in the North Pacific, in *The Geophysics of the Pacific Ocean Basin and Its Margin, Geophys. Monogr.,* vol. 19, edited by G. H. Sutton et al., pp. 205–226, AGU, Washington, D. C., 1976.

Hoffman, P., Evolution of an early Proterozoic continental margin: The Coronation geosyncline and associated aulacogens of the northwest Canadian Shield, *Phil. Trans. Roy. Soc. London, Ser. A., 273,* 547–581, 1973.

Hoffman, A. W., and S. R. Hart, An assessment of local and regional isotopic equilibrium in the mantle, *Earth Planet. Sci. Lett., 38,* 44–62, 1978.

Holmes, A., *Principles of Physical Geology,* 2nd ed., 1288 pp., Ronald, New York, 1965.

Horai, K., Effects of past climatic changes on the thermal field of the earth, *Earth Planet. Sci. Lett., 6,* 29–42, 1969.

Horai, K., and S. Uyeda, Terrestrial heat flow in volcanic areas, in *The Earth's Crust and Upper Mantle, Geophys. Monogr.,* vol. 13, pp. 95–109, edited by P. J. Hart, AGU, Washington, D. C., 1969.

Hsu, K. J., et al., *Initial Reports of the Deep Sea Drilling Project,* vol. 42, part 1, 1249 pp., U.S. Government Printing Office, Washington, D. C., 1978.

Hunter, D. R., Crustal development in the Kaapvaal Craton, 2, The Proterozoic, *Precambrian Res., 1,* 295–326, 1974.

Hurley, P. M., Distribution of age provinces in Laurasia, *Earth Planet. Sci. Lett., 8,* 189–196, 1971.

Hurley, P. M., and J. R. Rand, Pre-drift continental nuclei, *Science, 164,* 1229–1242, 1969.

Irving, A. J., On the validity of paleogeotherms determined from xenolith suites in basalts and kimberlites, *Amer. Mineral., 61,* 638–642, 1976.

Jessop, A. M., The distribution of glacial perturbation of heat flow in Canada, *Can. J. Earth Sci., 8,* 162–166, 1971.

Jessop, A. M., and T. Lewis, Heat flow and heat generation in the Superior Province of the Canadian Shield, *Tectonophysics, 50,* 55–77, 1978.

Jessop, A. M., M. Hobart, and J. G. Sclater, *World Wide Compilation of Heat Flow Data, Geothermal Ser.,* no. 5, Department of Energy, Mines and Resources, Ont., 1976.

Jordan, T. H., The continental tectosphere, *Rev. Geophys. Space Phys., 13,* 1–12, 1975.

Karig, D. E., Ridges and basins of the Tonga-Kermadec island arc system, *J. Geophys. Res., 75,* 239–254, 1970.

Karig, D. E., Structural history of the Mariana island arc system, *Geol. Soc. Amer. Bull., 82,* 323–344, 1971.

Karig, D. E., et al. *Initial Reports of the Deep Sea Drilling Project,* vol. 31, 927 pp., U.S. Government Printing Office, Washington, D. C., 1974.

Katz, M. B., Earth Precambrian granulites—Greenstones, transform mobile belts and ridge-rifts in early crust, in *The Early History of the Earth,* edited by B. F. Windley, pp. 147–158, John Wiley, New York, 1976.

Keen, C. E., Thermal history and subsidence of rifted continental margins—Evidence from wells on the North Scotian and Labrador shelves, *Can. J. Earth Sci., 16,* 505–522, 1979.

Killeen, P. G., and K. S. Heier, A uranium and thorium enriched province of the Fennoscandian Shield in southern Norway, *Geochim. Cosmochim. Acta, 39,* 1515–1524, 1975.

King, P. B., Tectonic map of North America, 1:5,000,000, U.S. Geol. Surv., Washington, D. C., 1969.

Kossinna, E., Die Liefen des Weltmeeres, *Inst. Meereskunde Veroeff. Geogr. Naturwiss., 9,* 70 pp., 1921.

Kristoffersen, C., and M. Talwani, The extinct triple-junction south of Greenland and the Tertiary motion of Greenland relative to North America, *Geol. Soc. Amer. Bull., 88,* 1037–1049, 1977.

Kutas, R. I., Investigation of heat flow in the territory of the Ukraine, *Tectonophysics, 41,* 139–145, 1977.

LaBrecque, J. L., D. V. Kent, and S. C. Cande, Revised magnetic polarity time scale for Late Cretaceous and Cenozoic time, *Geology, 5,* 330–355, 1977.

Lachenbruch, A. H., Crustal temperature and heat production: Implications of the linear heat flow relation, *J. Geophys. Res., 75,* 3291–3300, 1970.

Lachenbruch, A. H., Heat flow in the Basin and Range Province and thermal effects of tectonic extension, *Tectonophysics,* in press, 1979.

Lachenbruch, A. H., and C. M. Bunker, Vertical gradients of heat production in the continental crust, 2, Some estimates from borehole data, *J. Geophys. Res., 76,* 3852–3860, 1971.

Lachenbruch, A. H., and J. H. Sass, Heat flow in the United States and the thermal regime of the crust, in *The Earth's Crust, Geophys. Monogr.,* vol. 20, edited by J. G. Heacock, pp. 626–675, AGU, Washington, D. C., 1977.

Ladd, J. W., South Atlantic sea floor spreading and Caribbean tectonics, Ph.D. thesis, 251 pp. Columbia Univ., New York, 1974.

Lambert, I. B., and K. S. Heier, The vertical distribution of uranium, thorium, and potassium in the continental crust, *Geochim. Cosmochim. Acta, 31,* 377–390, 1967.

Lambert, R. S. J., Archean thermal regimes, crustal and upper mantle temperatures and a progressive evolutionary model for the earth, in *The Early History of the Earth,* edited by B. F. Windley, 363–387, John Wiley, New York, 1976.

Langseth, M. G., and M. A. Hobart, Interpretation of heat flow measurements in the Vema fracture zone, internal report, 12 pp., Lamont-Doherty Geol. Observ., Palisades, N. Y., 1976.

Langseth, M. G., and G. W. Zielinski, Marine heat flow measurements in the Norwegian-Greenland Sea and in the vicinity of Iceland, in *Geodynamics of Iceland and the North Atlantic Area,* edited by L. Kristansson, pp. 277–295, D. Reidel, Hingham, Mass., 1974.

Larson, R. L., Late Jurassic sea-floor spreading in the eastern Indian Ocean, *Geology, 3,* 69–71, 1975.

Larson, R. L., and T. W. C. Hilde, A revised time scale of magnetic reversals for the Early Cretaceous and Late Jurassic, *J. Geophys. Res., 80,* 2586–2594, 1975.

Lawver, L. A., J. W. Hawkins, and J. G. Sclater, Magnetic anomalies and crustal dilation in the Lau Basin, *Earth Planet. Sci. Lett., 33,* 27–35, 1975*a*.

Lawver, L. A., J. R. Curray, and D. G. Moore, Magnetics in the Andaman Sea and the effect of high sedimentation rates (abstract), *Eos Trans. AGU, 56,* 1064, 1975*b*.

Lee, W. H. K., and S. Uyeda, Review of heat flow data, in *Terrestrial Heat Flow, Geophys. Monogr.,* vol. 8, edited by W. H. K. Lee, pp. 87–190, AGU, Washington, D. C., 1965.

Lewis, T. J., and A. E. Beck, Analysis of heat flow data—Detailed observations in many holes in a small area, *Tectonophysics, 41,* 41–59, 1977.

Lister, C. R. B., On the thermal balance of a mid-ocean ridge, *Geophys. J. Roy. Astron. Soc., 26,* 515–535, 1972.

Lister, C. R. B., On the penetration of water into hot rock, *Geophys. J. Roy. Astron. Soc., 39,* 465–509, 1974.

Lister, C. R. B., Estimators for heat flow and deep rock properties based on boundary layer theory, *Tectonophysics, 41,* 157–171, 1977.

Lonsdale, P., and K. Klitgord, Structure and tectonic history of the eastern Panama Basin, *Geol. Soc. Amer. Bull., 59,* 981–999, 1978.

Louden, K., Magnetic anomalies in the West Philippine Basin, in *The Geophysics of the Pacific Ocean Basin and Its Margin, Geophys. Monogr.,* vol. 19, edited by G. H. Sutton et al., pp. 253–268, AGU, Washington, D. C., 1976.

Lubimova, E. A., B. G. Polyak, Ya. B. Smirnov, R. I. Kutas, F. V. Firsov, S. I. Sergienko, and L. N. Liusova, Heat flow in the USSR. in *Catalogue of Data, 1964–1972,* Soviet Geophysical Committee, Academy of Sciences of the USSR, Moscow, 1973.

Luyendyk, B. P., K. C. MacDonald, and W. B. Bryan, Rifting history of the Woodlark Basin, southwest Pacific, *Geol. Soc. Amer. Bull., 84,* 1125–1134, 1973.

McKenzie, D. P., Some remarks on heat flow and gravity anomalies, *J. Geophys. Res., 72,* 6261–6273, 1967.

McKenzie, D. P., Some remarks on the development of sedimentary basins, *Earth Planet. Sci. Lett., 40,* 25–32, 1978.

McKenzie, D. P., and N. Weiss, Speculations on the thermal and tectonic history of the earth, *Geophys. J. Roy. Astron. Soc., 42,* 131–174, 1975.

Menard, H. W., and S. M. Smith, Hyposometry of ocean basin provinces, *J. Geophys. Res., 71,* 4305–4326, 1966.

Ministry of Geology, Russian tectonic atlas, 16 sheets, Moscow, 1969.

Minster, J. B., T. H. Jordan, P. Molnar, and E. Harris, Numerical modeling of instantaneous plate tectonics, *Geophys. J. Roy. Astron. Soc., 36,* 541–576, 1974.

Molnar, P., and P. Tapponier, Cenozoic tectonics of Asia; effects of a continental collision, *Science, 189,* 419–426, 1976.

Molnar, P., T. Atwater, J. Mammerickx, and S. M. Smith, Magnetic anomalies, bathymetry and the tectonic evolution of the South Pacific since the Late Cretaceous, *Geophys. J. Roy. Astron. Soc., 40,* 383–420, 1975.

Moorbath, S., The oldest rocks and the growth of continents, *Sci. Amer., 236,* 92–105, 1977.

Mori, T., and D. H. Green, Pyroxenes in the system $Mg_2Si_2O_6$-$CaMgSi_2O_6$ at high pressure, *Earth Planet. Sci. Lett., 26,* 277–286, 1975.

Mueller, S., A new model of the continental crust, in *The Earth's Crust, Geophys. Monogr.* vol. 20, edited by J. G. Heacock, pp. 289–318, AGU, Washington, D. C., 1978.

Naqui, S. M., V. Divakara Rao, and H. Narain, The protocontinental growth of the Indian Shield and the antiquity of its rift valleys, *Precambrian Res., 1,* 345–398, 1974.

Norton, I., and J. G. Sclater, A model for the evolution of the Indian Ocean and the breakup of Gondwanaland, *J. Geophys. Res., 84,* 6803–6830, 1979.

Okal, E. A., The effect of intrinsic oceanic upper mantle heterogeneity on regionalization of long-period Rayleigh-wave phase velocities, *Geophys. J. Roy. Astron. Soc., 49,* 357–370, 1977.

Okal, E. A., and D. L. Anderson, A study of lateral inhomogeneities in the upper mantle by multiple *ScS* travel-time residuals, *Geophys. Res. Lett., 2,* 313–316, 1975.

Oldenburgh, D. W., A physical model for the creation of the lithosphere, *Geophys. J. Roy. Astron. Soc., 43,* 425–451, 1975.

Padovani, E. R., and J. L. Carter, Aspects of the deep crustal evolution beneath south central New Mexico, in *The Earth's Crust, Geophys. Monogr.,* vol. 20, edited by J. G. Heacock, pp. 19–56, AGU, Washington, D. C., 1977.

Palmasson, G., On heat flow in Iceland in relation to the mid-Atlantic ridge, *Soc. Sci. Islandica, 38,* 111–117, 1967.

Parker, R. L., and D. W. Oldenburg, Thermal model of ocean ridges, *Nature, 242,* 137–139, 1973.

Parsons, B., and D. P. McKenzie, Mantle convection and the thermal structure of the plates, *J. Geophys. Res., 83,* 4485–4496, 1978.

Parsons, B., and J. G. Sclater, An analysis of the variation of ocean floor bathymetry and heat flow with age, *J. Geophys. Res., 82,* 803–827, 1977.

Phair, G., and D. Gottfried, The Colorado Front Range, Colorado, USA, as a uranium and thorium province, in *The Natural Radiation Environment,* edited by J. A. S. Adams and W. M. Lowder, pp. 7–38, University of Chicago Press, Chicago, Ill., 1964.

Pitman, W. C., III, and M. Talwani, Sea floor spreading in the North Atlantic, *Geol. Soc. Amer. Bull., 83,* 619–646, 1972.

Pitman, W. C., III, R. L. Larson, and E. M. Herron, *Magnetic Lineations of the Oceans, Map Chart Ser.,* vol. MC-6, Geological Society of America, Boulder, Colo., 1974.

Polyak, B. G., and Y. A. Smirnov, Relationship between terrestrial heat flow and the tectonics of continents, *Geotectonics,* Engl. Transl., *4,* 205–213, 1968.

Rabinowitz, P. D., and J. L. LaBrecque, The mesozoic south Atlantic and evolution of its continental margins, *J. Geophys. Res., 84,* 5973–6002, 1979.

Rao, R. U. M., and A. M. Jessop, A comparison of the thermal characters of shields, *Can. J. Earth Sci., 12,* 347–360, 1975.

Rao, R. U. M., G. V. Rao, and H. Narain, Radioactive heat genera-

tion and heat flow in the Indian Shield, *Earth Planet. Sci. Lett., 30,* 57–64, 1976.
Reid, A. M., C. H. Donaldson, R. W. Brown, I. Ridley, and J. B. Dawson, Mineral chemistry of peridotite xenoliths from the Lashine volcano, Tanzania, *Phys. Chem. Earth, 9,* 525–544, 1975.
Richardson, S. W., and E. R. Oxburgh, Heat flow, radiogenic heat production and crustal temperatures in England and Wales, *J. Geol. Soc. London, 135,* 323–337, 1978.
Richter, F. M., Convection and the large-scale circulation of the mantle, *J. Geophys. Res., 78,* 8735–8745, 1973.
Richter, F. M., and B. Parsons, On the interaction of two scales of convection in the mantle, *J. Geophys. Res., 80,* 2529–2541, 1975.
Roy, R. F., D. D. Blackwell, and F. Birch, Heat generation of plutonic rocks and continental heat flow provinces, *Earth Planet. Sci. Lett., 5,* 1–12, 1968.
Roy, R. F., D. D. Blackwell, and E. R. Decker, Continental heat flow, in *The Nature of the Solid Earth,* edited by E. C. Robertson et al., pp. 506–543, McGraw-Hill, New York, 1972.
Royden, L., J. G. Sclater, and R. P. Von Herzen, Continental margin subsidence and heat flow: Important parameters in formation of petroleum hydrocarbons, *Bull. Amer. Ass. Petrol. Geol.,* in press, 1980.
Rybach, L., Radioactive heat production in rocks and its relation to other petrophysical parameters, *Pure Appl. Geophys., 114,* 309–317, 1976.
Sass, J. H., and A. Lachenbruch, Thermal regime of the Australian continental crust, in *The Earth, Its Origin Structure and Evolution,* edited by M. W. McElhinny, pp. 301–351, Academic, New York, 1978.
Sass, J. H., A. H. Lachenbruch, and A. M. Jessop, Uniform heat flow in a deep hole in the Canadian Shield and its paleoclimatic implications, *J. Geophys. Res., 76,* 8586–8596, 1971.
Schouten, H., and K. Klitgord, Mesozoic magnetic anomalies in western North Atlantic, *Map MF 915,* U.S. Geol. Surv., Reston, Va., 1977.
Schubert, G., C. Froideveaux, and D. A. Yuen, Oceanic lithosphere and asthenosphere: Thermal and mechanical structure, *J. Geophys. Res., 81,* 3525–3540, 1976.
Sclater, J. G., and P. A. F. Christie, Continental stretching: An explanation of the post–Mid-Cretaceous subsidence of the Central North Sea Basin, submitted to *J. Geophys. Res.,* 1979.
Sclater, J. G., and J. Crowe, A heat flow survey at anomaly 13 on the Reykjanes Ridge: A critical test of the relation between heat flow and age, *J. Geophys. Res., 84,* 1593–1602, 1979.
Sclater, J. G., and J. Francheteau, The implications of terrestrial heat flow observations on current tectonic and geochemical models of the crust and upper mantle of the earth, *Geophys. J. Roy. Astron. Soc., 20,* 509–542, 1970.
Sclater, J. G., R. N. Anderson, and M. L. Bell, The elevation of ridges and evolution of the central eastern Pacific, *J. Geophys. Res., 76,* 7888–7915, 1971.
Sclater, J. G., R. P. Von Herzen, D. L. Williams, R. N. Anderson, and K. Klitgord, The Galapagos spreading centre: Heat flow low on the north flank, *Geophys. J. Roy. Astron. Soc., 38,* 609–626, 1974.
Sclater, J. G., J. Crowe, and R. N. Anderson, On the reliability of oceanic heat flow averages, *J. Geophys. Res., 81,* 2997–3006, 1976*a*.
Sclater, J. G., D. E. Karig, L. A. Lawver, and K. Louden, Heat flow, depth, and crustal thickness of the marginal basins of the South Philippine Sea, *J. Geophys. Res., 81,* 309–318, 1976*b*.
Sclater, J. G., C. Bowin, R. Hey, H. Hoskins, J. Peirce, J. Phillips, and C. Tapscott, The Bouvet triple junction, *J. Geophys. Res., 81,* 1857–1869, 1976*c*.
Sclater, J. G., S. Hellinger, and C. Tapscott, Paleobathymetry of the Atlantic Ocean, *J. Geol., 85,* 509–552, 1977.
Sclater, J. G., H. Dick, I. O. Norton, and D. Woodruffe, A geophysical and petrological study of the antarctic plate boundary east and west of Bouvet Island, *Earth Planet. Sci. Lett., 37,* 393–400, 1978.
Sclater, J. G., L. Royden, S. Semken, C. Burchfiel, L. Stegena, and F. Horvath, The Miocene through present development of the intra-Carpathian basins, *Earth Planet Sci. Lett.,* in press, 1980.
Simmons, G., and K. Horai, Heat flow data, 2, *J. Geophys. Res., 73,* 6608–6629, 1968.
Simmons, G., and A. Nur, Granites: Relation of properties insitu to laboratory measurements, *Science, 162,* 789–791, 1968.
Simpson, E., J. G. Sclater, B. Parsons, I. Norton, and L. Meinke, Mesozoic magnetic lineations in the Mozambique Basin, *Earth. Planet Sci. Lett., 43,* 260–264, 1979.
Sipkin, S. A., and T. H. Jordan, Lateral heterogeneity of the upper mantle determined from the travel times of *ScS, J. Geophys. Res., 80,* 1474–1484, 1975.
Sleep, N. H., Thermal effects of the formation of Atlantic continental margins by continental breakup, *Geophys. J. Roy. Astron. Soc., 24,* 325–350, 1971.
Smith, D., and S. Levy, Petrology of the Green Knobs diatreme and implications for the upper mantle below the Colorado Plateau, *Earth Planet. Sci. Lett., 29,* 107–125, 1976.
Smithson, S. B., Modeling continental crust: Structural and chemical constraints, *Geophys. Res. Lett., 5,* 749–752, 1978.
Sollogub, V. B., et al., New D.S.S. data on the crustal structure of the Baltic and Ukranian shields, *Tectonophysics, 20,* 67–84, 1973.
Steckler, M. S., and A. B. Watts, Subsidence of the Atlantic-type continental margin off New York, *Earth Planet. Sci. Lett., 41,* 1–13, 1978.
Swanberg, C. A., Vertical distribution of heat production in the Idaho batholith, *J. Geophys. Res., 77,* 2508–2513, 1972.
Swanberg, C. A., M. D. Chessman, G. Simmons, S. B. Smithson, G. Grønlie, and K. S. Heier, Heat flow–heat generation studies in Norway, *Tectonophysics, 23,* 31–48, 1974.
Sweeney, J. F., Subsidence of the Sverdrup Basin, Canadian arctic islands, *Geol. Soc. Amer. Bull., 88,* 41–48, 1977.
Sykes, L. R., and M. Sbar, Intraplate earthquakes, lithospheric stresses and the driving mechanism of plate tectonics, *Nature, 245,* 298–302, 1973.
Talwani, M., C. C. Windisch, and M. G. Langseth, Reykjanes Ridge crest: A detailed geophysical study, *J. Geophys. Res., 76,* 473–517, 1971.
Tarney, J., and B. F. Windley, Chemistry, thermal gradients and evolution of the lower continental crust, *J. Geol. Soc. London, 134,* 153–172, 1977.
Tarney, J., I. W. D. Dalziel, and M. J. de Wit, Marginal basin 'Rocas Verdes' complex from S. Chile; a model for Archean greenstone belt formation, in *The Early History of the Earth,* edited by B. F. Windley, pp. 131–146, John Wiley, New York, 1976.
Tilling, R. I., D. Gottfried, and F. C. W. Dodge, Radiogenic heat production of contrasting magma series: Bearing on interpretation of heat flow, *Geol. Soc. Amer. Bull., 81,* 1447–1462, 1970.
Urien, C. M., and J. J. Zambrano, The geology of the basins of the Argentine continental margin and Malomas Plateau, in *The Ocean Basins and Margins,* vol. 1, *The South Atlantic,* edited by A. Nairn and F. Stehli, pp. 135–170, John Wiley, New York, 1973.
Uyeda, S., Heat flow, in *Crust and Upper Mantle of the Japanese Area,* edited by S. Miyamura and S. Uyeda, pp. 97–105, Earthquake Research Institute, University of Tokyo, Tokyo, 1972.
van Hinte, J. E., A Jurassic time scale, *Amer. Ass. Petrol. Geol. Bull., 60*(4), 489–497, 1976*a*.
van Hinte, J. E., A Cretaceous time scale, *Amer. Ass. Petrol. Geol. Bull., 60*(4), 498–516, 1976*b*.
van Niekerk, C. B., and A. J. Burger, A new age for the Ventersdorp acidic lavas, *Trans. Geol. Soc. S. Afr., 81,* 155–163, 1978.
Veizer, J., $^{87}Sr/^{86}Sr$ evolution of seawater during geologic history and its significance as an index of crustal evolution, in *The Early History of the Earth,* edited by B. F. Windley, pp. 569–578, John Wiley, New York, 1976.
Von Herzen, R. P., and W. H. K. Lee, Heat flow in ocean regions, in *The Earth's Crust and Upper Mantle, Geophys. Monogr.,* vol. 13, edited by P. J. Hart, AGU, pp. 88–94, Washington, D. C., 1969.
Watanabe, T., M. G. Langseth, and R. N. Anderson, Heat flow in back-arc basins, of the western Pacific, in *Island Arcs, Deep Sea Trenches, and Back-Arc Basins,* edited by M. Talwani and W. Pitman III, pp. 137–162, AGU, Washington, D. C., 1977.
Watts, A. B., and W. B. F. Ryan, Flexure of the lithosphere and continental margin basins, *Tectonophysics, 36,* 25–44, 1976.
Watts, A. B., and J. K. Weissel, Tectonic history of the Shikoku marginal basin, *Earth Planet. Sci. Lett., 25,* 239–250, 1975.
Watts, A. B., J. K. Weissel, and F. J. Davey, Tectonic evolution of the South Fiji marginal basin, in *Island Arcs, Deep Sea trenches, and Back-Arc Basins,* edited by M. Talwani and W. Pitman III, pp. 419–428, AGU, Washington, D. C., 1977.
Weissel, J. K., Evolution of the Lau Basin by the growth of small plates, in *Island Arcs, Deep Sea Trenches, and Back-Arc Basins,* edited by M. Talwani and W. Pitman III, pp. 429–436, AGU, Washington, D. C., 1977.
Weissel, J. K., and D. E. Hayes, Evolution of the Tasman Sea, *Earth Planet. Sci. Lett., 36,* 77–84, 1970.
Weissel, J. K., D. E. Hayes, and E. M. Herron, Plate tectonic syn-

thesis: The relative motions of the Australian, New Zealand and antarctic continental fragments since the Early Cretaceous, *Mar. Geol., 25,* 231–277, 1977.

Williams, D. L., and R. P. Von Herzen, Heat loss from the earth: New estimate, *Geology, 2,* 327–328, 1974.

Williams, D. L., R. P. Von Herzen, J. G. Sclater, and R. N. Anderson, The Galapagos spreading center: Lithospheric cooling and hydrothermal circulation, *Geophys. J. Roy. Astron. Soc., 38,* 587–608, 1974.

Wiltshire, H. G., and E. D. Jackson, Problems in determining mantle geotherms from pyroxene compositions of ultramafic rocks, *J. Geol., 83,* 313–329, 1975.

Windley, B. F., *The Evolving Continents,* 385 pp., John Wiley, New York, 1978.

Windley, B. F., and J. V. Smith, Archean high-grade complexes and modern continental margins, *Nature, 260,* 671–675, 1976.

Wood, B. J., and S. Banno, Garnet-orthopyroxene and orthopyroxene-clinopyroxene relationships in simple and complex systems, *Contrib. Mineral. Petrol., 42,* 109–124, 1973.

(Received September 28, 1978;
accepted August 30, 1979.)